PHYTOCHEMICAL AND PHARMACOLOGICAL SCREENING OF *SANSEVIERIA ROXBURGHIANA* SCHULT. & SCHULT. (FAMILY: AGAVACEAE)

Thesis submitted
by
Niloy Bhattacharjee

Doctor of Philosophy (Pharmacy)

Department of Pharmaceutical Technology
Faculty Council of Engineering & Technology
Jadavpur University
Kolkata, India
2018

JADAVPUR UNIVERSITY

KOLKATA 700032

WEST BENGAL, INDIA

INDEX NO: 177/13/Ph

1. **Title of the thesis:**

   Phytochemical and Pharmacological Screening of *Sansevieria Roxburghiana* Schult. & Schult. (Family: Agavaceae).

2. **Name, Designation & Institution of the supervisor:**

Dr. Saikat Dewanjee

Assistant professor

Department of Pharmaceutical Technology

Jadavpur University,

188, Raja S C Mullik Road, Kolkata 700032

West Bengal, India.

3. **List of Publications:**

A. Related to the thesis works (2)

i. Bhattacharjee N, Dua TK, Khanra R, Joardar S, Nandy A, Saha A, De Feo V, Dewanjee S. Protocatechuic acid, a phenolic from *Sansevieria roxburghiana* leaves, suppresses diabetic cardiomyopathy via stimulating glucose metabolism, ameliorating oxidative stress and inhibiting inflammation. Front Pharmacol. 2017;8:251. doi: 10.3389/fphar.2017.00251. (**Impact factor: 4.400; PMID: 28533752**).

ii. Bhattacharjee N, Khanra R, Dua TK, Das S, De B, Zia-Ul-Haq M, De Feo V, Dewanjee S. *Sansevieria roxburghiana* Schult. & Schult. F. (family: Asparagaceae) attenuates type 2 diabetes and its associated cardiomyopathy. PLoS One. 2016;11:e0167131. doi: 10.1371/ journal.pone. 0167131. (**Impact factor: 2.806; PMID: 27893829**).

B. Other publications obtained during the period of doctoral research (10)

i. Dewanjee S, Das S, Das AK, **Bhattacharjee N,** Dihingia A, Dua TK, Kalita J, Manna P. (2018). Molecular mechanism of diabetic neuropathy and its pharmacotherapeutic targets.

European Journal of Pharmacology. European Journal of Pharmacology 833, 472-523. **(Impact factor: 3.040; PMID: 29966615)**

ii. Dewanjee S, **Bhattacharjee N.** (2018). MicroRNA: a new generation therapeutic target in diabetic nephropathy. Biochemical Pharmacology. 155, 32-47. (**Impact factor: 4.235; PMID: 29940170**)

iii. Das S, Joardar S, Manna P, Dua TK, **Bhattacharjee N,** Khanra N, Khanra R, Bhowmick S, Kalita J, Saha A, Ray S, De Feo V, Dewanjee, S. (2018). Carnosic acid, a natural diterpene, attenuates arsenic-induced hepatotoxicity via reducing oxidative stress, MAPK activation, and apoptotic cell death pathway. Oxidative Medicine and Cellular Longevity. 2018; Article ID 1421438. doi: 10.1155/2018/1421438. (**Impact factor: 4.593; PMID: 29854073**)

iv. Dewanjee S, Dua TK, **Bhattacharjee N,** Das A, Gangopadhyay M, Khanra R, Joardar S, Riaz, M, De Feo V, Zia-Ul-Haq M. Natural products as alternative choice for P-glycoprotein (P-gp) inhibition. Molecules. 2017;22:871. doi:10.3390/molecules22060871. (**Impact factor: 2.861; PMID: 28587082**).

v. Khanra R, **Bhattacharjee N,** Dua TK, Nandy A, Saha A, Kalita J, Manna P. Taraxerol, a pentacyclic triterpenoid, from *Abroma augusta* leaf attenuates diabetic nephropathy in type 2 diabetic rats. Biomed Pharmacother. 2017;94:726-741. (**Impact factor: 2.759; PMID: 28802226**).

vi. Dewanjee S, Joardar S, **Bhattacharjee N,** Dua TK, Das S, Kalita J, Manna P. Edible leaf extract of *Ipomoea aquatica* Forssk. (Convolvulaceae) attenuates doxorubicin-induced liver injury via inhibiting oxidative impairment, MAPK activation and intrinsic pathway of apoptosis. Food Chem Toxicol. 2017;105:322-336. (**Impact factor: 3.778; PMID: 28478100**).

vii. Khanra R, Dewanjee S, Dua TK, **Bhattacharjee N.** Taraxerol, a pentacyclic triterpene from *Abroma augusta* leaf, attenuates acute inflammation via inhibition of NF-κB signaling. *Biomed. Pharmacother.* 2017;88:918-923. (**Impact factor: 2.759; PMID: 28587082**).

viii.Bhattacharjee N, Barma S, Konwar N, Dewanjee S, Manna P. Mechanistic insight of diabetic nephropathy and its pharmacotherapeutic targets: An update. Eur J Pharmacol. 2016;791:8-24. (**Impact factor: 2.896; PMID: 27568833**).

ix. Dua TK, Dewanjee S, Khanra R, **Bhattacharya N,** Bhaskar B, Zia-Ul-Haq M, De Feo V. The effects of two common edible herbs, *Ipomoea aquatica* and *Enhydra fluctuans*, on cadmium-induced pathophysiology: a focus on oxidative defense and anti-apoptotic mechanism. J. Transl. Med. 2015;13:245. doi: 10.1186/s12967-015-0598-6. (**Impact factor: 3.786; PMID: 26215156**).

x. Dewanjee S, Dua TK, Khanra R, Das S, Barma S, Joardar S, **Bhattacharjee N,** Zia-Ul-Haq M, Jaafar HZ. Water spinach, *Ipomoea aquatica* (Convolvulaceae), ameliorates lead toxicity by

inhibiting oxidative stress and apoptosis. *PLoS One.* 2015;10:e0139831. doi: 10.1371/journal.pone.0139831. (**Impact factor: 2.806; PMID: 26473485**).

4. List of patents: Nil

5. List of presentations in national/international seminar/conferences: (3)

i. Bhattacharjee N, Saha A, Dewanjee S. Protocatechuic acid, a phenolic from *Sansevieria roxburghiana* leaves, attenuates hyperglycemia through regulating IRS1/PI3K/Akt/AMPK /p 38/GLUT4 signaling in type 2 diabetic rats. Oral presentation in national seminar entitled "Natural resources for drug discovery and development" Dibrugarh University, Dibrugarh, Assam (February 24-25, 2018), Abstract book pp. 29. (**Awarded: Best oral presentation award**)

ii. Bhattacharjee N, Saha A, Dewanjee S. Protocatechuic acid attenuates diabetic cardiomyopathy through regulating PKC/NF-κβ/PARP signaling in type 2 diabetic rats. Oral presentation in international conference entitled "3rd International conference on innovations in pharmaceutical sciences (ICIPS-2018)", School of Pharmacy, Guru Nanak Institutions, Ibrahimpatnam, Hyderabad, Telangana (August 3-4, 2018), Abstract book pp. 48.

iii. Bhattacharjee N, Dewanjee S. Exploration of antidiabetic effect *Sansevieria roxburghiana* Schult. & Schult. F. (family: Asparagaceae) rhizomes. Poster presentation in national seminar entitled "Recent advances and scope in herbal technology: challenges and prospects", Assam University, Silchar, Assam (September 9-10, 2016), Abstract book pp. 25.

CERTIFICATE FROM THE SUPERVISOR

This is to certify that the thesis entitled "**Phytochemical and Pharmacological Screening of *Sansevieria Roxburghiana* Schult. & Schult. (Family: Agavaceae)**" submitted by **Sri. Niloy Bhattacharjee** who got his name registered on February 6, 2013 for the award of Ph. D. (Pharmacy) degree of Jadavpur University is absolutely based upon his own work under the supervision of **Dr. Saikat Dewanjee** and that neither his thesis nor any part of the thesis has been submitted for any degree/diploma or any other academic award anywhere before.

……..

(Dr. Saikat Dewanjee)
Assistant professor
Department of Pharmaceutical Technology
Jadavpur University
Kolkata 700032
West Bengal, India.

Acknowledgements

I wish to express my sincere gratitude to my supervisor, ***Dr. Saikat Dewanjee****, Assistant Professor, Department of Pharmaceutical Technology, Jadavpur University, Kolkata, India for his sincere, professional and precise guidance to achieve this goal.*

I sincerely acknowledge ***Department of Science and Technology (DST), New Delhi, India*** *for financial support through DST-Inspire fellowship [DST/INSPIRE Fellowship/2012 (1690-2012)].*

I express my sincere gratitude to ***Prof. Biswajit Mukherjee,*** *Department of Pharmaceutical Technology, Jadavpur University, Kolkata, India, for his cordial help during the period of my research. I am also thankful to other faculties of Department of Pharmaceutical Technology, Jadavpur University, Kolkata, India, for their cordial and expert help.*

I wish to acknowledge the authorities of ***Jadavpur University*** *for providing necessary supports throughout the tenure of my doctoral research. It has been an excellent opportunity to work in Jadavpur University with the outstanding facilities being offered to me.*

I sincerely acknowledge the Taxonomists, Central National Herbarium, Botanical Survey of India, Shibpur, India for their kind support in identification of the plant specimens for my research.

I prefer to express my sincere gratitude to ***Prof. Muhammad Zia-Ul-Haq,*** *Lahore College for Women University, Pakistan and* ***Prof. Vincenzo De Feo,*** *Department of Pharmacy, Salerno University, Italy for their professional cooperation, thoughtful scientific input, and feedback in my research work.*

I also wish to express my deepest gratitude to ***Prof. Achintya Saha*** *Department of Chemical Technology, University of Calcutta, Kolkata, India for his cordial supports to complete the in silico studies in my doctoral research.*

I deeply appreciate the warm welcome and the encouragement I have received from all of my ***fellow researchers*** *working at the same laboratory. I am also sincerely acknowledging all of my professional and personal* ***friends*** *for accepting nothing but only excellence from me.*

I would like to express my forlorn mind for the ***soul of innocent rats*** *without their immolation, it has been impossible to complete this work.*

My greatest acknowledgement and gratitude goes to ***my mother, my wife, and my in-laws*** *for their unconditional support, inspiration, and sacrifice for me to complete this assignment.*

Finally, I am grateful to almighty without whose blessings I couldn't have completed my research work.

Date:

Place: ***(Niloy Bhattacharjeee)***

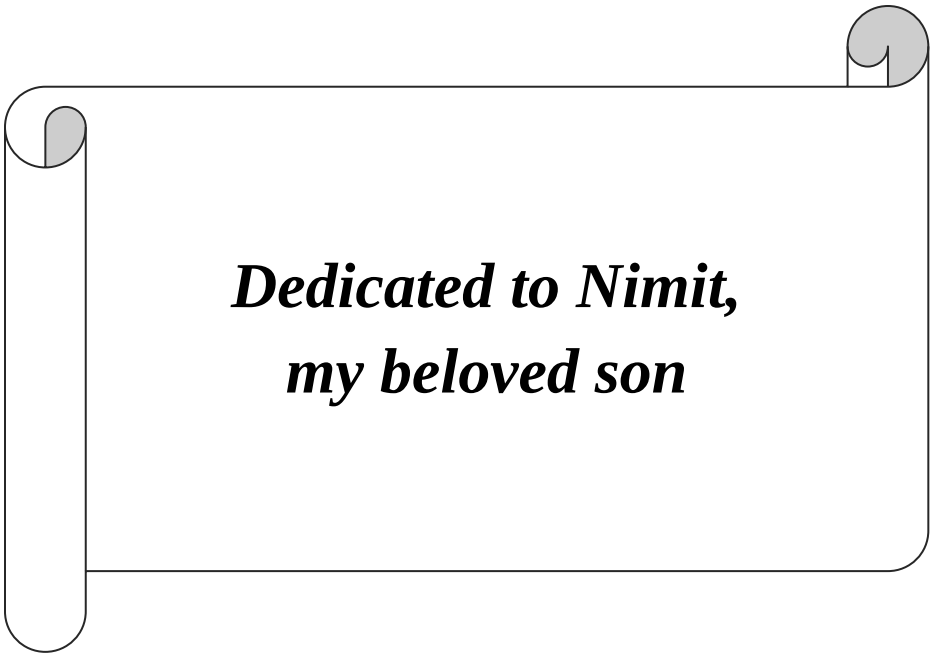
Dedicated to Nimit,
my beloved son

Preface

Sansevieria roxburghiana Schult. & Schult. F. (Family: Agavaceae) is a stem less, evergreen, and perennial monocot-herb with stout rootstock. The leaves are green, transversely marked with darker green lines on both sides. The leaves grow flat, strap-shaped/narrowly lanceolate, with subulate point. The raceme spike-like flowering stem grows and the flowers come in clusters of pedicels and jointed. This plant is commonly called as "Indian bowstring-hemp" or 'murva' in Ayurveda. It is widely distributed in Eastern coastal region in India. It is also found in Bangladesh, Myanmar, Sri Lanka, Indonesia, and tropical Africa. *S. roxburghiana* rhizome has been traditionally used to treat cancer, diabetes, oxidative damage, and inflammatory diseases. Phytochemical data revealed presence of saponins, phenolics, flavonoids, alkaloids, anthocyanins, terpenoids, and phytosterols in *S. roxburghiana* rhizome. In this thesis, it has been attempted to represent a comprehensive drug discovery research with *S. roxburghiana* rhizome. Despite the anti-diabetic effect of the crude extract of *S. roxburghiana* rhizome has been reported earlier against streptozotocin-induced type 1 diabetic rats; however, the report largely failed to fetch any conclusive evidence regarding the mechanism and the scaffold/s responsible for anti-diabetic effect. Therefore, present research has been undertaken not only to validate folklore claim of anti-diabetic activity by *S. roxburghiana* rhizome against type 2 diabetic rats, but also to identify bioactive scaffold for the said activity. Considering the claimed anti-oxidant and anti-inflammatory effects of *S. roxburghiana* rhizome, it has been intended to evaluate the prophylactic effect of *S. roxburghiana* rhizome against diabetes-mediated micro-vascular complications in the myocardial tissues. Finally, it has been anticipated to reveal mechanistic insights behind the protective effect of crude extract and bioactive scaffold. The thesis has been framed as follows:

Chapter 1: Introduction, it is a brief introductory section to give an impression of plant-based drug discovery and the objective of the overall research;

Chapter 2: Literature review of *S. roxburghiana*;

Chapter 3: Phytochemical analysis of *S. roxburghiana* rhizome;

Chapter 4: Toxicity studies of *S. roxburghiana* rhizome and protocatechuic acid;

Chapter 5: Protective role of *S. roxburghiana* rhizome against type 2 diabetes and diabetic cardiomyopathy;

Chapter 6: Protective role of protocatechuic acid against type 2 diabetes and diabetic cardiomyopathy.

Index

Figure captions

Table captions

1.1. Introduction

Medicinal plants have immense influence in the healthcare system in the people of different societies. The use of herbs for the treatment of diseases began long ago (Schulz et al., 2001). Methods of folk healing commonly employ the curative effect of traditional herbs. These traditional herbs were employed as the drug discovery tool over past few centuries (Atanasov et al., 2015). The new drug discovery encompasses the identification of therapeutically significant new chemical moieties, possessing all the requirements to be a drug (Katiyar et al., 2012). These new chemical moieties would be obtained either through chemical synthesis or from natural reservoirs. Initial successful stories of drug discovery rely on synthetic compounds; however, it has been proven to be less effective in terms of overall success (Katiyar et al., 2012). On the other hand, plants contain plenty of new molecules with diverse/complex chemical structures, which offer enormous scope in drug discovery. Before the advancement of high throughput bioassay, ~ 80% of drug candidates were purely natural compounds or their semisynthetic analogs (Katiyar et al., 2012). Despite nature-derived small-molecules remain integral components of the drug discovery pipeline; natural product-based drug discovery is considerably declining over past three decades (Stratton et al., 2015). On other hand, interest on natural product-based drug discovery is shifting from small-molecules toward big molecule biologicals such as antibodies, nucleic acid including miRNAs, therapeutic polypeptides etc. (Projan et al., 2004). However, considering the research output between 1950 and 2010, Pye et al claimed that implementation of innovative discovery methods will still retain scopes to discover novel small molecules with unique structural and biological properties in future from natural products (Pye et al. 2017).

1.2. Natural product-based drug discovery: history to present scenario

The history of natural product-based drug discovery has been astonishingly successful over the past century evidenced from the antitumor agents namely, taxol, vinblastine, vincristic, and doxorubicin, the immune-suppressants such as cyclosporine, and rapamycin, and the cholesterol lowering agent-statins remain the top-selling drugs today (Gonzalez-Sabin, 2012). The rational drug discovery from medicinal plants has been begun in the early of 19th century when morphine was first isolated in the year of 1806 from *Paparver somniferum* (Sertürner, 1817; Atanasov et al., 2015). Many bioactive phytochemicals viz. quinine, codeine, digitoxin, caffeine, salicylic acid, atropine, codeine, capsaicin, colchicine, cocaine etc. were subsequently isolated from medicinal plants in 20th century, which are still in use (Balunas and Kinghorn, 2005; Atanasov et al., 2015). Preceding World War II, a progression in the identification of pharmacologically active scaffolds from plants and microorganisms has been achieved. The antibiotics, such as

penicillin, streptomycin etc. were isolated during that time (Atanasov et al., 2015). In the post-war epoch, new scaffolds namely reserpine from *Rauwolfia serpentina*, vinblastine from *Catharanthus roseus*, pilocarpine from *Pilocarpus jaborandi*, vancomycin from *Amycolatopsis orientalis*, erythromycin from *Saccharopolyspora erythraea* etc. were isolated (Klohs et al., 1954; Dias et al., 2012; Moudi et al., 2013; Atanasov et al., 2015). A total of 19 natural product-based drugs have been accepted for marketing globally between 2005 and 2010. Among them, 7 were classified as natural product-derived small molecules in their original forms as drugs, 10 were the semi-synthetic analogs of natural product-derived small molecules, and 2 were natural product-derived drugs (Mishra and Tiwari, 2011). Several natural product-based small molecules are now in the different phases of clinical trials and may be chosen as the drugs in future (Mishra and Tiwari, 2011). 2015 has been a breakthrough in the natural product-based drug discovery, when William C Campbell, Satoshi Omura, and Youyou Tu have been awarded Nobel Prize in physiology or medicine for their discovery of avermectins and artemisinin. Among the derivatives of avermectins, ivermectin (Figure 1.1A) could attenuate the incidence of onchocerciasis and lymphatic filariasis (Shen, 2015). On other hand, artemisinin (Figure 1.1B) has been found to reduce the mortality of malaria patients (Shen, 2015).

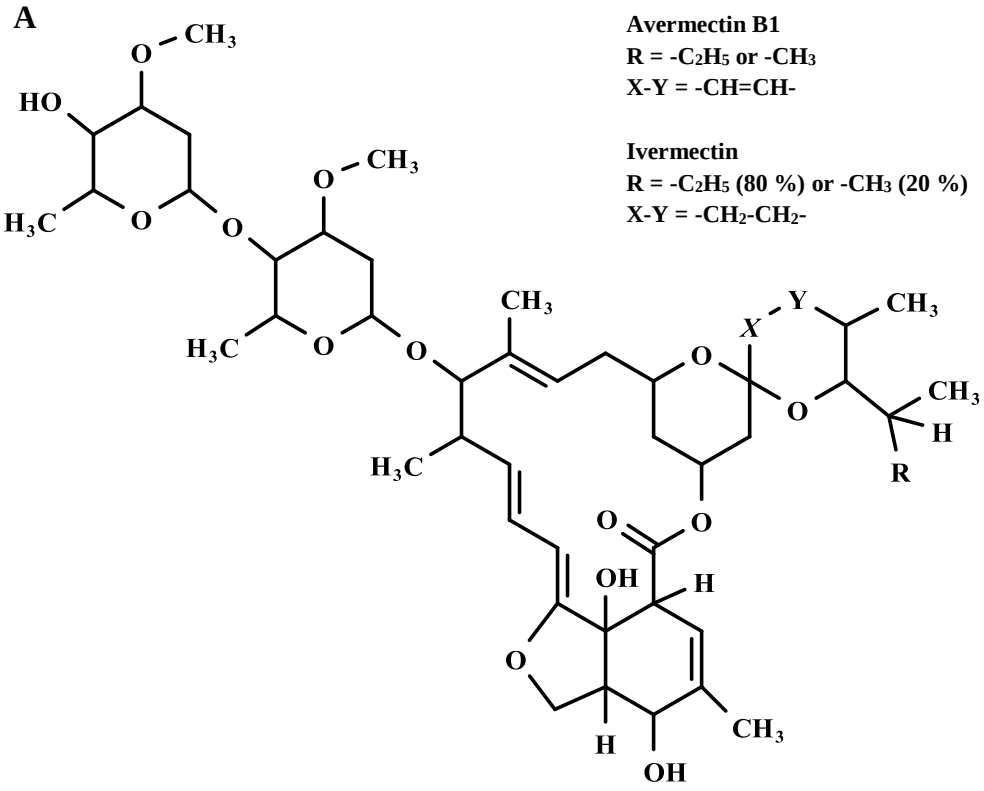

B

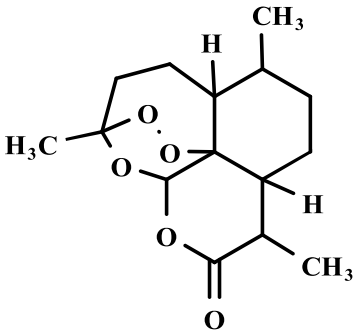

Figure 1.1. Chemical structures of avermectins and analogs (A), and artemisinin (B).

Despite wonderful history of natural product-based drug discovery, the trends in drug discovery have moved towards synthetic compounds in the early 90's after the advancement of high-throughput screening of compound (synthetic) libraries. The difficulty in developing library of small molecule analogs due to great structural complexity, lack of efficient de-replication methodologies, and time consuming purification steps argue against the compatibility with high-throughput screening in natural product-based drug discovery (Gonzalez-Sabin, 2012). However, some innovative approaches such as liquid chromatography with UV/VIS diode array detection coupled with ESI^+/ESI-time-of-flight mass spectroscopy (MS), high performance liquid chromatography (HPLC) bioactivity profiling-microtiter plate technique hyphenated with capillary probe nuclear magnetic resonance (NMR) spectroscopy could able to redirect the interest to some extent toward natural product-based drug discovery (Lang et al., 2008; Nielsen et al., 2011). In the past, natural product-based drug discovery has been time consuming especially in the process of structure elucidation and in the bioassay of limited number of sample at a time. However, introduction of sophisticated chromatographic and spectroscopic techniques has accelerated the drug discovery process from natural products. Modern equipments such as HPLC, higher magnetic field-strength NMR, capillary NMR and robotics to automate high-throughput bioassays accelerated the pathway of lead discovery from natural products even in minute quantity. The conjugation of spectroscopy with chromatography ("hyphenated" techniques) such as LC-NMR, LC-NMR-MS, LC-solid phase extraction (SPE)-NMR, and LC-SPE-NMR-MS further speed up the identification of scaffolds present within complex mixture of crude natural product (Corcoran and Spraul, 2003; Lewis et al., 2005; Sandvoss et al., 2005; Pham et al., 2005). Koehn and Carter have pointed out some unique features of the phytochemicals viz. higher number of chiral centers, more steric complexity, higher number of oxygen atoms, lower ratio of

aromatic ring atoms: total heavy atoms, higher number of solvated H-bond acceptors and donors, grater molecular rigidity, broader distribution of molecular properties, and diversity in ring systems (Koehn and Carter, 2005). These distinctive features of nature-derived small molecules could impart challenges for the researchers to develop analogs with improved therapeutic efficacy, pharmacokinetic properties, and less toxicity. Therefore, the main focus of the natural product researchers is often directed toward identifying small molecule leads which are therapeutically active in their original forms.

1.3. The approaches of plant drug research

The research in drug discovery from medicinal plants involves a multilayered approach combining botanical, phytochemical, biological, and molecular techniques. Selection of plant species is a crucial step in plant-based drug discovery. Based on extensive ethnomedicinal survey followed by comprehensive literature review the plant species is chosen for drug discovery process. The selected plant is then collected and authenticated with the involvement of a Taxonomist. The plant is then extracted with suitable solvent, fractionated, and subjected to lead discovery process either employing bioassay guided fractionation or by random isolation of

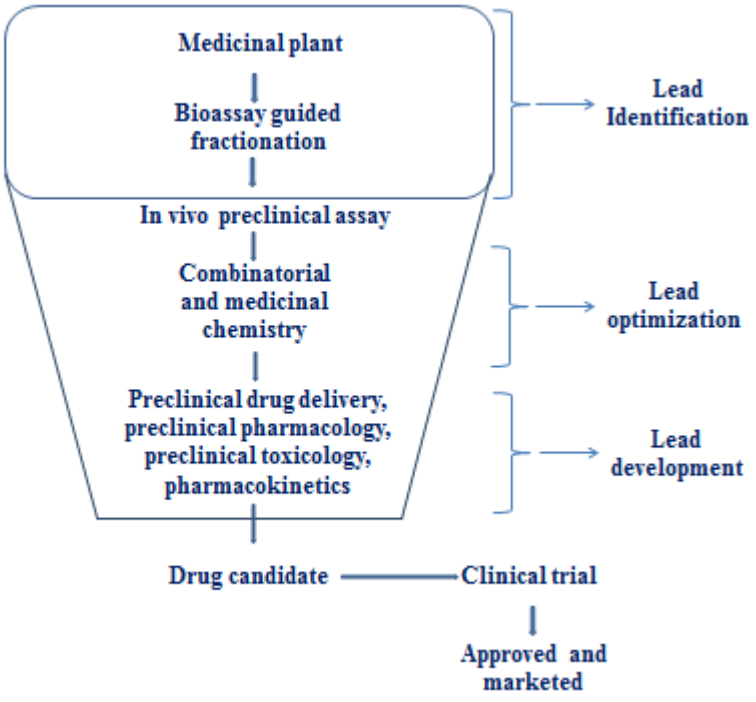

Figure 1.2. A schematic flow of generic approach of medicinal plant-based drug development (Koehn and Carter, 2005).

phytochemicals followed by preclinical assays. Lead identification is the first step in a lengthy drug discovery process (Balunas and Kinghorn, 2005). Lead optimization involving combinatorial and medicinal chemistry is the second step of drug discovery process. Finally, the drug candidate is developed employing preclinical drug delivery, pharmacology, toxicology, pharmacokinetics evaluations (Balunas and Kinghorn, 2005). Finally, the drug candidate is subjected to clinical trial and approved molecule is a natural product-derived drug. A consideration attention is paid to find out the molecular mechanism involving different biological and molecular techniques in lead development process. A schematic flow of typical medicinal plant-based drug discovery has been depicted in figure 1.2. However, this drug discovery is very time consuming and complicated process as compared to the drug discovery from the library of synthetic agents. The process of natural product-based drug discovery requires more time as compared with synthetic drugs. However, the recent advancement in separation methods, spectroscopic techniques, robotic-based high throughput bioassays, and other biochemical analytical techniques will surely accelerate drug discovery process from medicinal plants. Advancement in the knowledge of molecular mechanisms, cell biology and genomics helps to identify different molecular targets in a disease pathogenesis. Therefore, it is now easier to design in vitro cell based or enzymatic assay for a particular target disease for further execution of high throughput bioassays for lead identification. Despite it is challenging to employ high throughput screening in natural product-based drug discovery, but techniques like HPLC bioactivity profiling via high throughput bioassays-microtiter plate technique hyphenated with capillary probe NMR ensures rapid lead identification from natural products.

Conjugation of chemical process in natural product-based drug discovery often found to be advantageous over generic phytochemical approach (Koehn and Carter, 2005). In this approach, natural product is extracted, concentrated, fractionated and purified to yield bioactive molecule preferably a single bioactive scaffold. The known compounds are avoided to avoid the replication of earlier observation. LC-MS systems and natural-product databases could greatly aid to exclude the process of dereplication (Strege, 1999). De novo structure elucidation is done by advanced spectroscopic techniques. The novel bioactive compounds were screened on the basis of activity profile to meet with the required criteria for potency and selectivity. The primary structure-activity relationship (SAR) studies are performed and the lead optimization process is further intensified. Once the possibility of regulating biological response via preliminary chemical modification is established, the lead is subsequently processed toward additional optimization by

traditional medicinal chemistry. Figure 1.3. depicts involvement of chemical methods lead discovery from natural products.

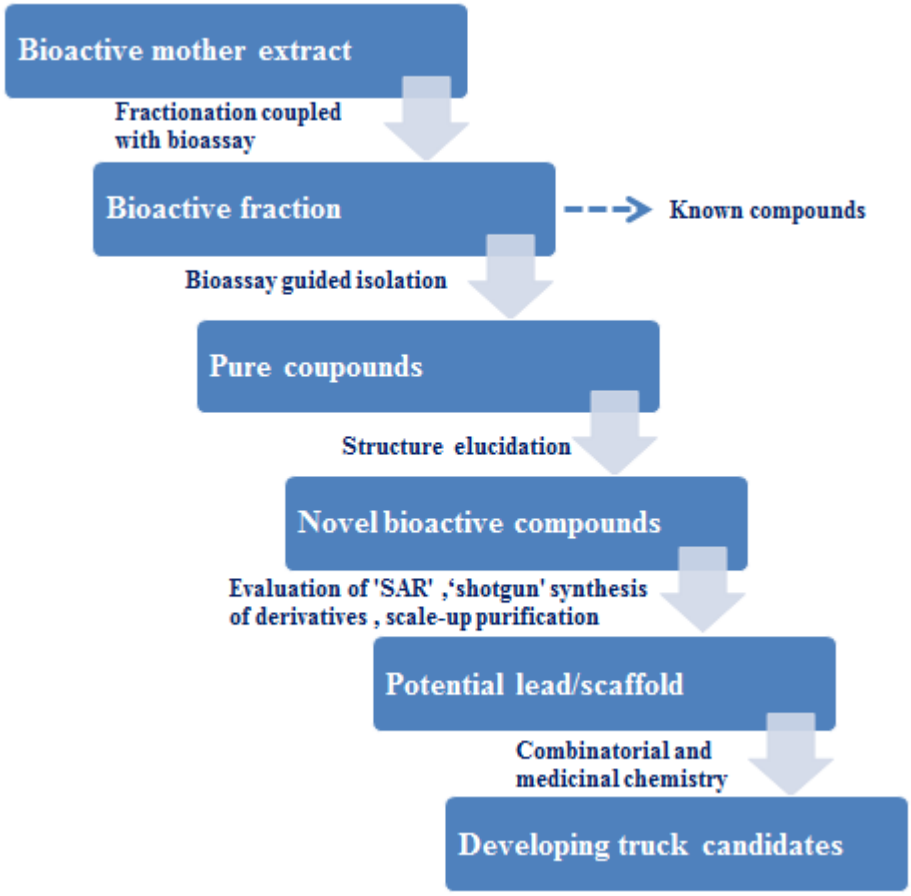

Figure 1.3. Chemical approach in natural product-based drug discovery.

1.4. Phytotherapeuticals, alternative to phytochemicals as the therapeutic intervention

Phytotherapeutic approach is more traditional approaches, which relies on traditional knowledge and use medicinal plants as therapeutic intervention. Phytotherapy represents a pragmatic approach for herbal practitioners employing evidenced based medicines as therapeutic agents. Phytotherapy intends medical uses of plants, extracts, fractions, tinctures, and polyherbals for therapeutic purposes (Calixto, 2000). Phytotherapeutic agents are not normally employed as emergency drugs as these normally do not possess an immediate action (Akerele, 1993; Calixto, 2000).Phytotherapeuticals generally are not evaluated in controlled clinical trials or in rigorous biomedical studies. In some countries, traditional wisdom is considered sufficient to license

phytotherapeuticals as medicines, while in other countries, phytotherapy is considered as a form of traditional/folklore therapy. Development of phytotherapeuticals commonly follows reverse pharmacological approach (Surah, 2011). Generally, rational drug discovery either from chemical libraries or from natural product is extremely expensive and time consuming, and critically inefficient (Surah, 2011). Additionally, post-marketing failures of hit drugs is a major anxiety

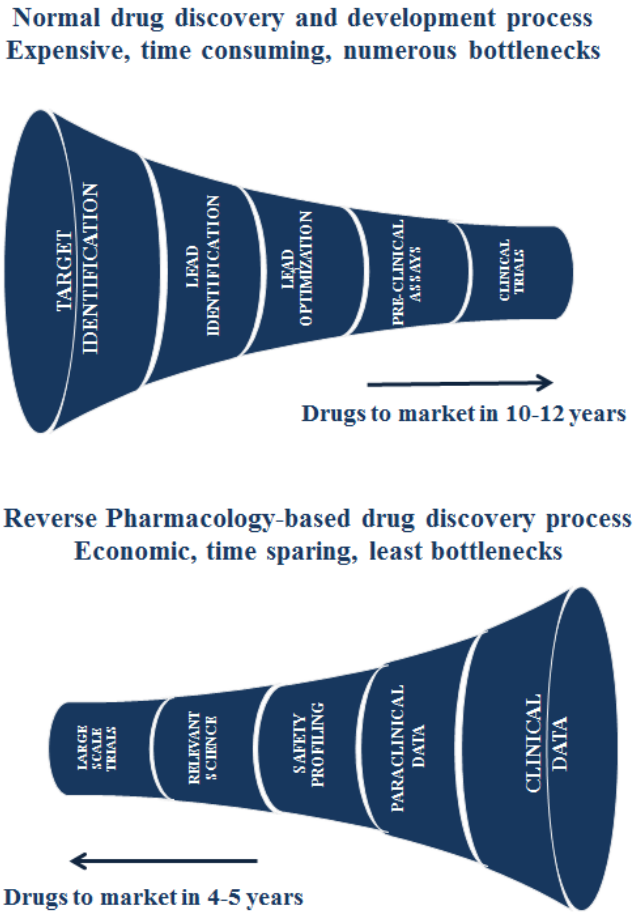

Figure 1.4. Comparison between rational and reverse pharmacology-based drug discoveries.

for pharmaceutical industries (Surah, 2011). Therefore, Paradigm in drug development is shifting towards reversing the rational drug discovery path. Ethnopharmacology and traditional medicines appear to be a re-emerging drug discovery tool, which follow reverse pharmacology approach (Figure 1.4). The noticeable feature in this approach is the documented clinical data in traditional literature. The integration between traditional knowledge and applications of modern scientific tools ensures to deliver better and safer phytotherapeuticals (Patwardhan and Mashelkar, 2009).

The traditional wisdom-inspired reverse pharmacology communicates to reverse the rational 'laboratory-to-clinic' method of drug discovery to 'clinic-to-laboratories' (Patwardhan et al., 2008). It is an economic and time sparing method of drug discovery. Advancement of modern molecular techniques and sophisticated analytical tools ensure to deliver safe, therapeutically defined, standardized, and reproducible quality phytotherapeutic agents. However, critics have still a narrow view on phytotherapy due to treatment with complex mixture, where many are unknown. On the other hand, herbalists claimed that the multifactorial pathogenesis in a disease would be only treated with multicomponent phytotherapeuticals to achieve multimodal therapeutic intervention. Anyhow, integration between the legacy of traditional medicine and modern scientific application can accelerate the development of novel phytotherapeuticals with excellent efficacy with minimal toxicity. It has been reported that about 70% of the physicians in France and Germany frequently prescribe phytotherapeutic agents (Pal and Shukla, 2003). India is one of the countries having long successful history of herbalism and most of the Indians primarily rely on herbal medicines in their primary healthcare (Sen and Chakraborty, 2017). Aspecton®, an authorized oral drops containing a specific thyme extract (KMTv24497), has been found to be effective against human rhinovirus serotype 1A and influenza A virus (Lenza et al., 2018). Mistletoe, a *Viscum album* L. extract (Iscador) has been used as a phototherapeutic agent used in the treatment in cancer in various European countries (Maldacker, 2006). The standardized ginkgo (*Ginkgo biloba* L.) extract (EGb 761) containing ~24% flavonoid glycosides has been extensively used in the treatment of early-stage Alzheimer's disease, vascular dementia, claudication, and vascular tinnitus (Gertz and Kiefer, 2004; Reitz et al.; 2012). Diabrid, poly herbal antidiabetic formulation comprising *Gymnema sylvestre*, *Momordica charantia*, *Eugenia jambolana*,*Trigonella foenum-graeceium* extracts is under clinical trial in India (Aslam et al., 2016). With the growing interest of patients towards herbal therapy, US Food & Drug Administration (FDA) has relaxed their recommendations in selling of herbal supplements (Gottlieb, 2000). Over last decade, a considerable number of researchers involved in drug development mainly focus in developing phytotherapeuticals against different ailments (Aslam et al., 2016).

1.5. Origin of research problem and objective

Since time immemorial, healing with traditional medicinal plants has found their usefulness against various ailments (Petrovska, 2012). The demand for plant-derived products is undoubtedly increasing around the world (Jamshidi-Kia et al., 2018). Despite plants remain indispensible source of therapeutic agents, the majority of plant species is yet to be examined.

Additionally, many of traditionally important medicinal plants are still to be scientifically explored and most of the scientifically explored medicinal plants were only screened on basis of preclinical 'Hippocratic' pharmacological assay of chemically undefined and unpurified crude extract to validate folklore claims (Mahwasane et al., 2013; Yuan et al., 2016). Therefore, beside investigation of unexplored species, it is equally important to execute a systematic approach with partially explored medicinal plants via scientific validation of folklore claims employing preclinical assay couple with molecular approach to find out the therapeutic mechanism, thorough phytochemical analysis and lead identification.

In this thesis, it has been attempted to represent a comprehensive drug development research with *Sansevieria roxburghiana* Schult. & Schult. F. (Family: Agavaceae) rhizome. *S. roxburghiana* is a traditional medicinal plant mentioned in the traditional literatures of Indian subcontinent, Myanmar, and tropical Africa (Haldar et al., 2010a; Haldar et al., 2010b; Saravanan et al., 2015). The plant is traditionally used as cardiotonic, expectorant, febrifuge, purgative, antidiabetic, tonic, anti-inflammatory, and anti-rheumatic (Obydulla, 2016). *S. roxburghiana* rhizome exhibited antitumor (Haldar et al., 2010a), antidiabetic (Haldar et al., 2010b), antioxidant (Haldar et al., 2010b), and antimicrobial properties (Sethi, 2013; Sardessai et al., 2013); whole plant also possesses antimicrobial (Philip et al., 2011a; Philip et al., 2011b), analgesic (Roy et al., 2012), antioxidant (Roy et al., 2012). However, the biological evaluations have been restricted within observational data. Researchers did neither highlight any mechanistic insight nor attempt to correlate the activities with respect to the phytochemicals. Therefore, their claims may only serve as scientific validation of folklore claims rather than to establish any justified scientific conclusion. Haldar and co-workers reported anti-diabetic effect of the crude extract of *S. roxburghiana* rhizome against streptozotocin-induced type 1 diabetic rats (Haldar et al., 2010b). However, their claim failed to fetch any conclusive evidence regarding the mechanism and the scaffold/s responsible for anti-diabetic effect. Secondly, the selection of type 1 animal model of diabetes is not very substantial for screening of an oral hypoglycemic agent. Considering the aforementioned opinions, it has been aimed to find out the protective effect of *S. roxburghiana* rhizome against experimentally induced type 2 diabetes and associated micro-vascular complication (cardiomyopathy) in rats. It was further envisioned to establish the molecular mechanism behind the pharmacological effect. Finally, the bioactive scaffold has been identified in *S. roxburghiana* rhizome as the conclusive evidence.

The primary objective of this work was scientific exploration of anti-diabetic activity of *S. roxburghiana* rhizome and to identify bioactive scaffold for the said activity. Considering the

folklore claim of anti-oxidant and anti-inflammatory effects of *S. roxburghiana* rhizome, it has been intended to evaluate the prophylactic effect of *S. roxburghiana* rhizome against diabetes-mediated micro-vascular complication in the cardiac tissues. Finally, it has been anticipated to reveal mechanistic insights behind the protective effect of crude extract and bioactive scaffold. Several scientific tools viz. pharmacology, toxicology, biochemistry, molecular biology, genetics, and phytochemistry have been employed to accomplish the plan of work.

The research work of this thesis has been represented as follows:

- Phytochemical analysis of *S. roxburghiana* rhizome;
- Toxicity studies of *S. roxburghiana* rhizome and protocatechuic acid (identified scaffold);
- Protective role of *S. roxburghiana* rhizome against type 2 diabetes and diabetic cardiomyopathy;
- Protective role of protocatechuic acid against type 2 diabetes and diabetic cardiomyopathy.

References

Akerele O. Summary of WHO guidelines for the assessment of herbal medicines. Herbal Gram. 1993;28:13-19.

Aslam MS, Ahmad MS, Mamat AS, Ahmad MZ, Salam F. An update review on polyherbal formulation: a global perspective. Sys Rev Pharm. 2016;7:35-41.

Atanasov AG, Waltenberger B, Pferschy-Wenzig E-M, Linder T, Wawrosch C, Uhrin P, Temml V, Wang L, Schwaiger S, Heiss EH, Rollinger JM, Schuster D, Breuss JM, Bochkov V, Mihovilovic MD, Kopp B, Bauer R, Dirsch VM, Stuppner H. Discovery and resupply of pharmacologically active plant-derived natural products: A review. Biotechnol Adv. 2015;33:1582-1614.

Balunas MJ, Kinghorn AD. Drug discovery from medicinal plants. Life Sci. 2005;78:431-441.

Calixto JB. Efficacy, safety, quality control, marketing and regulatory guidelines for herbal medicines (phytotherapeutic agents). Braz J Biol Res. 2000;33:179-189.

Chakraborty R. Revival, modernization and integration of Indian traditional herbal medicine in clinical practice: Importance, challenges and future. J Tradit Complement Med. 2017;7:234-244.

Corcoran O, Spraul M. LC-NMR-MS in drug discovery. Drug Discov Today. 2003;8:624-631.

Dias DA, Urban S, Roessner U. A Historical Overview of Natural Products in Drug Discovery. Metabolites. 2012; 2:303-336.

Gertz HJ, Kiefer M. Review about *Ginkgo biloba* special extract EGb 761 (Ginkgo), 2004;10:261-264.

Gonzalez-Sabin J. Natural products: back to the future in drug discovery. Biochem Pharmacol (Los Angel). 2012;1:e112.

Gottlieb S. US relaxes its guidelines on herbal supplements. BMJ, 2000;320:207.

Haldar PK, Kar B, Bala A, Bhattacharya S, Mazumder UK. Antitumor activity of *Sansevieria roxburghiana* rhizome against Ehrlich ascites carcinoma in mice. Pharm Biol. 2010a;48:1337-1343.

Haldar PK, Kar B, Bhattacharya S, Bala A, Kumar SRB. Antidiabetic activity and modulation of antioxidant status by *Sansevieria roxburghiana* rhizome in streptozotocin-induced diabetic rats. Diabetologia Croatica. 2010b;39:115-123.

Jamshidi-Kia F, Lorigooini Z, Amini-Khoei H. Medicinal plants: Past history and future perspective. J Herbmed Pharmacol. 2018;7:1-7.

Katiyar C, Gupta A,Kanjilal S Katiyar S. Drug discovery from plant sources: An integrated approach. Ayu. 2012;33:10-19.

Klohs MW, Draper MD, Keller F, Petracek FJ. The Isolation of Reserpine from *Rauwolfia canescens* Linn. J Am Chem Soc. 1954;76:1381-1381.

Koehn FE, Carter GT. The evolving role of natural products in drug discovery. Nat Rev Drug Discov. 2005;4:206-220.

Lang G, Mayhudin NA, Mitova MI, Sun L, van der Sar S, Blunt JW, Cole AL, Ellis G, Laatsch H, Munro MH. Evolving trends in the dereplication of natural product extracts: new methodology for rapid, small-scale investigation of natural product extracts. J Nat Prod. 2008;71:1595-1599.

Lenza E, Müllera C, Mostafa A, Dzieciolowski J, Kanrai P, Dam S, Cwientzek U, Prenner L-N, Pleschka S. Authorised medicinal product Aspecton® Oral Drops containing thyme extract KMTv24497 shows antiviral activity against viruses which cause respiratory infections. J Herb Med. 2018; Doi: 10.1016/j.hermed.2018.02.003.

Lewis RJ, Bernstein MA, Duncan SJ, Sleigh CJ. A comparison of capillary-scale LC-NMR with alternative techniques: spectroscopic and practical considerations. Magn Reson Chem. 2005;43:783-789.

Mahwasane ST, Middleton L, Boaduo N. An ethnobotanical survey of indigenous knowledge on medicinal plants used by the traditional healers of the Lwamondo area, Limpopo province, South Africa. S Afr J Bot. 2013;88:69-75.

Maldacker J. Preclinical investigations with mistletoe (*Viscum album* L.) extract Iscador. Arzneimittel-Forschung. 2006;56:497-507.

Mishra BB, Tiwari VK. Natural products: an evolving role in future drug discovery. Eur J Med Chem. 2011;46:4769-4807.

Moudi M, Go R, Yien CYS, Nazre M. Vinca Alkaloids. Int J Prev Med. 2013;4:1231-1235.

Nielsen KF, Månsson M, Rank C, Frisvad JC, Larsen TO. Dereplication of microbial natural products by LC-DAD-TOFMS. J Nat Prod. 2011;74:2338-2348.

Obydulla O. *Sansevieria roxburghiana* Schult. & Schult. F., Agavaceae: phytochemistry, traditional uses and its pharmacological activities-a review. World Sci News 2016;59:24-34.

Pal SK, Shukla Y. Herbal medicine: current status and the future. Asian Pacific J Cancer Prev. 2003;4:281-288.

Patwardhan B, Vaidya ADB, Chorghade M, Joshi SP. Reverse pharmacology and systems approaches for drug discovery and development. Curr Bioact Compd. 2008;4:201-212.

Patwardhan B, Mashelkar RA. Traditional medicine-inspired approaches to drug discovery: can Ayurveda show the way forward? Drug Discov Today. 2009;14:804-811.

Petrovska BB. Historical review of medicinal plants' usage. Pharmacogn Rev. 2012;6:1-5.

Pham LH, Vater J, Rotard W, Mügge C. Identification of secondary metabolites from *Streptomyces violaceoruber* TU22 by means of on-flow LC-NMR and LC-DAD-MS. Magn Reson Chem. 2005;43:710-723.

Philip D, Kaleena PK, Valavittan K, Kumar GCP. Phytochemical screening and antimicrobial activity of *Sansevieria roxburghiana*. Middle-East J Sci Res. 2011a;10:512-518.

Philip D, Kaleena PK, Valavittan K. GC-MS analysis and antibacterial activity of chromatographically separated pure fractions of leaves of *Sansevieria roxburghiana*. Asian J Pharm Clin Res. 2011b;4:130-133.

Projan SJ, Gill D, Lu Z, Herrmann SH. Small molecules for small minds? The case for biologic pharmaceuticals. Expert Opin Biol Ther. 2004;4:1345-1350.

Pye CR, Bertin MJ, Lokey RS, Gerwick WH, Linington RG. Retrospective analysis of natural products provides insights for future discovery trends. Proc Natl Acad Sci USA. 2017;114:5601-5606.

Roy J, Kuddus M, Begum B, Hasan C. Evaluation of analgesic, cytotoxic and antioxidant activities of *Sansevieria roxburghiana* Schult. and Schult. f. Asian Pac J Trop Biomed. 2012; 2012:S723-S726.

Sandvoss M, Bardsley B, Beck TL, Lee-Smith E, North SE, Moore PJ, Edwards AJ, Smith RJ. HPLC-SPE-NMR in pharmaceutical development: capabilities and applications. Magn Reson Chem. 2005;43:762-770.

Saravanan KS, Madhavan V, Yoganarasimhan S. Pharmacognostical studies on the Rhizome of *Sansevieria roxburghiana* Schult. & Schult. f.-a botanical source for Murva-an Ayurveda drug. Spatula DD. 2015;5:161-169.

Sardessai Y, Angle GP, Joshi A, Bhobe M. Significant antimicrobial activity exerted by the ethanolic extract of rhizomes of *Sansevieria roxburghiana*. Int J Pharm Photon. 2013;104:327-334.

Schulz, V., Hänsel, R. & Tyler, V.E. (2001) Rational Phytotherapy. A Physician's Guide to Herbal Medicine, 4th Ed., Springer-Verlag, Berlin, Germany.

Sertürner FW. Über das Morphium, eine neue salzfähige grundlage, und die mekonsäure, als hauptbestandteile des opiums. Ann Phys. 1817;25:56-90.

Sethi P. Biological characterization of the rhizome of *Sansevieria roxburghiana* Schult. & Schult. F. (Agavaceae). J Med Plant Res. 2013;7:1201-1203.

Shen B. A new golden age of natural products drug discovery. Cell. 2015;163:1297-1300.

Stratton CF, Newman DJ, Tana DS. Cheminformatic comparison of approved drugs from natural product versus synthetic origins. Bioorg Med Chem Lett. 2015;25:4802-4807.

Strege MA. High-performance liquid chromatographic-electrospray ionization mass spectrometric analyses for the integration of natural products with modern high-throughput screening. J Chrom B. 1999;725;67-68.

Surah Y-J. Reverse pharmacology applicable for botanical drug development-inspiration from the legacy of traditional wisdom. J Tradit Complement Med. 2011;1:5-7.

Yuan H, Ma Q, Ye L, Piao G. The traditional medicine and modern medicine from natural products. Molecules 2016;21:559.

2.1. Introduction

A vigilant and comprehensive literature review is indispensable for executing any research at any stage. Review of literature encompasses systematic identification of all the relevant information related to the research to be executed. The principal feature of literature review includes comprehensive interpretation of all existing literatures available till date to find out any gap/problem, which would be addressed through the research. Similarly, the initial point in designing a plant-based drug discovery research scheme is a complete literature review, including the traditional uses, scientifically validated pharmacological activities, reported phytochemical profile (if any), and mechanistic insight (if any). A literature review should recognize the up-to-date evidence of efficacy and safety of herbal medicine for the proposed therapeutic intervention. Since the clinical data serve as a primary criterion in plant-based drug discovery, the data obtained from experienced traditional practitioners/herbalists would serve as the principal documental evidence to select a plant species for further research. However, lack of large number of clinical trials makes it difficult to achieve meta-analysis data for herbal drugs. Additionally, the efficacy of a specific treatment may vary with the skill and experience of traditional practitioners. Therefore, scientific validation of folklore claim also serves as an indispensible database for selecting of a research plant. In present time, World Wide Web (Web) is a prevalent medium to disseminate information within a short time (Poornisri and Priya, 2015). Personalized Web searching of PubMed, Scopus, Web of Science, and Google Scholar could provide relevant published information till date (Falagas et al., 2008; Poornisri and Priya, 2015). After selection of a plant species and target disease, it is important to design a research approach. Large number of existing literature would aid in formulating a research approach. Newer concepts are often preferred over classical approaches. It has been observed that, present day drug discovery programme principally target enzymes, signal proteins or mRNAs or even microRNAs in a disease pathogenesis rather than overall effect in a disease model (Zhang et al., 2010; Bull and Doig, 2015; Connelly et al., 2016; Bhattacharjee et al., 2017). Thorough understanding of disease pathogenesis would aid to frame and execute a plan of work. Up-to-date literature review can help to give a better impression of pathogenic pathway of the targeted disease. Finally, detailed literature review of phytochemicals is a necessary requisite to exclude/include the process of de-replication (Strege, 1999). Considering the aforementioned arguments, a thorough literature survey has been conducted before and throughout the tenure of research.

Sansevieria is a genus under Agavaceae family comprising ~60 species of flowering monocot herbs native to Africa, Arabian Peninsula, Madagascar and southern Asia (Klimko et al., 2017).

Sansevieria roxburghiana Schult and Schult F. is an ornamental herb under genus *Sansevieria* commonly known as 'Indian bowstring hemp' (Rajalekshmi et al., 2015). The whole plant is traditionally used as cardiotonic, expectorant, febrifuge, purgative, tonic, and in rheumatism (Rajalekshmi et al., 2015; Rajalekshmi et al., 2017). *S. roxburghiana* rhizome is mucilaginous and is used in consumptive complaints, chronic coughs and cold, and in ear pain (Rajalekshmi et al., 2015; Rajalekshmi et al., 2015). *S. roxburghiana* rhizome has been reported to possess antitumor (Haldar et al., 2010a), antidiabetic (Haldar et al., 2010b), antioxidant (Haldar et al., 2010b), analgesic (Obydulla, 2016), and antimicrobial properties (Sethi, 2013; Sardessai et al., 2013). The plant has been reported to contain alkaloids, flavonoids, homoisoflavonoids, tannins, saponins, carotenoids, fatty acids, flavonoid glycosides, and phytosterols (Obydulla, 2016).

2.2. Botanical hierarchy (Obydulla, 2016; http://plants.usda.gov)

Kingdom: Plantae

Subkingdom: Tracheobionta

Superdivision: Spermatophyta

Division: Magnoliophyta

Class: Liliopsida

Subclass: Liliidae

Order: Liliales

Family: Agavaceae

Genus: *Sansevieria* Thunb.

Species: *Sansevieria roxburghiana* Schult. & Schult. F.

2.3. Synonyms (Obydulla, 2016; http://indiabiodiversity.org/biodiv/species/show/33281)

Acyntha roxburghiana Schult. & Schult. F. Kuntze

Cordyline roxburghiana Schult. & Schult. F. Merr.

Sansevieria zeylanica Roxb.

2.4. Common names

Indian bowstring hemp, Bowstring hemp.

2.5. Vernacular names

English: Indian bowstring hemp

Bengali: Lankh hi pang

Hindi: Marul, Marahri, Murva

Kannada: Heggurutike

Malayalam: Hatukapel

Marathi: Murhari

Sanskrit: Muruva

Sanskrit: Murva

Tamil: Marul-kalang

Telugu: Ishaura-koda-udr

2.6. Distribution

S.roxburghiana is mostly distributed in the tropical area of southern and southeastern Asia, tropical Africa (Figure 2.1.). The species is abundant in eastern coast of India, Sri Lanka, Indonesia, Malaysia, Bangladesh, and Myanmar. *S. roxburghiana* arises wild and also cultivated as fiber plant in India. In addition, it also frequently grows as an ornamental plant in other places. The plant has been introduced in Mauritius.

Figure 2.1. The distribution of *S.roxburghiana* in the worldmap.

2.7. Morphological description

S. roxburghiana is a stem less, evergreen, and perennial monocot-herb with stout rootstock. The leaves are simple, green, and transversely marked with darker green lines on both sides (Figure 2.2.). The leaves grow flat, strap-shaped/narrowly lanceolate, with subulate point (Figure 2.2.). The leaves are generally 50-75 cm long; however, leaves can grow up to 1.2 m long. The adult leaves are ascending and slightly re-curving, deeply concave channeled down the face, rounded or very obtusely keeled on the back. The leaf surface is generally smooth, but the lower surface is slightly rough. *S. roxburghiana* produces light-green six-stellate flowers during autumn. The raceme spike-like flowering stem grows 60 cm or more long and the flowers come in clusters of

pedicels (6-9 cm) and jointed near the middle, with the tube (6-7.5 mm) and lobes (8.5- 9.5 mm) (Figure 2.2.). Fruits appear as globose berries, indehiscent with 1-3 globose seeds. Rootstock are short and rhizomous, often stoloniferous (Figure 2.2.). Creeping rhizome is a characteristic feature of *S. roxburghiana* (Figure 2.2.) (http://eol.org/data_objects/4962632; Huxley, 1992).

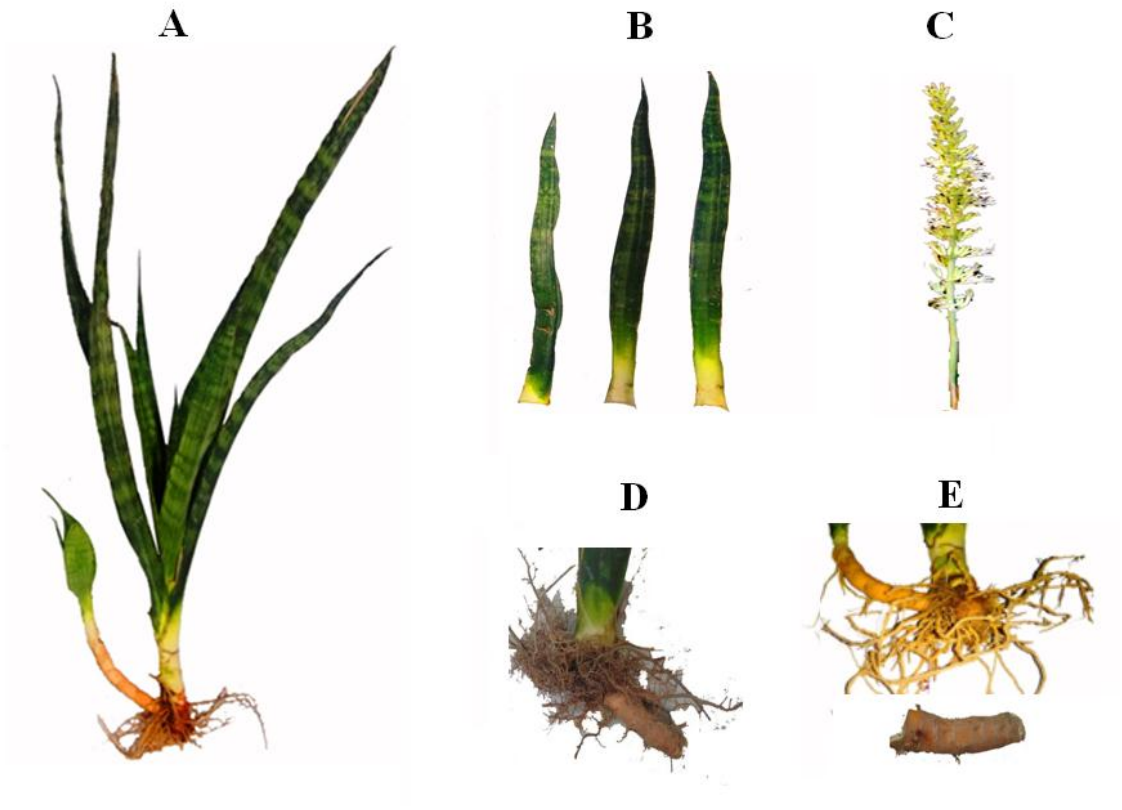

Figure 2.2. The morphological features of *S. roxburghiana*. A. The whole plant; B. Simple strap-shaped/narrowly lanceolate leaves; C. Raceme spike-like flowering stem, D. Short and stout rootstock; E. Creeping rhizome.

2.8. Chemical Constituents

S. roxburghiana contains alkaloids, flavonoids, homoisoflavonoids, tannins, saponins, carotenoids, fatty acids, flavonoid glycosides, and phytosterols (Obydulla, 2016). 16 bioactive compounds have been reported in GC-MS analysis of methanolic extract of *S. roxburghiana* leaves (philip et al., 2011a). The compounds are dodecanoic acid (**1**), diethyl phthalate (**2**), 6-methyl-1-octanol (**3**), 2-propyldecan-1-ol (**4**), 2(4H)-benzofuranone (**5**), 3,3-dimethylhexanal (**6**), di-isobutyl phthalate (**7**), 3,4-dimethoxy benzoic acid anhydride (**8**), 1,2-benzenedicarboxylic acid bis(2-ethylhexyl) ester (**9**), palmitaldehyde diallyl acetal (**10**), delta undecalactone (**11**), 1-butyl,2-(8-methylnonyl) phthalate (**12**), n-hexadecanoic acid (**13**), 6,10,14-trimethyl-2-pentadecanone

(**14**), 2,5-dimethoxy benzhydrazide (**15**), and methyl hexadecanoate (**16**) (philip et al., 2011a). The plant is found to contain a triterpene, lupeol (**17**), and a homoisoflavonoid, cambodianol (**18**) (Figure 2.3.) (Roy et al., 2013). It also contains an alkaloid, sansevierine (Dodge, 1897; Obydulla, 2016).

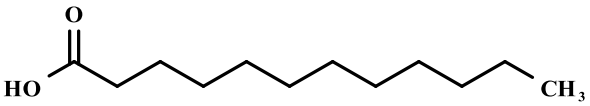

1

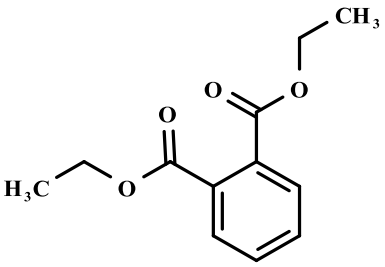

2

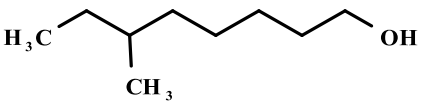

3

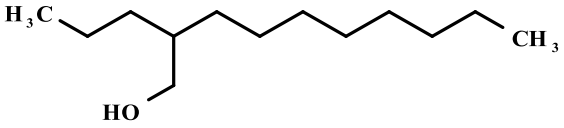

4

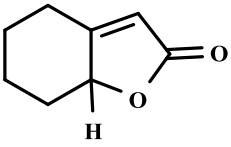

5

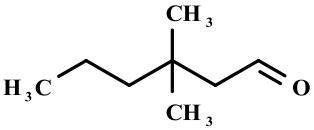

6

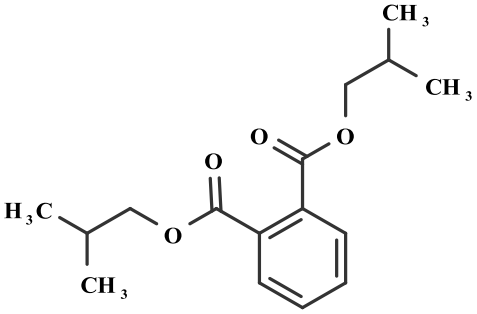

7

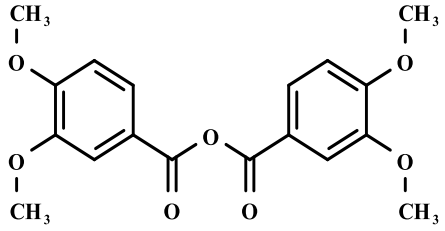

8

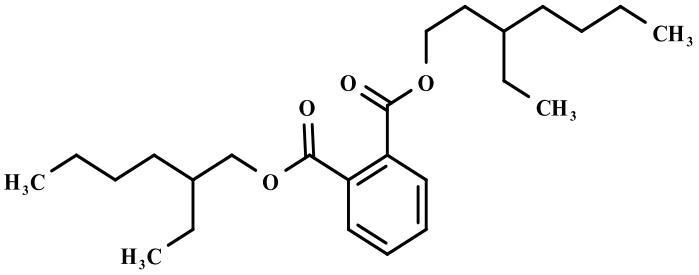

9

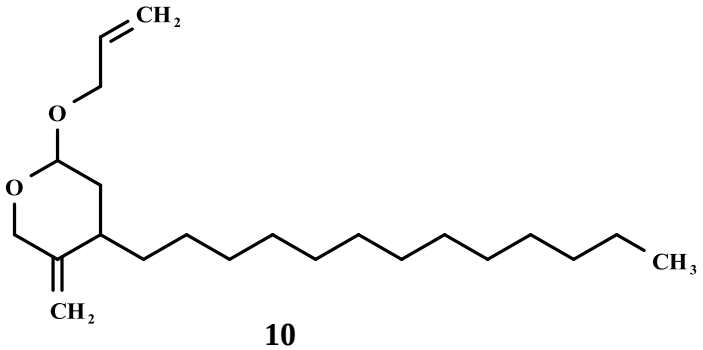

10

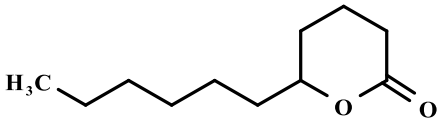

11

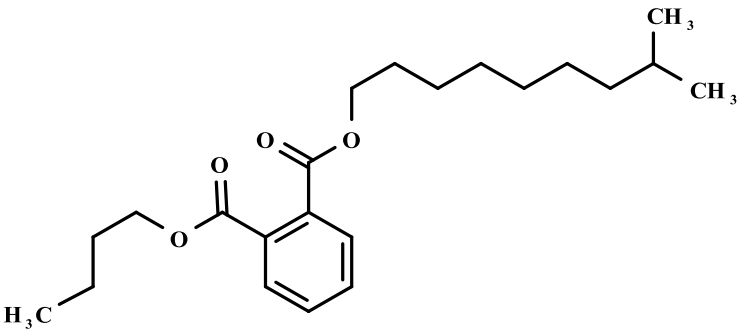

12

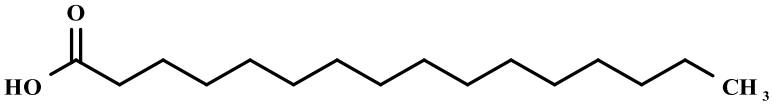

13

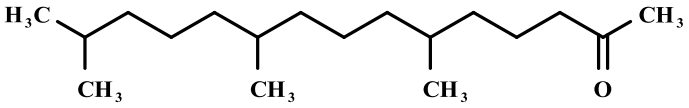

14

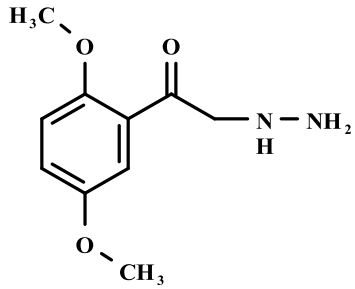

15

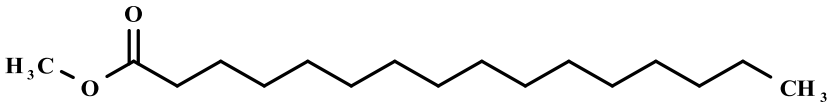

16

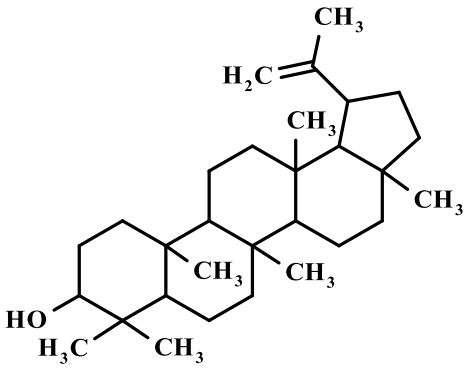

17

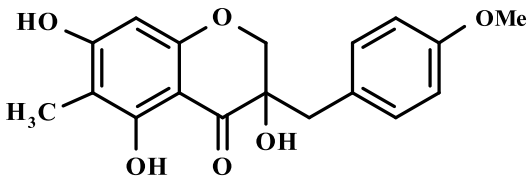

18

Figure 2.3. The structures of identified compounds in *S. roxburghiana*.

2.9. Ethnomedicinal uses

S. roxburghiana has been traditionally used for the treatment of different diseases. The whole plant of *S. roxburghiana* is traditionally used as cardiotonic, expectorant, febrifuge, purgative, tonic (Dhiman, 2006; Pulliah, 2006; Khare, 2007). Additionally, it is possessing ethnomedicinal significance in glandular enlargement, in bone setting, and in rheumatism (Dhiman, 2006; Pulliah, 2006; Khare, 2007). The root is used as a febrifuge in snake bite and hemorrhoids (Khan & Khanum, 2005; Kirtikar & Basu, 1935). Rhizome of the plant is used in consumptive complaints, cough, common cold, toothache, and ear pain (sethi, 2013). Leaves are used to treat pimples, skin diseases, and asthma (singh et al., 2014). The roasted leaves are emollient. In southern Western Ghats of India, Kani tribes of Agasthiyarmalai biosphere reserve use the leaf of this plant for the treatment of ear pain and juice of rhizome for long standing coughs (Prakash et al., 2008). In Bangladesh, juice of the tender shoot is used to clear sticky phlegm from the throat of children; juice from young leaves is applied topically to treat ear infection.

2.10. Scientifically explored pharmacological activities

Literature review revealed that *S. roxburghiana* exhibit wide range of medicinal activities. The earlier researches with the plant were enlisted hereunder.

2.10.1. Anticancer activity

Hydroalcoholic extract of *S. roxburghiana* rhizome exhibited antitumor activity against Ehrlich Ascites Carcinoma (EAC) in Swiss albino mice (Haldar et al., 2010a). The extract could significantly reduce tumor volume, packed cell volume, and viable cell count and increased the life span of EAC bearing mice. Additionally, extract treatment significantly attenuate redox stress in EAC bearing mice.

2.10.2. Antimicrobial activity

The antimicrobial effect of various extracts of *S. roxburghiana* leaf and rhizome was determined by agar disk diffusion method. Methanol and acetone extracts of leaf revealed significant antimicrobial activity against Gram-positive bacteria, such as *Micrococcus luteus, Bacillus cereus, Enterococcus spp.,* and *Staphylococcus aureus* and Gram-negative bacteria, such as *Proteus vulgaris, Pseudomonas aeruginosa, Pseudomonas fluorescence, Salmonella typhi, Salmonella paratyphi, Klebsiella pneumoniae, Shigella sonnei,* and *Escherichia coli, fungal strains Cryptococcus* spp. and *Candida albican*. Ethyl acetate extract of rhizome also exhibited appreciable antimicrobial activity against most of the pathogens tested. The leaf extract showed better antimicrobial activity than rhizomes (Philip et al., 2011b). In another study, ethanolic extract of rhizome of *S. roxburghiana* showed antibacterial effect against Gram negative bacteria such as *Salmonella Typhi, Pseudomonas fluorescens, Pseudomonas aeruginosa* and *Escherichia coli* (Sethi, 2013).

2.10.3. Analgesic activity

Methanolic extract and all fractions of the whole plant of *S. roxburghiana* has been reported to exhibit significant peripheral analgesic activity. Analgesic activity was tested by acetic acid induced writhing model in mice. The ethyl acetate soluble fraction produced maximum writhing inhibition and the effect was comparable to that of standard drug, diclofenac sodium (Roy et al., 2012).

2.10.4. **Antioxidant activity**

Methanolic extract and all fractions of the whole plant of *S. roxburghiana* has been reported to possess radical scavenging and antioxidant activity. Antioxidant effect was measured by 1,1-diphenyl-2-picrylhydrazyl (DPPH) radical scavenging assay (Roy et al., 2012). Another report revealed that, methanol, acetone and ethyl acetate extracts of *S. roxburghiana* leaves exhibited strong radical (DPPH, NO) scavenging and antioxidant effects in a concentration-dependent manner. However, methanol extract showed better radical scavenging and antioxidant potentials as compared to acetone and ethyl acetate extracts due to presence of high quantity of alkaloids, sterols, flavonoids, and saponins in the methanol extract of *S. roxburghiana* leaves (Philip et al., 2012).

2.10.5. Antidiabetic activity

Hydroalcoholic extract of *S. roxburghiana* rhizome has been claim to exhibit antihyperglycemic and antihyperlipidemic effects in streptozotocin-induced type 1 diabetic rats (Haldar et al.,

2010b). The extract could significantly restore body mass, serum parameters, and endogenous redox status of diabetic rats to near normal status (Haldar et al., 2010b).

2.11. Discussion

Through the literature review, an overall picture of *S. roxburghiana* has been summarized. It has been found that *S. roxburghiana* rhizome possesses ethnomedicinal significance as anti-diabetic agent. Additionally, the crude extract of *S. roxburghiana* rhizome exhibited anti-hyperglycemic and anti-hyperlipidemic effects in streptozotocin-induced type 1 diabetic rats. However, their claim could not fetch any conclusive evidence regarding the mechanism and the scaffold/s responsible for anti-diabetic effect. Secondly, the selection of type 1 model of diabetes is not very convincing approach in the development of oral hypoglycemic agent/s. Considering the aforementioned opinions, the research proposal has been framed to evaluate protective effect and mechanism of *S. roxburghiana* rhizome against experimentally induced type 2 diabetes. Furthermore, the crude extract of *S. roxburghiana* rhizome possesses significant anti-oxidant and anti-inflammatory (evidenced from analgesic and anti-rheumatic activities) effects. Therefore, it has further aimed to find out the prophylactic mechanism of *S. roxburghiana* rhizome against a diabetic micro-vascular complication, diabetic cardiomyopathy. This drug discovery research mainly focus to identify target specific bioactive scaffold *S. roxburghiana* rhizome against diabetes and diabetic cardiomyopathy. The research frame has been designed on the basis of literature survey on *S. roxburghiana*. The experimental methods were premeditated on the basis of extensive literature review on molecular signaling involved in diabetic pathophysiology and the experimental methodologies related to this topic.

References

Bhattacharjee N, Dua TK, Khanra R, Joardar S, Nandy A, Saha A, De Feo V, Dewanjee S. Protocatechuic acid, a phenolic from *Sansevieria roxburghiana* leaves, suppresses diabetic cardiomyopathy via stimulating glucose metabolism, ameliorating oxidative stress and inhibiting inflammation. Front Pharmacol. 2017;8:251.

Bull SC, Doig AJ. Properties of protein drug target classes. PLoS One. 2015;10:e0117955.

Connelly CM, Moon MH, Schneekloth Jr JS. The emerging role of RNA as a therapeutic target for small molecules. Cell Chem Biol. 2016;23:1077-1090.

Dhiman AK. Ayurvedic drug plants, Dayal publishing house, New Delhi, 2006.

Falagas ME, Pitsouni EI, Malietzis GA, Pappas G. Comparison of PubMed, Scopus, Web of Science, and Google Scholar: strengths and weaknesses. FASEB J. 2008;22:338-342.

Haldar PK, Kar B, Bala A, Bhattacharya S, Mazumder UK. Antitumor activity of *Sansevieria roxburghiana* rhizome against Ehrlich ascites carcinoma in mice. Pharm Biol. 2010a;48:1337-1343.

Haldar PK, Kar B, Bhattacharya S, Bala A, Kumar SRB. Antidiabetic activity and modulation of antioxidant status by *Sansevieria roxburghiana* rhizome in streptozotocin-induced diabetic rats. Diabetologia Croatica. 2010b;39:115-123.

Huxley A. The new RHS dictionary of gardening. MacMillan Press, UK, 1992.

Khan IA, Khanum IA. Medicinal and aromatic plants of india, Ukkaz publications, Hyderabad, 2005.

Khare CP. Indian medicinal plants, an illustrated dictionary, Springer, Berlin, 2007.

Kirtikar KR, Basu BD. Indian medicinal plants, New Delhi, 1935.

Klimko M, Nowińska R, Wilkin P, Wiland-Szymańska J. pollen morphology of some species of the genus *Sansevieria petagna* (Asparagaceae). Acta Biol Cracov Bot. 2017;59/2:63-75.

Obydulla O. *Sansevieria roxburghiana* Schult. & Schult. F., Agavaceae: phytochemistry, traditional uses and its pharmacological activities-a review. World Sci News 2016;59:24-34

Philip D, Kaleena PK, Valavittan K. GC-MS analysis and antibacterial activity of chromatographically separated pure fractions of leaves of *Sansevieria roxburghiana*. Asian J Pharm Clin Res. 2011a;4:130-133.

Philip D, Kaleena PK, Valivittan K, Girish Kumar CP. Phytochemical screening and antimicrobial activity of *Sansevieria roxburghiana* Schult. and Schult. F. Middle-East J Sci Res. 2011b;10512-10518.

Philip D, Kaleena PK, Valivittan K. Antioxidant potential of *Sansevieria roxburghiana* Schult. and Schult. F. Asian J Pharm Clinical Res. 2012;5:166-169.

Poornisri K, Priya SR. A literature review on personalized web search. Int J Modern Trend Eng Res. 2015;2:473-479.

Prakash JW, Raja RDA, Anderson NA, Williams C, Regini GS, Bensar K, Jajeev R, Kirula S, Jeeva S, Das SCM. Ethnomedicinal plants used by Kani tribes of Agastiyarmalai biosphere reserve, Southern Western Ghats. Indian J Trad Knowledge. 2008;7:410-413.

Pulliah T. Encyclopedia of World Medicinal Plants. Regency publications, New Delhi, 2006.

Rajalekshmi M, Shreedhara CS, Lobo R, Setty MM. Quality Standards of Rhizome of *Sansevieria roxburghiana* Schult and Schult F. Adv Sci Lett. 2017;23:1767-1772.

Rajalekshmi M, Shreedhara CS, Lobo R. Quality control parameters of rhizomes of *Sansevieria roxburghiana* Schult & Schult F. Nat Prod Chem Res. 2015;3:6.

Roy J, Aktar F, Haq MR, Begum B. Hasan CM. A rare homoisoflavonoid cambodianol from *Sansevieria roxburghiana*. Asian J Chem. 2013;25:5113-5114.

Roy J, Kuddus M, Begum B, HasanC. Evaluation of analgesic, cytotoxic and antioxidant activities of *Sansevieria roxburghiana* Schult. and Schult. F. Asian Pac J Trop Biomed. 2012;2:S723-S726.

Sardessai Y, Angle GP, Joshi A, Bhobe M. Significant antimicrobial activity exerted by the ethanolic extract of rhizomes of *Sansevieria roxburghiana*. Int J Pharm Photon. 2013;104:327-334.

Sethi P. Biological characterisation of the rhizome of *Sansevieria roxburghiana* Schult. & Schult. F. (Agavaceae). J Med Plants Res. 2013;7:1201-1203.

Singh SK, Patel JR, Dubey PK, Thakur S. A review on antiasthmatic activity of traditional medicinal plants. Int J Pharm Sci Res. 2014;5:4109-4116.

Strege MA. High-performance liquid chromatographic-electrospray ionization mass spectrometric analyses for the integration of natural products with modern high-throughput screening. J Chrom B. 1999;725;67-68.

Zhang S, Chen L, Jung EJ, Calin GA. Targeting microRNAs with small molecules: between dream and reality. Clin Pharmacol Ther. 2010;87:754-758.

Web references

http://eol.org/data_objects/4962632

http://indiabiodiversity.org/biodiv/species/show/33281

http://plants.usda.gov

3.1. Introduction

Phytochemicals are generally non-nutrient secondary metabolites of plants, which are present in various parts of plants like leaves, wood, roots, rhizomes, bark, flowers, fruits, and seeds (Acamovic and Brooker, 2005; Nandagopalan et al., 2016). These continue to provide wonderful structural diversity and complexity in comparison to standard synthetic molecules, which presents excellent opportunity to discover novel therapeutic lead against different ailments (Dias et al., 2012). It has been reported that approximately one-half of all licensed and approved medicines are either directly obtained from natural products or their chemically modified forms (Kennedy and Wightman, 2011). Additionally, phytochemicals can also serve as drug precursors, drug prototypes, and pharmacological probes. The plant secondary metabolites can be categorized into different groups viz. alkaloids, terpenoids, carotenoids, flavanoids, tannins, glycosides etc. on the basis of their chemical structures, physico-chemical nature, composition, and/or the biosynthesis. Despite the principal interest in drug discovery still trust on synthetic chemistry methods in conjugation with molecular modeling and combinatorial chemistry, natural product-derived small molecules still continue to impress in their original forms as drugs, drug precursors, templates for synthetic modification, and pharmacological probes. Andrographolide, atropine, berberine, codeine, colchicine, digitoxin, ephedrine, etoposide, glycyrrhizin, papavarine, pilocarpine, reserpine, silymarin, taxol, vinblastine, vincristine etc. are few of many phytochemicals used in their original forms as drugs (Kong et al., 2003). Besides phytochemicals, the interest on phytotherapeuticals is also growing progressively over the past few decades. Flavocoxid (Primus Pharmaceuticals, US), a proprietary blend of natural flavonoids from *Scutellaria baicalensis* and *Acacia catechu*, is used as medical food for the therapeutic intervention of osteoarthritis (https://www.primuDFSRx.com). Standardized *Ginkgo biloba* extract (EGb 761®, Dr. Willmar Schwabe Pharmaceuticals, France) has been approved for treatment of dementia, cognition disorders, neurological disorders, vascular disorders, and Alzheimer's disease (Reitz et al.; 2012, https://adisinsight.springer.com/drugs/800002008). Sativex (GW Pharmaceuticals, UK), a standardized extract of *Cannabis sativa*, is used for the treatment of patients with neuropathic pain (Guy and Stott, 2005). Some phytochemicals have been found to be the small-molecule drug precursors. Isolation of paclitaxel from the barks of *Taxus brevifolia* is not a feasible method to meet with the commercial demand, as it could only yield 0.014% w/w of paclitaxel (Kingston, 2000). However, 10-Deacetylbaccatin III could be isolated in relatively large amounts from *Taxus baccata*, which could be chemically converted into paclitaxel (Denis and Greene, 1988). Therefore, 10-Deacetylbaccatin III can serve as a precursor for paclitaxel. Diosgenin, a steroidal sapogenin extracted from the tubers of *Dioscorea* species, is a precursor of other therapeutically

important steroids including progesterone, and cortisone (Jayachandran et al, 2016). (-)-Shikimic acid, an important intermediate of secondary metabolism in plants and microorganisms, can serve as a precursor of antiviral oseltamivir (Abrecht et al., 2004). Some phytochemicals can serve as the drug prototypes, which mean "the first compound discovered in a series of chemically related therapeutic agents" (Sneader, 1996). These chemicals may possess undesirable physicochemical, toxicological, solubility, bioavailability properties, which restrict their clinical applications. However, their analogs have been developed with higher therapeutic indices. Podophyllotoxin (toxic and poor water solubility), camptothecin (toxic and poor water solubility) have been reported to be drug prototypes of several clinically important antineoplastic agents including etoposide, topotecan, and even paclitaxel (Lee et al., 2005; Rahier et al., 2005). Guanidine, a phytochemical from *Galega officinalis*, possesses significant hypoglycemic activity; however, it is too toxic for clinical application. On other hand, some chemical analogs have been developed and metformin was found to be clinically suitable hypoglycemic agent (Krentz and Bailey, 2005). In addition, plant secondary metabolites can serve as pharmacological probes, which help researchers to understand the intracellular molecular signal transductions and biochemical mechanisms related to the pathological states and in turn aid in designing of novel therapeutic agents. Genistein, an isoflavone in soybean, serves to probe the interaction between protein tyrosine kinases and cyclic nucleotide-gated channels (Molokanova and Kramer, 2001). Different ester derivatives of phorbol, a diterpenoid from *Croton tiglium* seeds, have been extensively used in biomedical researches related to tumor pathogenesis (Montesano and Orci, 1985; Droms and Malkinson, 1991).

Plant-derived small molecules provide many novel bioactive molecules; some of them have led to therapeutically important drugs which are available in the market today. The global market value of plant based products exceeds $200 billion per annum. Therefore, drug discovery from medicinal plants has fetched the focus of researchers and industries. The conjugation of the traditional knowledge and application of modern scientific appliances can lead to new avenue in natural product based drug discovery. Introduction of high throughput screening, high resolution screening, hyphenated-chromatographic techniques (LC-NMR, GC-MS, LC-MS, LC-NMR-MS, LC-solid phase extraction-NMR, LC-solid phase extraction-NMR-MS), higher magnetic field-strength-NMR, capillary-NMR etc. have provided excellent opportunities in the natural product-based drug discovery in a rapid way. In this work, it has been aimed to identify pharmacologically active constituent/s in *S. roxburghiana* rhizomes useful against type 2 diabetes and its associated microvascular complication within myocardial tissue. This chapter deals with the thorough phytochemical investigation of *S. roxburghiana* rhizomes. The pharmacologically

active extract was subjected to qualitative chemical assays to identify the classes of secondary metabolites present within the test material. A phytochemical fingerprinting of the bioactive extract has been performed employing GC-MS analysis. Finally, the pharmacologically active extract was subjected to isolate the secondary metabolites, which were further subjected to preclinical assays for identifying pharmacologically active lead/scaffold(s).

3.2. Materials and methods

3.2.1. Collection and identification of plant

S. roxburghiana rhizomes were collected from Kharagpur (22.59° N, 88.26° E), West Midnapore district, West Bengal, India in December, 2013. The plant was authenticated (Ref. no. CNH/Tech.II/2015/37/316 dated 20.08.2015) by the Taxonomists of Botanical Survey of India, Shibpur, Howrah, India. A voucher specimen JU/PT/PC/05/2015 was submitted at the Advanced Pharmacognosy Research Laboratory, Department of Pharmaceutical Technology, Jadavpur University, India.

3.2.2. Extraction and phytochemical analysis

The rhizomes were dried in an incubator (40 ± 5 ºC, 72 h) and crushed into powder. The powdered rhizome (~5 kg) was macerated with methanol for 72 h at 30 ± 5 ºC with constant stirring. Particulate matters were removed by filtration and resulting extract was dried under vacuum in a rotary vacuum evaporator at 45 ± 5 ºC to obtain a semisolid mass (567 g, yield ~ 11.34 % w/w). The crude extract was dissolved in water and water soluble extract was fractioned with n-hexane to remove fat and waxes to yield defatted extract, DFSR (421 g).

The qualitative phytochemical analysis of DFSR was performed by preliminary phytochemical assays for alkaloids, terpenoids, carotenoids, flavanoids, tannins, steroids, anthocyanins, saponins etc. (Ghosh et al., 2010). DFSR was further subjected to GC-MS analysis employing gas chromatography system (Agilent 5975C, USA) following the protocol detailed by Das et al using HP-5MS capillary column (length 30 m plus Duraguard 10 m, film 0.25 µm, diameter 0.25 mm narrow bore) (Das et al., 2016). Briefly, the sample and internal standard were dissolved in CH_3OH:H_2O (1:1) was distributed into eppendorf tube (50 µl) and evaporated to dryness. The residue was redissolved in of methoxyamine hydrochloride and subsequently shaken for 90 min at 30 ºC and then of N-methyl-N-trimethylsilyltrifluoroacetamide was added and shaken at 37 ºC for 30 min for trimethylsilylation of acidic protons to increase volatility of metabolites. 2 µl of fatty acid methyl esters markers (a mixture of internal retention index markers was prepared using fatty acid methyl esters of C8, C10, C12, C14, C16, C18, C20, C22, C24, and C26 linear chain length) dissolved in chloroform was added for GC-MS analysis in an Agilent 5975C gas

chromatography system, USA following the method of Kind et al. (2009). Agilent J & W HP-5MS capillary column (USA) of length 30 m plus Duraguard 10 m, diameter 0.25 mm narrow bore, film 0.25 µm was used in this study. Injection was made in sandwich mode with fast plunger speed without viscosity delay or dwell time. The analysis was performed under the following oven temperature programme: oven ramp 60 ºC (1 minute hold) to 325 ºC at 10 ºC/ min, 10 min hold before cool-down, 37.5 min run time. The injection temperature was set at 250 ºC; the MS transfer line at 290 ºC and the ion source at 230ºC. Helium was used as the carrier gas at a constant flow rate of 0.723 ml/min (carrier linear velocity 31.141 cm/s). Samples (1 µl) were injected via the split mode (split ratio 1:5) onto the GC column. Identification of the metabolites was carried out by comparing the fragmentation patterns of the mass spectra and retention times (R_t) with those present in Agilent Fiehn Metabolomics library using Agilent retention time locking (RTL) method. Automated mass spectral deconvolution and identification system (AMDIS) was used to de-convolute GC-MS results and to identify chromatographic peaks.

3.2.3. Isolation of phytochemicals from DFSR

DFSR (~ 250 g) was chromatographed in a normal phase silica gel column and eluted with n-hexane-ethyl acetate and ethyl acetate-CH_3OH with increasing polarity, to yield 8 major fractions (A-H). Fraction A (~ 1.8 g) was further chromatographed with n-hexane-CH_2Cl_2 and CH_2Cl_2-CH_3OH with increasing polarity to yield 6 sub-fractions (A_{1-6}). The sub-fraction A_3 (~ 215 mg) was further column chromatographed with n-hexane-$CHCl_3$ and $CHCl_3$-CH_3OH with increasing polarity to yields compound 1 (~ 31 mg). Fraction B (~ 2.5 g) was further chromatographed with n-hexane-ethyl acetate and ethyl acetate- CH_3OH with increasing polarity to yield 4 sub-fractions (B_{1-4}). The sub-fraction B_2 (~ 615 mg) was further column chromatographed with n-hexane-CH_2Cl_2 and CH_2Cl_2-CH_3OH with increasing polarity to yields compound 2 (~ 21 mg). Fraction C (~ 1.2 g) was further chromatographed with n-hexane-ethyl acetate and ethyl acetate-CH_3OH with increasing polarity to yield 3 sub-fractions (C_{1-3}). The sub-fraction C_3 (~ 475 mg) was further column chromatographed with n-hexane-$CHCl_3$ and $CHCl_3$-CH_3OH with increasing polarity to yields compound 3 (~ 17 mg). Fraction D (~ 917 mg) was further chromatographed with n-hexane-CH_2Cl_2 and CH_2Cl_2-CH_3OH with increasing polarity to yield 3 sub-fractions (D_{1-3}). The sub-fraction D_2 (~ 386 mg) was further column chromatographed using same solvent system to yield compound 4 (~ 42 mg). Fraction E (~ 26.8 g) was further chromatographed with n-hexane-CH_2Cl_2 and CH_2Cl_2-CH_3OH with increasing polarity to yield 4 sub-fractions (E_{1-4}). The sub-fraction E_3 (~11.1 g) was further column chromatographed using same solvent system and finally purified by preparative TLC using solvent system CH_2Cl_2: acetone: acetic acid (10: 1.5: 0.5, v/v/v) to yield compound 5 (~ 3.7 g). Fraction G (~ 2.4 g) was further chromatographed with

n-hexane-CH_2Cl_2, CH_2Cl_2-CH_3COCH_3 and finally CH_3COCH_3-CH_3OH with increasing polarity to yield 3 sub-fractions (G_{1-3}). The sub-fraction G_2 (~ 873 mg) was further column chromatographed using same solvent system to yield compound 6 (~ 22 mg). The structures have been elucidated employing physicochemical data, ^1H and ^{13}C NMR interpretation, and mass spectroscopic data (Gutzeit et al., 2007; Martin et al., 2000). Different stages of work from extraction to isolation were depicted in Figure 3.1.

Figure 3.1. Different stages of work from extraction, column chromatography and TLC studies for separation of pure compound from DFSR.

3.3. Results

3.3.1. Phytochemical analysis of DFSR

Preliminary phytochemical analysis revealed presence of terpenoids, steroids, flavonoids, saponins, alkaloids, anthocyanins, carotenoids, and phenolic compounds in DFSR.

GC-MS analysis revealed presence of different compounds mainly phenolic compounds, sugar alcohols, sterols, amino acids and saturated fatty acids. The chromatogram and the list of identified compounds have been depicted in Figure 3.2. and Table 3.1., respectively. Amongst the identified compounds, ferulic acid, caffeic acid, heptadecanoic acid, sinapyl alcohol, gallic acid, 4-hydroxycinnamic acid, 4-hydroxy-3-methoxybenzoic acid, myristic acid, protocatechuic acid, oleic acid, vanillin, hydroquinone, 4-hydroxybenzaldehyde, kaempferol, ergosterol and stigmasterol were important to serve as markers for this test material with respect to observed pharmacological activity.

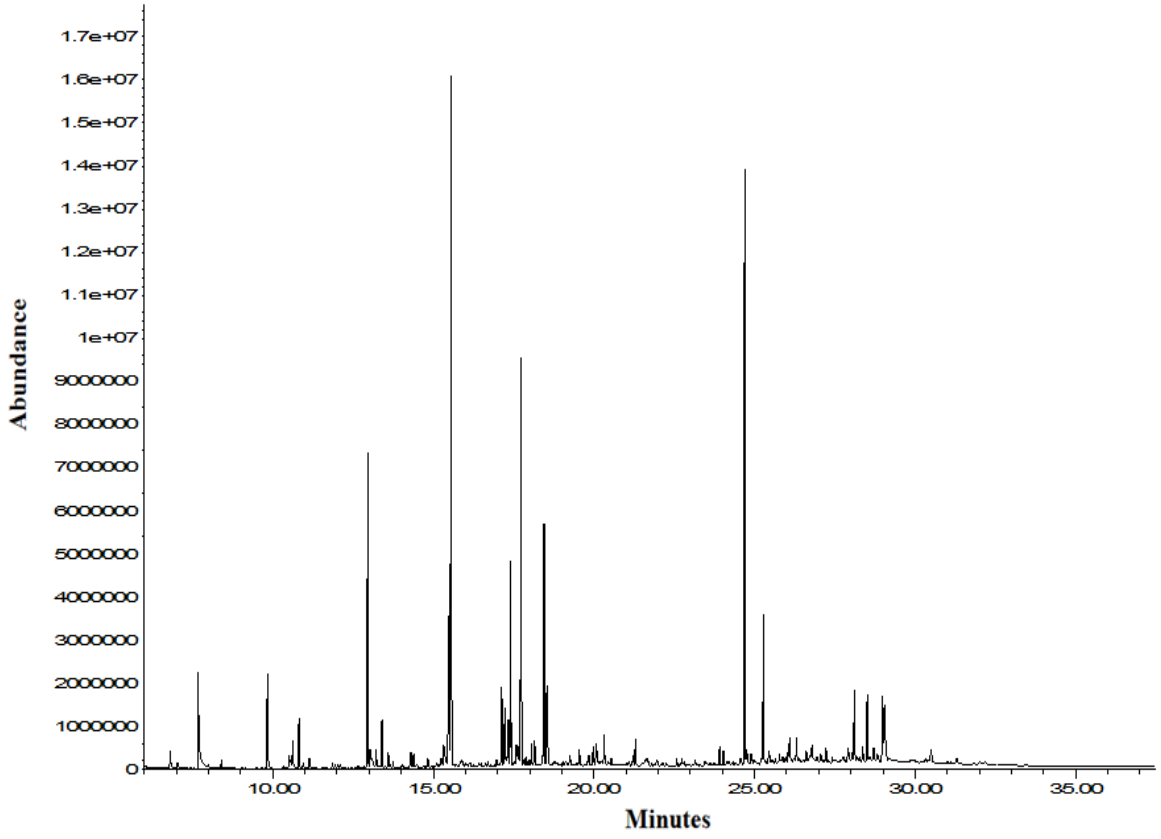

Figure 3.2. GC-MS chromatogram of DFSR.

Table 3.1. List of identified phytochemicals identified within DFSR by GC-MS analysis as compared with library R_t.

Sl no.	Components	Peak area	Library R_t	Sample R_t
1	Internal standard (Ribitol)	151584	15.6	15.34
2	Lactic acid	2216064	6.85	6.8
3	Glycolic acid	854377	7.05	7.02
4	Oxalic acid	182557	7.88	7.84
5	Glycerol	8247817	9.83	9.94
6	Phosphoric acid	521818	9.97	9.85
7	Glycine	16899	10.46	10.27
8	Succinic acid	266,929	10.51	10.35
9	Glyceric acid	2110087	10.73	10.61
10	Tartronic acid	455597	11.52	10.95

11	D-malic acid	180684	12.79	12.65
12	D-threitol	26159855	12.95	12.95
13	L-pyroglutamic acid	408701	13.22	13.09
14	L-glutamic acid	320199	13.23	13.09
15	2-(4-hydroxyphenyl)ethanol	330289	13.84	13.64
16	4-(2-hydroxyethyl)phenol (tyrosol)	288248	13.86	13.86
17	3-hydroxy-3-methylglutaric acid	153391	14.23	14.02
18	4-hydroxybenzoic acid	1939041	14.51	14.27
19	D-Lyxose	710192	14.74	14.83
20	Xylitol	16381882	15.38	15.48
21	4-hydroxy-3-methoxybenzoic acid	299570	15.99	15.83
22	Glycerol-1-phosphate	153180	16.06	15.9
23	3,4-dihydroxybenzoic acid	337086	16.59	16.41
24	Citric acid	172128	16.61	16.48
25	Myristic acid	526047	16.89	16.63
26	Fructose	6379741	17.18	17.12
27	D-mannose	17239303	17.29	17.4
28	Gluconic acid lactone	3113690	17.3	17.21
29	D-glucose	17528559	17.43	17.4
30	D-mannitol	37552154	17.81	17.73
31	4-hydroxycinnamic acid	1458690	17.85	17.62
32	Gallic acid	445635	18.01	17.84
33	Gluconic acid	21741500	18.3	18.44
34	Palmitic acid	7613397	18.85	18.53
35	Ferulic acid	199873	19.31	19.08
36	Heptadecanoic acid	133002	19.8	19.46
37	Linoleic acid	1759168	20.4	20.06
38	Oleic acid	766893	20.5	20.1
39	Stearic acid	2614472	20.68	20.31
40	D-glucose-6-phosphate	164109	21.56	22.14
41	Arachidic acid	271853	22.37	21.96
42	Behenic acid	227724	23.9	23.48
43	D-(+)Trehalose	62851888	24.75	24.69

44	Kaempferol	149694	26.93	26.7
45	Chlorogenic acid	759266	27.18	27.06
46	Cholesterol	1049716	27.56	27.23
47	Ergosterol	32477	28.09	27.79
48	Stigmasterol	6724413	28.44	28.11

3.3.2. Phytochemicals isolated from DFSR

Compound 1 (White needles, Lupeol, 3β-Lup-20(29)-en-3-ol); m.p. 213-215 °C; ^{1}H NMR data (400 MHz; CDCl3): δ 4.67 (1H, s, 29b), 4.56 (1H, s, H-29a), 3.21 (1H, dd, J= 2.0, 6.0 Hz, H-3), 1.65, 1.02, 0.97, 0.95, 0.84, 0.79, 0.76 (21H, 7 s, 7 CH_3); ^{13}C NMR data (100 MHz; CDCl3): δ 151.2 (C-20), 109.3 (C-29), 79.2 (C-3), 55.8 (C-5), 50.6 (C-9), 48.5 (C18), 48.2 (C-19), 43.1 (C-17), 43.0 (C-14), 41.1 (C-8), 40.2 (C-22), 39.0 (C-4), 38.9 (C-1), 38.4 (C-13), 37.5 (C10), 35.7 (C-16), 34.3 (C-7), 29.8 (C-21), 28.2 (C-23), 27.6 (C-2), 27.2 (C-15), 25.3 (C-12), 21.2 (C-11), 19.7 (C30), 18.6 (C-6), 18.2 (C-28), 16.2 (C-25), 16.0 (C-26), 15.6 (C-24), 14.9 (C-27); ESIMS: 427 $[M + H]^+$.

Compound 2 (White needles, Stigmasterol; Stigmasta-5,22-dien-3β-ol): m.p. 168-170 °C; ^{1}H NMR data (400 MHz; CDCl3): δ 5.36 (1H, d, J =4.8 Hz, H-6), 5.14 (1H, dd, J = 8.8, 14.2 Hz, H-22), 5.02 (1H, dd, J = 8.8, 14.8 Hz, H-23), 3.54 (1H, dd, J=1.2 and 4.5 Hz, H-3), 1.03 (3H, s, H-19), 0.93 (3H, d, J = 6.4 Hz, H-21), 0.87 (3H, d, J = 7.2 Hz, H-26), 0.83 (3H, t, J = 7.4 Hz, H-29), 0.80 (3H, d, J = 8.4 Hz, H-27), 0.68 (3H, s, H-18); ^{13}C NMR data (100 MHz; CDCl3): δ 140.8 (C-5), 138.3 (C-22), 129.3 (C-23), 121.7 (C-6), 71.8 (C-3), 56.8 (C-14), 56.1 (C-17), 51.2 (C-24), 50.2 (C-9), 45.8 (C-25), 42.3 (C-13), 40.7 (C-20), 39.8 (C-12), 37.4 (C-4), 37.3 (C-1), 36.5 (C-10), 32.0 (C-8), 31.8 (C-7), 29.2 (C-16), 28.2 (C-2), 25.4 (C-28), 24.4 (C-15), 21.2 (C-21), 21.1 (C-11), 19.8 (C-27), 19.4 (C-26), 19.0 (C-19), 12.0 (C-29), 11.9 (C-18); ESIMS: 413 $[M + H]^+$.

Compound 3 (White needles, Ergosterol, Ergosta-5,7,22-trien-3β-ol): m.p. 157-158 °C; ^{1}H NMR data (400 MHz; $CDCl_3$): δ 5.57 (1H, dd, J = 3.0, 5.5 Hz, H-6), 5.38 (1H, dd, J = 3.0, 5.4 Hz, H-7), 5.22 (1H, m, H-23), 5.17 (1H, m, H-22), 3.63 (1H, m, H-3), 1.03(3H, d, J = 7.2 Hz, H-21), 0.94 (3H, s, H-18), 0.92 (3H, d, J = 7.2 Hz, H-28), 0.84 (3H, d, J = 7.2 Hz, H-26), 0.82 (3H, d, J = 7.2 Hz, H-27), 0.63 (3H, s, H-19); ^{13}C NMR data (100 MHz; $CDCl_3$): δ 141.5 (C-8), 139.9 (C-5), 135.8 (C-22), 132.1 (C-23), 119.7 (C-6), 116.4 (C-7), 70.4 (C-3), 55.8 (C-17), 54.7 (C-14), 46.3 (C-9), 43.0 (C-13), 42.9 (C-24), 0.9 (C-5), 40.4 (C-20), 39.2 (C-12), 38.5 (C-1), 37.1 (C-10), 33.2 (C-25), 32.0 (C-12), 28.4 (C-16), 23.1 (C-15), 21.2 (C-11), 21.2 (C-21), 20.0 (C-27), 19.6 (C-26), 17.7 (C-19), 16.2 (C-28), 12.1 (C-18); ESIMS: 397 $[M + H]^+$.

Compound 4 (Yellowish amorphous solid, Cambodianol, (3R)-3,5,7-Trihydroxy-6-methyl-3-(40-methoxybenzyl)-4-chromanone): m.p. 167-170 °C; ^{1}H NMR data (400 MHz; $CDCl_3$): δ 11.28 (1H, s, OH-5), 7.08 (1H, d, J = 8.4 Hz, H-2'), 6.76 (2H, d, J = 8.4 Hz, H-3', 5'), 6.07 (1H, s, H-8), 4.96 (1H, s, OH-3), 4.19 (1H, m, H-2), 4.04 (1H, m, H-2), 3.87 (3H, s, OCH_3-4'), 2.97 (1H, d, J = 14.0 Hz, H-9), 2.92 (1H, d, J = 14.0 Hz, H-9), 2.0 (3H, s, CH_3-6); ^{13}C NMR data (100 MHz; $CDCl_3$): δ 200.5 (C-4), 166.5 (C-7), 163.9 (C-5), 162.6 (C-8a), 159.8 (C-4'), 133.4 (C-2'), 133.1 (C-6'), 127.9 (C-1'), 115.4 (C-3'), 115.4 (C-5'), 106.5 (C-6), 101.5 (C-4a), 95.7 (C-8), 73.8 (C-3), 73.2 (C-2), 56.2 (C-4', -OCH_3), 41.4 (C-9), 7.9 (C-6, -CH_3); ESIMS: 331 $[M + H]^+$.

Compound 5 (Brownish white amorphous solid, Protocatechuic acid, 3,4-Dihydroxybenzoic acid) m.p. 220-221 °C; ^{1}H NMR data (400 MHz; DMSO-d6): δ 12.33 (1H, s, COOH-7), 9.67 (1H, d, J = 3.2 Hz, OH-2), 9.33 (1H, d, J = 3.2 Hz, OH-3), 7.32 (1H, d, J = 2.0 Hz, H-1), 7.27 (1H, dd, J = 8.4, 2.0 Hz, H-6), 6.76 (1H, d, J = 8.4 Hz, H-5); ^{13}C NMR data (100 MHz; DMSO-d6): δ 168.1 (-COOH), 149.6 (C-4), 145.1 (C-3), 122.7 (C-6), 122.0 (C-1), 116.9 (C-2), and 115.4 (C-5); ESIMS: 155 $[M + H]^+$.

Compound 6 (Colourless gummy solid, Vanillic acid, 4-Hydroxy-3-methoxybenzoic acid): m.p. 211-212 °C; ^{1}H NMR (400 MHz, DMSO-d6): δ 12.51 (1H, s, COOH-7), 9.82 (1H, d, J = 2.8 Hz, OH-2), 7.43 (1H, d, J = 2.4 Hz, H-1), 7.44 (1H, d, J = 8.2 Hz, H-5), 6.86 (1H, d, J = 8.4 Hz, H-6), 3.82 (1H, d, J = 3.2 Hz, OCH_3-3); ^{13}C NMR (100 MHz, DMSO-d6): δ 167.9 (-COOH), 151.7 (C-3), 147.6 (C-4), 124.4 (C-1), 130.1 (C-6), 116.7 (C-2), 114.9 (C-5), 55.7 (-OCH_3); ESIMS: 169 $[M + H]^+$.

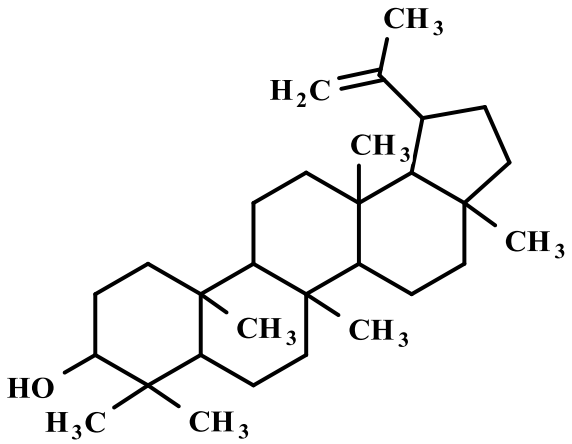

Compound 1

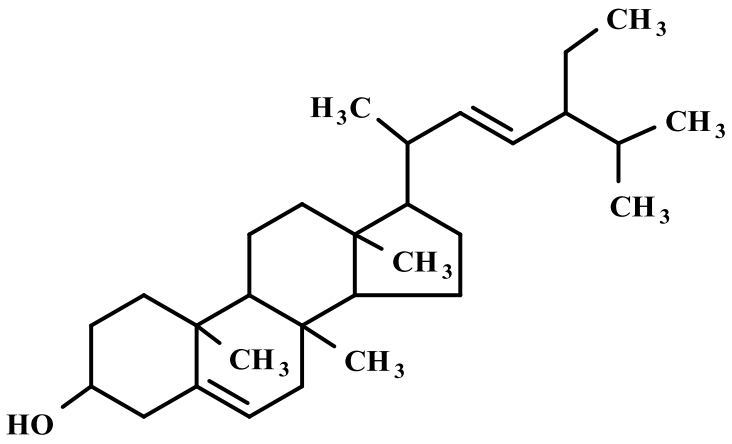

Compound 2

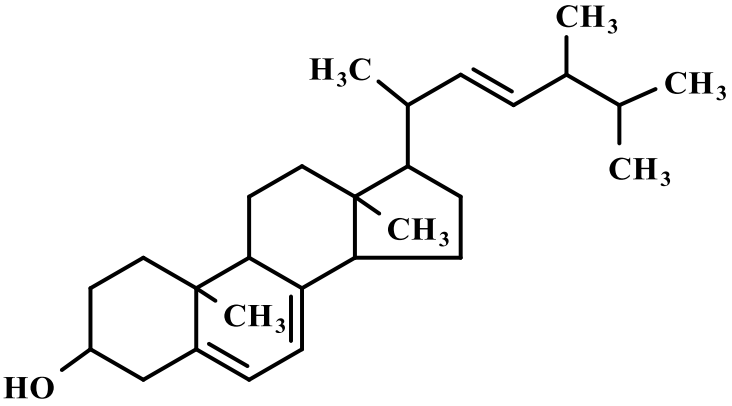

Compound 3

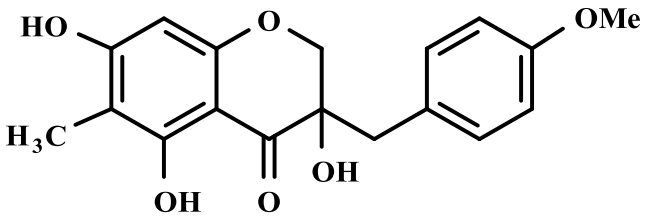

Compound 4

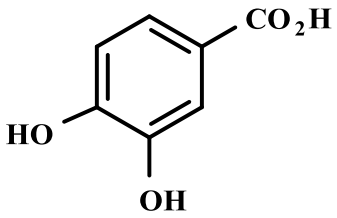

Compound 5

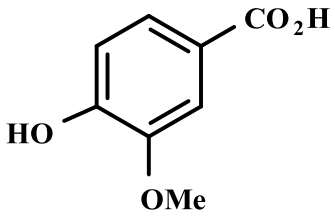

Compound 6

Figure 3.3. The structures of the isolated compounds from DFSR.

By interpreting ^{1}H NMR, ^{13}C NMR data the isolated compounds were identified. The structures of compound 1-6 were depicted in Figure 3.3. The structure of compound 1, lupeol, has been previously reported and it has also been reported to be present in whole plant of *S. roxburghiana* (Aher et al., 2010; Roy et al., 2013). However, our method of isolation is different and simple as well the yield value is found to be superior to previous report. A doublet of doublet at δ 3.20 (J= 2.0, 6.0 Hz) is due to the proton attached secondary carbinol at H-3. Two broad singlets were seen at δ 4.67 and 4.56 due to the two exomethylene protons (H-29a and b). Seven singlets were appeared between 0.76 and 1.65 correspond to 7 CH_3. 13C NMR data showed seven methyl groups at C-23 (δ 28.2), C-30 (δ 19.7), C-28 (δ 18.2), C-25 (δ 16.2), C-26 (δ 16.0), C-24 (δ 15.6), and C-27 (δ 14.9). The deshielded signal at δ 79.2 corresponds to C-3 bearing -OH group. The structure of compound 2, stigmasterol, has been previously reported (Agarwal et al., 1985, Jamal et al., 2009); however, this is the first time ergosterol was isolated from *S. roxburghiana* rhizomes. In ^{1}H NMR spectrum, H-3 proton appears as double doublet at δ 3.54 (J=1.2 and 4.8 Hz). H-6 olefinic H appears as doublet at δ 5.36 (J =4.8 Hz). H-22 and H-23 olefinic protons appear at as double doublet at δ 5.14 (J = 8.8, 14.2 Hz) and δ 5.02 (J = 8.8, 14.8 Hz), respectively. Signals at region between δ 0.68 and δ 1.03 correspond to -CH_3 groups in H-19 (δ 1.03), H-21 (δ 0.93), H-26 (δ 0.87), H-29 (δ 0.83), H-27 (δ 0.80), and H-18 (δ 0.68). ^{13}C NMR data revealed C28-sterol stigmastane skeleton. ^{13}C NMR data revealed the signals at δ 140.8 (C-5), δ 138.3 (C-22), δ 129.3 (C-23), and δ 121.7 (C-6) correspond to the alkene carbons. The δ 71.8 corresponds to C-3 β-OH group. CH_3 carbons were observed between δ 21.4 and 11.9 regions viz. C-21 (δ 21.2), C-27 (δ 19.8), C-26 (δ 19.4), C-19 (δ 19.0), C-29 (δ 12.0), C-18 (δ 11.9). The structure of compound 3, ergosterol, has been previously reported (Martinez et al., 2015; Alexandre et al., 2017); however, this is the first time ergosterol was isolated from *S. roxburghiana* rhizomes. ^{1}H

NMR data revealed $\Delta^{5,7}$ structure by signals δ 5.57 (dd, J = 3.0, 5.5 Hz) and δ 5.38 (dd, J = 3.0, 5.4 Hz) diagnostic for olefin hydrogens of H-6 and H-7. δ 3.63 (H-3) indicate the existence of H-linked to carbinolic C. Double bonds were observed at signals δ 5.22 (m) and δ 5.17 (m) relative to H-22 and H-23. Signals at region between δ 0.63 and δ 1.1 correspond to methyl groups in δ 1.03 (21-CH_3), δ 0.94 (18-CH_3), δ 0.92 (28-CH_3), δ 0.84 (26-CH_3); δ 0.82 (27-CH_3), and δ 0.63 (19-CH_3). ^{13}C NMR data revealed C28-sterol ergostane skeleton. Signals at region between δ 116.4 and 141.5 correspond to C-7 (δ 116.4), C-6 (δ 119.7), C-23(δ 132.1), C-22 (δ 135.8), C-5 (δ 139.9), and C-8 δ (141.5). CH_3 carbons were observed between δ 28.4 and 12.1 regions, while hydroxyl group was observed in C-3 (δ 70.3). The structure of compound 4, cambodianol, has been previously reported and it has also been reported to be present in whole plant of *S. roxburghiana* (Liu et al., 2009; Roy et al., 2013). In the ^{1}H NMR data, four proton signals at δ 4.19, δ 4.04, δ 2.97, and δ 2.92 and four carbon signals in the ^{13}C NMR spectrum at δ 73.8, δ 73.2, δ 200.5, and δ 41.4 indicate the presence of 3-hydroxy-3-benzyl-4-chroma-none. An AA'BB' spin system at δ 7.08 (d, J = 8.4 Hz) and 6.76 (d, J = 8.4 Hz) revealed the C-4 in ring B was oxygenated. Additionally, a -OH proton (δ 11.28, s), an aromatic proton (δ 6.07, s), a -CH_3 signal (δ 2.0, s), and a -OCH_3 signal (δ 3.87, s) was observed in ^{1}H NMR spectra. Four aromatic carbons with oxygen function were observed at δ 166.5, δ 163.9, δ 162.6, and δ 159.8 in the ^{13}C NMR spectra. The structure of compound 5, protocatechuic acid, has been previously reported; however, this is the first time protocatechuic acid was isolated from *S. roxburghiana* rhizomes by our group (Ou et al., 2012; López-Martínez et al., 2015; Bhattacharjee et al., 2017). ^{1}H-NMR spectral data revealed two -OH protons (δ 9.67 and δ, 9.33), a -COOH proton (δ 12.33, s), and three aromatic protons (7.32, 7.27 and 6.76). ^{13}C-NMR spectral data revealed the presence of 7 carbon atoms in the molecule. The C-1-6 resonated at δ 122.7, δ 116.9, δ 145.1, δ 149.6, δ 115.4, and δ 122.7, respectively. C-7 (-COOH) resonated at 168.1. The higher δ of C-7 is due to the effect of strong intermolecular H-bonding. The structure of compound 6, vanillic acid, has been previously reported; however, this is the first time vanillic was isolated from *S. roxburghiana* rhizomes (Chang et al., 2009; López-Martínez et al., 2015). ^{1}H-NMR spectral data revealed one -OH proton (δ 9.82), a -COOH proton (δ 12.51), and three aromatic protons (7.44, 7.44 and 6.86). The C-1-6 resonated at δ 124.4, δ 116.7, δ 151.7, δ 147.6, δ 114.9, and δ 130.1, respectively. C-7 (-COOH) resonated at 167.9. The higher δ of C-7 is due to the effect of strong intermolecular H-bonding. -OCH_3 resonated at δ 55.7.

3.4. Discussion

Isolation and identification of the secondary metabolites in a plant are the initial steps toward natural product-based drug discovery. Classical research approach relies on extraction, qualitative

assays for phytochemicals, fractionation considering nature of phytochemicals present within mother extract and chromatographic separation to isolate targeted phytochemicals or random isolation of phytochemicals from fractions. On the other hand, modern research implements bioassay guided fractionation following chromatographic separation of phytochemicals from bioactive fraction(s). In this study, DFSR was subjected to phytochemical analysis. Qualitative phytochemical analysis revealed presence of steroids, flavonoids, alkaloids, triterpenoids and phenolic compounds in DFSR. GC-MS analysis further recognized different compounds mainly phenolic compounds, sugar alcohols, sterols, amino acids and saturated fatty acids in *S. roxburghiana* rhizomes. Six compounds viz. lupeol, stigmasterol, ergosterol, cambodianol, protocatechuic acid, and vanillic acid were isolated from DFSR employing chromatographic separation techniques. The isolated compounds were screened for pharmacological assays to identify the bioactive scaffold(s) and the activity of scaffold has been discussed in the subsequent section of this thesis.

References

Abrecht S, Harrington P, Iding H, Karpf M, Trussadi R, Wirz B, Zutter U. The synthetic development of the anti-influenza neuraminidase inhibitor oseltamivir phosphate (Tamiflu®): a challenge for synthesis & process research. Chimia. 2004;58:621-629.

Acamovic T, Brooker JD. Biochemistry of plant secondary metabolites and their effects in animals. Proc Nutr Soc. 2005;64:403-412.

Agarwal PK, Jain DC, Gupta RK, Thakur RS. Carbon-13 NMR spectroscopy of steroidal sapogenins and steroidal saponins. Phytochemistry. 1985;24:2476-2496.

Aher AN, Pal SC, Yadav SK, Patil UK, Bhattacharya UK. Isolation and characterization of phytoconstituents from *Casuarina equisetifolia* (Casuarinaceae). Asian J Chem. 2010;22:3429-3434.

Alexandre TR, Lima ML, Galuppo MK, Mesquita JT, do Nascimento MA, dos Santos AL, Sartorelli P, Pimenta DC, Tempone AG. Ergosterol isolated from the basidiomycete *Pleurotus salmoneostramineus* affects *Trypanosoma cruzi* plasma membrane and mitochondria. J Venom Anim Toxins Incl Trop Dis. 2017;23:30.

Bhattacharjee N, Dua TK, Khanra R, Joardar S, Nandy A, Saha A, De Feo V, Dewanjee S. Protocatechuic acid, a phenolic from *Sansevieria roxburghiana* leaves, suppresses diabetic cardiomyopathy via stimulating glucose metabolism, ameliorating oxidative stress, and inhibiting inflammation. Front Pharmacol. 2017;8:251.

Chang SW, Kim KH, Lee IIK, Choi SU, Ryu SY, Lee KR. Phytochemical Constituents of *Bistorta manshuriensis*. Nat Prod Sci. 2009;15:234-240.

Das S, Dutta M, Chaudhury K, De B. Metabolomic and chemometric study of *Achras sapota* L. fruit extracts for identification of metabolites contributing to the inhibition of α-amylase and α-glucosidase. Eur Food Res Technol. 2016;242:733-743.

Denis JN, Greene AE, Guenard D, Gueritte-Voegelein F, Mangatal L, Potier P. Highly efficient, practical approach to natural taxol. J Am Chem Soc. 1988;110:5917-5919.

Dias DA, Urban S, Roessner U. A historical overview of natural products in drug discovery. Metabolites. 2012;2:303-336.

Droms KA, Malkinson AM. Phorbol ester-induced tumor promotion by downregulation of protein kinase C. Mol Carcinog, 1991;4:1-2.

Ghosh J, Das J, Manna P, Sil PC. Protective effect of the fruits of *Terminalia arjuna* against cadmium-induced oxidant stress and hepatic cell injury via MAPK activation and mitochondria dependent pathway. Food Chem. 2010;123:1062-1075.

Guy GW, Stott CG. The development of Sativex® -a natural cannabis based medicine. In: Mechoulam R. (ed) Cannabinoids as therapeutics (Milestones in drug therapy). Birkhäuser, Switzerland, 2005;pp. 231-263.

Jamal AK, Yaacob WA, Din LB. A chemical study on *Phyllanthus Columnaris*. Eur J Sci Res. 2009;28:76-81.

Jayachandran KS, Vasanthi AHR, Gurusamy N. Steroidal saponin diosgenin from *Dioscorea bulbifera* protects cardiac cells from hypoxia-reoxygenation injury through modulation of pro-survival and pro-death molecules. Pharmacogn Mag. 2016;12:S14-S20.

Kennedy DO, Wightman EL. Herbal extracts and phytochemicals: plant secondary metabolites and the enhancement of human brain function. Adv Nutr. 2011;2:32-50.

Kind T, Wohlgemuth G, Lee DY, Lu Y, Palazoglu M, Shahbaz S, Fiehn O. Fiehnlib-mass spectral and retention index libraries for metabolomics based on quadrupole and time-of-flight gas chromatography/mass spectrometry. Anal Chem. 2009;81:10038-10048.

Kingston DGI. Recent advances in the chemistry of taxol. J Nat Prod. 2000:63:726-734.

Kong JM, Goh NK, Chia LS, Chia TK. Recent advances in traditional plant drugs and orchids. Acta Pharmacol Sin. 2003;24:7-21.

Krentz AJ, Bailey CJ. Oral antidiabetic agents: current role in type 2 diabetes mellitus. Drugs. 2005;65:385-411.

Lee KH, Xiao Z. Podophyllotoxins and analogs. In: Cragg GM, Kingston DGI, Newman DJ (eds) Anticancer agents from natural products. CRC press, Taylor and Francis, Boca Raton, US, 2005;pp. 95-122.

Liu J, Mei W-L, Wu J, Zhao Y-X, Peng M, Dai H-F. A new cytotoxic homoisoflavonoid from *Dracaena cambodiana*. J Asian Nat Prod Res. 2009;11:192-195.

López-Martínez LM, Santacruz-Ortega H, Navarro R-E, Sotelo-Mundo RR, González-Aguilar GA. A 1H NMR Investigation of the interaction between phenolic acids found in mango (*Manguifera indica* cv Ataulfo) and papaya (*Carica papaya* cv Maradol) and 1,1-diphenyl-2-picrylhydrazyl (DPPH) Free Radicals. PLoS ONE. 2015;10:e0140242.

Martinez M, Alvarez ST, Campi MG, Bravo JA, Vila JL. Egosterol from the mushroom *Laetiporus* Sp.; isolation and structural characterization. Rev Bol Quim. 2015;32:90-94.

Molokanova E, Kramer RH. Mechanism of inhibition of cyclic nucleotide-gated channel by protein tyrosine kinase probed with genistein. J Gen Physiol. 2001;117:219-234.

Montesano R, Orci L. Tumor-promoting phorbol esters induce angiogenesis in vitro. Cell. 1985;42:469-477.

Nandagopalan V. Doss A. Marimuthu C. Phytochemical analysis of some traditional medicinal plants. Biosci Discov. 2016;7:17-20.

Ou CB, Pang Q, Chen X, Hou N, He C. Protocatechuic acid, a new active substance against the challenge. Poult Sci. 2012;91:1604-1609.

Rahier NJ, Thomas CJ, Hecht SM. Camptothecin and its analogs. In: Cragg GM, Kingston DGI, Newman DJ (eds) Anticancer Agents from Natural Products. CRC press, Taylor and Francis, Boca Raton, US, 2005;pp. 5-25.

Reitz C. Alzheimer's disease and the amyloid cascade hypothesis: a critical review. Int J Alzheimer's Dis. 2012; 2012:369808.

Roy J, Aktar F, Haq MR, Begum B, Hasan CM. A rare homoisoflavonoid cambodianol from *Sansevieria roxburghiana*. Asian J Chem. 2013;25:5113-5114.

Sneader W. Drug Prototypes and Their Exploitation. Hoboken: Wiley, England, 1996.

Web references

http://www.primuDFSRx.com

https://adisinsight.springer.com/drugs/800002008

4.1. Introduction

The physician, patients, and consumers are primarily interested to access safe and effectual drugs. Therefore, toxicity testing is one of the critical and unavoidable steps in drug discovery process (Parasuraman, 2011). The origin of toxicity studies was initiated in early in the sixteen century by Paracelsus who determined specific chemicals responsible for the observed toxicity of plants and animals (Parasuraman, 2011). The US FDA (Food and Drug Administration) proposed that it is essential to screen every new molecule for preclinical pharmacological and toxicological potential in vivo (Parasuraman, 2011). Preclinical toxicity profiling of chemicals plays a critical role in risk assessment and risk mitigation (Bluemel et al., 2012). Depending on the objective and therapeutic regimen, pre-clinical toxicity studies can be categorized as acute, sub-acute, sub-chronic, and chronic toxicity studies. Different regulatory agencies namely the Organization for Economic Co-operation and Development (OECD) and the International Conference on Harmonization (ICH), US FDA, and World Health Organization (WHO) provided the guidelines for the toxicity testing of pharmaceutical agents (Parasuraman, 2011; https://www.fda.gov/, http://www.ich.org/). In 1920, J. W. Trevan introduced the concept of the 50 % lethal dose (LD_{50}) to experimental animals for determination of the toxic dose of a chemical. Acute toxicity is usually an initial step to assess and evaluate toxic characteristics of the compounds. Acute toxicity studies are performed on experimental animals to determine LD_{50} values, which are the doses of test materials causing death to 50 % of the population of experimental animals. The acute toxicity studies provide impressions to select therapeutic doses, to reveal of toxic incidence, and to provide idea relevant to acute overdosing. In sub-acute toxicity studies, the pharmaceutical agents are administered generally to the rodents in a daily basis for the tenure of 28 days (Han et al., 2015; Olaniyan et al., 2015). The clinical sign, mortality, body weight, dietary intake, water intake, behavioral patterns, haematological parameters, biochemical parameters, and urinal parameters are generally recorded along with the organ weight and histological assessment (Han et al., 2015). The sub-acute toxicity data give the impression of toxicity of the chemicals following repeated administration. Additionally, it helps to establish doses for the chronic studies. In sub-chronic toxicity studies, the pharmaceutical agents are administered daily for the tenure of at least 90 days (Parasuraman, 2011). Behavioral patterns (daily), body weight variations (weekly), hematological (monthly), biochemical (monthly), and cardiovascular parameters (monthly) are observed. Gross pathological changes including histopathological analyses are performed (Parasuraman, 2011). Chronic toxicity studies are performed with at least one rodent and one non-rodent species. The test compounds are administered repeatedly for more than 90 days (Parasuraman, 2011). The animals are observed periodically and all the parameters in sub-

chronic studies (Parasuraman, 2011) along with mutagenicity, carcinogenicity, teratogenicity, geno-toxicity, neurotoxicity, and toxicokinetics are measured (Kimm-Brinson and Ramsdell, 2001; Zepnik et al., 2003; Oliveira et al., 2010; http://www.oecd.org/dataoecd/20/52/37622194; http://ecb.jrc.ec.europa.eu/documents/Testing-Methods/ANNEXV/B32web1988; http://alttox.org/(non-animalmethodsoftoxicitytesting).

Medicinal plants have a long and successful history in different traditional medicinal systems (Dewanjee et al., 2009; Boukandou Mounanga et al., 2015). According to the WHO, about 40-90 % of people in developing countries primarily rely on traditional medicine (Boukandou Mounanga et al., 2015). Regardless of their reliable uses, there is the lack of scientific evidence related to their mechanism of action and safety profile (Subramanian et al., 2018). Generally, it is claimed that medicinal plants and plant derived molecules are non-toxic (Dewanjee et al., 2009). However, many medicinal plants have been reported to possess deleterious health effects (Boukandou Mounanga et al., 2015). Indeed, among 1,500,000 plants were investigated and most of them were reported to contain toxic substances (Ishii et al., 1984; Boukandou Mounanga et al., 2015). Therefore, medicinal plants can be 'double edge sword', and proper caution must be taken before using them as the therapeutic intervention. Thorough toxicological profiling of medicinal plants is obligatory before using them as therapeutic agents. This chapter deals with the acute and sub-acute toxicity studies of the crude extract of *S. roxburghiana* rhizomes (SR) and protocatechuic acid.

4.2. Materials and Methods

4.2.1. Chemicals

The kits/reagents for biochemical assays for estimating different biochemical parameters were bought from Span diagnostic Ltd., India and Sigma-Aldrich, USA. All other reagents, solvents and chemicals used were of analytical grade.

4.2.2. Animals

Wistar rats (♂, 150 ± 25 g) were used in toxicity studies. Rats were housed in standard polypropylene cages under standard laboratory conditions of light:dark cycle (12 h:12 h), relative humidity (55 ± 5%), temperature (25 ± 2 °C), standard diet and water ad libitum. The animal experiments were performed at the Department of Pharmaceutical Technology, Jadavpur University, India (Committee for the Purpose of Control and Supervision on Experiments on Animals Reg. No. 0367/01/C/CPCSEA, University Grants Commission, Government of India, New Delhi). The animal experiment has been approved by the Jadavpur University animal ethical committee (Ref no. AEC/PHARM/1502/05/2015 dated 30.07.2015) and the principles of laboratory animals care were observed during experiment (Public Health Service, 2015).

4.2.3. Extraction

The powdered rhizomes were extracted with double distilled water containing 1 % of chloroform for 48 h at 30 ± 5 ºC with constant stirring. Particulate matters were removed by filtration and resulting extract was freeze-dried to obtain the powdered crude extract of *S. roxburghiana* rhizomes (SR, ~10.5 % w/w). Lyophilized powder was dissolved in distilled water containing tween 80 (1 %) before in vivo experiment. The isolation of protocatechuic acid was discussed in the chapter 3 of this thesis.

4.2.4. Oral acute toxicity study

Acute toxicity studies of SR and protocatechuic acid were performed following the standard protocol (Lorke, 1983). Briefly, all the animals were kept fasted overnight with free access to water before initiation of dosing. SR and protocatechuic acid were administered separately to two groups of rats (n = 20). The treatments were started with the initial doses of 25 mg/kg, body weight orally by oral gavage for both the compounds. The dose was increased to 2 folds in every alternative day up to the highest dose of 1600 mg/kg. A group of vehicle-treated 20 rats was kept as control. The animals were individually observed for behavioral changes and general toxicity symptoms after dosing for 48 h, with special attention being paid during the first 4 h after each dosing (Kifayatullah et al., 2015; Bello et al., 2016). The oral acute toxicity values were represented as median lethal dose (LD_{50}), which was calculated using probits scale.

4.2.5. Oral sub-acute toxicity study

The Wister rats were divided into five groups (n = 6) and were treated as follows:

Group I: Normal control (rats received only vehicle for 28 days);

Group II: Rats were treated with SR (50 mg/kg, body weight orally by oral gavage) once daily for 28 days;

Group III: Rats were treated with SR (100 mg/kg, body weight orally by oral gavage) once daily for 28 days;

Group IV: Rats were treated with protocatechuic acid (50 mg/kg, body weight orally by oral gavage) once daily for 28 days;

Group V: Rats were treated with protocatechuic acid (100 mg/kg, body weight orally by oral gavage) once daily for 28 days (Okoye et al., 2012; Yuet Ping et al., 2013).

The body weight, dietary intake, water intake, and behavioral patterns were monitored in a regular basis, with special attention being paid during the first 4 h after dosing (Kifayatullah et al., 2015). On day 29, the blood samples were collected from retro-orbital venous complex using local anesthetic, tetracaine ophthalmic drop (0.5 %; one drop). After blood collection, the rats

were exposed to CO_2 euthanasia followed by sacrificing via cervical dislocation. The haematological parameters viz. total erythrocyte count, haemoglobin (g/dl), total leucocytes count were measured following standard laboratory procedure. Lactate dehydrogenase (LDH), creatine kinase (CK), total cholesterol, HDL cholesterol, triglycerides, alanine aminotransferase (ALT), aspartate aminotransferase (AST), urea, uric acid, and creatinine in sera were assayed by using commercially available kits (Span Diagnostic Limited, India) following manufacturers' protocols. Troponin I and T contents in sera were estimated by enzyme-linked immunosorbent assay (ELISA) using commercially available kits (Kamiya Biomedical Company, US). For histological investigations, the liver, kidney, and heart were excised and immediately fixed in 10% buffered formalin. The fixed tissues were processed for paraffin sectioning. Sections (thickness ~ 5 µm) were stained with eosin & hematoxylin to assess under light microscope (Dewanjee et al., 2013).

4.2.6. Statistical analysis

Data were statistically calculated by utilizing one way ANOVA and expressed as mean ± SD. followed by Dunnett's *t*-test using computerized GraphPad InStat version 3.05, Graph pad software, U.S.A. The significance was considered when $p < 0.05$.

4.3. Results

4.3.1. Acute toxicity studies

The oral acute toxicity profile of SR and protocatechuic acid has been shown in Tables 4.1 and 4.2, respectively. The study revealed that, no death of rat was observed up to 100 and 200 mg/kg of SR and protocatechuic acid, respectively. The oral median lethal doses (LD_{50}) of the test materials were measured using probit scale. By taking probit as 5, the oral LD_{50} values of SR and protocatechuic acid were calculated to be 870 and 2089 mg/kg, respectively (Figures 4.1. and 4.2.).

Table 4.1. The oral acute toxicity profile of SR in rats.

	Doses (mg/kg)							LD_{50}
	25	50	100	200	400	800	1600	(mg/kg)
Number of alive animals	20	20	20	19	17	8	5	~ 870
Number of dead animals	0	0	0	1	3	12	15	(Probit analyzed)

Table 4.2. The oral acute toxicity profile of protocatechuic acid in rats.

	Doses (mg/kg)							LD_{50}
	25	50	100	200	400	800	1600	(mg/kg)
Number of alive animals	20	20	20	20	19	16	8	~ 2089
Number of dead animals	0	0	0	0	1	4	12	(Probit analyzed)

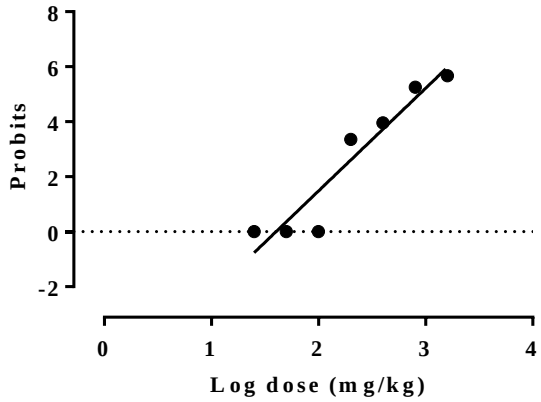

Figure 4.1. Probits vs Log dose curve to predict the oral LD_{50} value of SR.

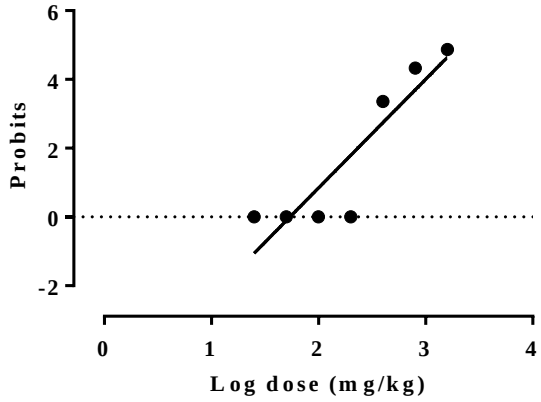

Figure 4.2. Probits vs Log dose curve to predict the oral LD_{50} value of protocatechuic acid.

4.3.2. Sub-acute toxicity study

In sub-acute toxicity study, the animals did not show any sign of behavioral abnormality viz. tremor, convulsions, and/or reflex in either SR (50 and 100 mg/kg) or protocatechuic acid (50 and 100 mg/kg) treated rats and no sign of toxicity was recorded in the wellness parameters during the 28-day observation period. The SR (50 and 100 mg/kg) and protocatechuic acid (50 and 100 mg/kg) treated rats did not exhibit any muscular numbness of the legs, salivation and diarrhoea. The food and water intake per day were also found to be normal. The body weights of SR (50 and 100 mg/kg) and protocatechuic acid (50 and 100 mg/kg) treated rats were comparable to that of normal rats (Table 4.3). No significant change was observed in the body weight gain with time in either SR or protocatechuic acid-treated rats.

Table 4.3. Effect on body weight changes of rats of sub-acute toxicity studies.

Groups	Schedule (Day)					
	1	**3**	**7**	**14**	**21**	**28**
Group I	162.25 ± 14.50	163.22 ± 16.37	167.54 ± 16.21	174.67 ± 16.45	181.50 ± 17.67	188.75 ± 18.50
Group II	160.11 ± 16.89	159.24 ± 17.01	164.33 ± 15.17	171.65 ± 16.22	175.42 ± 17.13	182.14 ± 16.67
Group III	156.48 ± 15.22	157.87 ± 16.17	161.36 ± 16.04	166.24 ± 15.72	171.12 ± 16.33	178.74 ± 17.65
Group IV	161.62 ± 15.89	162.98 ± 16.01	164.66 ± 16.33	168.45 ± 16.57	171.89 ± 16.18	174.87 ± 17.01
Group V	159.48 ± 15.22	161.67 ± 15.72	164.69 ± 17.50	170.52 ± 16.98	174.08 ± 16.54	178.87 ± 17.11

Values were expressed as mean ± SD (n = 6). Group I: Normal control; Group II: Normal rats + SR (50 mg/kg); Group III: Normal rats + SR (100 mg/kg); Group IV: Normal rats + protocatechuic acid (50 mg/kg); Group V: Normal rats + protocatechuic acid (100 mg/kg).

Table 4.4. Effect on hematological and serum biochemical parameters of rats of sub-acute toxicity studies.

Groups / Parameters	Group I	Group II	Group III	Group IV	Group V
Total erythrocyte count ($x10^6/mm^3$)	5.67 ± 0.33	5.72 ± 0.57	5.70 ± 0.82	5.62 ± 0.67	5.73 ± 0.54
Haemoglobin (g/dl)	11.08 ± 1.23	11.23 ± 1.02	11.14 ± 1.37	10.96 ± 1.22	11.27 ± 1.11
Total leucocytes count ($x10^3/mm^3$)	6.23 ± 0.55	6.11 ± 0.67	6.11 ± 0.43	6.18 ± 0.82	6.13 ± 0.62
LDH (U/l)	32.11 ± 2.50	33.67 ± 3.12	32.83 ± 3.58	31.52 ± 2.87	31.98 ± 3.50
CK (IU/ mg protein)	173.33 ± 16.50	175.15 ± 17.85	174.89 ± 15.86	174.21 ± 17.32	171.79 ± 16.33
Cholesterol (mg/dl)	89.25 ± 7.36	91.43 ± 8.17	88.72 ± 8.62	87.85 ± 8.18	89.79 ± 8.07
HDL-cholesterol (mg/dl)	35.06 ± 3.59	37.14 ± 2.89	34.93 ± 3.11	35.33 ± 3.51	36.02 ± 3.03
Triglycerides (mg/dl)	92.33 ± 9.55	93.27 ± 8.41	92.89 ± 7.99	91.76 ± 10.04	92.50 ± 7.13
ALT (IU/l)	62.21 ± 4.32	61.63 ± 6.12	58.74 ± 5.48	60.50 ± 5.11	58.12 ± 5.27
AST (IU/l)	47.17 ± 4.68	47.22 ± 5.08	45.33 ± 4.92	46.78 ± 4.14	45.65 ± 4.37
Urea (mg/dl)	20.29 ± 1.87	21.33 ± 2.54	20.14 ± 2.04	21.12 ± 1.33	20.50 ± 1.92
Uric acid (mg/dl)	2.05 ± 0.22	2.02 ± 0.26	2.02 ± 0.17	1.98 ± 0.13	2.01 ± 0.15
Creatinine (mg/dl)	0.41 ± 0.07	0.41 ± 0.04	0.45 ± 0.04	0.42 ± 0.07	0.40 ± 0.05
Troponin I (ng/ml)	1.31 ± 0.19	1.34 ± 0.22	1.29 ± 0.12	1.34 ± 0.12	1.29 ± 0.25
Troponin T(ng/ml)	470.50 ± 42.33	472.67 ± 49.18	462.11 ± 41.99	458.77 ± 50.08	472.33 ± 41.98

Values were expressed as mean ± SD (n = 6). Group I: Normal control; Group II: Normal rats + SR (50 mg/kg); Group III: Normal rats + SR (100 mg/kg); Group IV: Normal rats + protocatechuic acid (50 mg/kg); Group V: Normal rats + protocatechuic acid (100 mg/kg).

Hematological and serum biochemical parameters were shown in Table 4.4. The SR (50 and 100 mg/kg) and protocatechuic acid (50 and 100 mg/kg) treatments did not cause any significant change in total erythrocytes count and haemoglobin level, and total leucocytes count in experimental rats and the values remain almost comparable to that of normal rats. The levels of

LDH, CK, total cholesterol, HDL-cholesterol, triglycerides, ALT, AST, urea, uric acid, and creatinine, Troponin I, and Troponin II in the sera were estimated. The parameters remained within the normal range after 28 day treatments with SR (50 and 100 mg/kg) and protocatechuic acid (50 and 100 mg/kg). Also, no sign of structural abnormality was observed in the histological sections of liver (A), kidney (B) and heart (C) between the normal and treated rats (Figure 4.3.).

4.4. Discussion

Acute toxicity studies are performed to determine the short-term assessment of potential hazards of pharmacological agents when administered in a single dose (Arome and Chinedu, 2013). Acute toxicity data (LD_{50}) supply idea to perceive therapeutic doses, to estimate the therapeutic index, to reveal of toxic incidence, and to give idea relevant to acute overdosing. However, acute

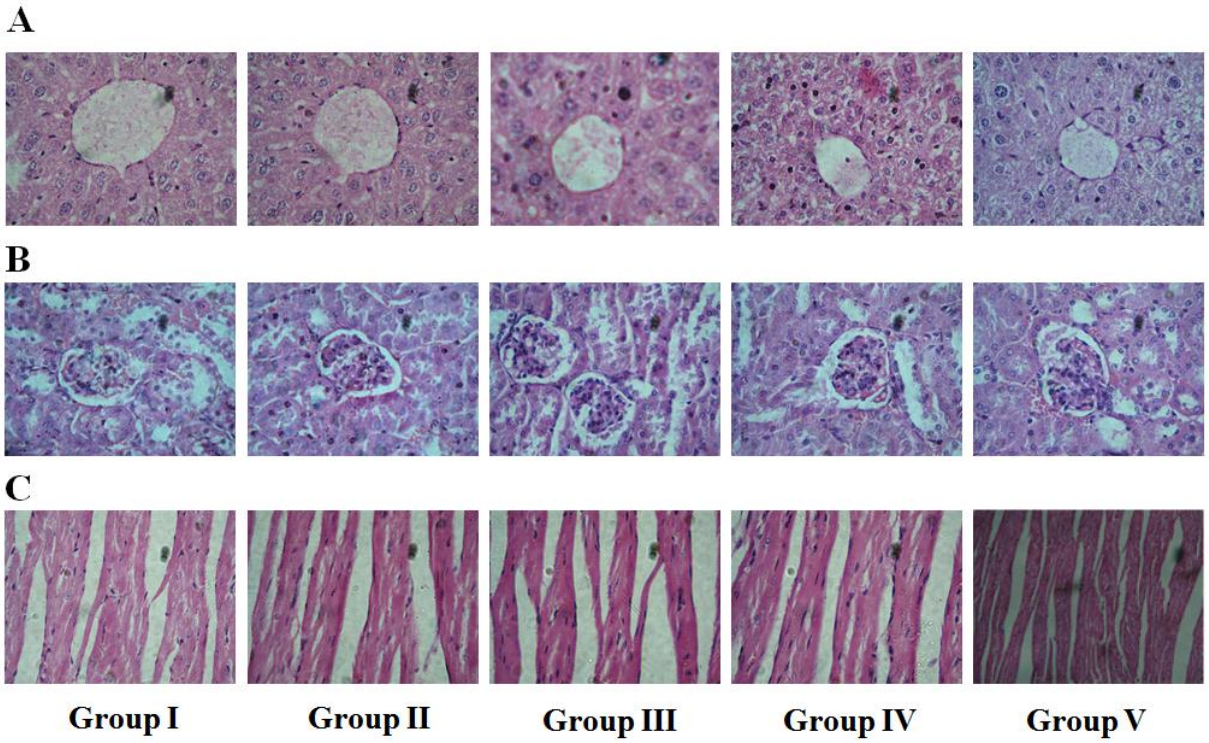

Figure 4.3. Histological sections of liver (A), kidney (B) and heart (C) of rats under different treatments. Group I: Normal control; Group II: Normal rats + SR (50 mg/kg); Group III: Normal rats + SR (100 mg/kg); Group IV: Normal rats + protocatechuic acid (50 mg/kg); Group V: Normal rats + protocatechuic acid (100 mg/kg).

toxicity studies do not reveal the effects of pharmacological agents on vital functions like the cardiovascular, central nervous system, and respiratory systems etc. (Jothy et al., 2011). The acute toxicity study of SR and protocatechuic acid revealed that, oral LD_{50} values were 870 and

2089 mg/kg, respectively in rats. Considering the LD_{50} values and therapeutic (antidiabetic) doses of the test substances, the doses of 50 and 100 mg/kg were chosen for sub-acute toxicity studies of both the test substances. Sub-acute toxicity studies are conducted to reveal the effect of pharmaceutical agents by different dose levels to various organs and to access the nature of toxicity under more realistic situation. Generally, 2-3 doses are normally used in sub-acute toxicity studies (Agrawal and Paridhavi, 2007; Olaniyan et al., 2016). In this study, SR (50 and 100 mg/kg) and protocatechuic acid (50 and 100 mg/kg) were subjected to sub-acute toxicity studies. The behavioral patterns, body weight variations, hematological, serum biochemical, and histological parameters were assessed. Blood parameters give an earliest diagnostic indication of pathological states. Hematological parameters can serve as the pathological and physiological indicators (Kanu et al., 2016). Total erythrocyte counts, haemoglobin levels, and total leucocytes counts following SR (50 and 100 mg/kg) and protocatechuic acid (50 and 100 mg/kg) treatments revealed that SR and protocatechuic acid are non-toxic at the selected doses. LDH, an enzyme present in the cytoplasm of liver, heart, kidneys, pancreas, skeletal muscles, lymph tissues, and blood cells, catalyzes the process of turning sugar into energy (Raddam et al., 2017). CK an enzyme present in the skeletal muscle, cardiac muscle, and the brain, bladder, stomach, and colon, catalyzes the phosphorylation of creatine (Kemp et al., 2004). The increased levels of these enzymes in the sera indicate the pathological incidences in the organs, where they present. The levels of LDH and CK in the sera remained almost comparable to that of normal control after SR (50 and 100 mg/kg) and protocatechuic acid (50 and 100 mg/kg) treatments, which reflected that the test materials do not possess any toxic happening to the aforementioned organs. AST is an enzyme distributed in the cytosol of almost all tissues (except) bone, with highest levels in liver and skeletal muscle. It catalyzes the inter-conversion of aspartate and α-ketoglutarate to oxaloacetate and glutamate (Ellinger et al., 2011). ALT, an enzyme present in liver, heart, kidneys, pancreas, spleen, and lung, which catalyzes the transfer of amino groups form L-alanine to α-ketoglutarate (Kim et al., 2008). ALT and AST serve as the markers of liver functions; however, ALT is more specific to the liver (Kim et al., 2008). The normal levels of AST and ALT in the sera indicated that SR (50 and 100 mg/kg) and protocatechuic acid (50 and 100 mg/kg) did not produce any sign of hepatotoxicity. Lipids are one of the important cellular components which regulate many cellular functions and homeostasis. Liver plays vital role in lipid biosynthesis, metabolism and transportation (Ghadir et al., 2010). Therefore, abnormality lipids profile in sera would indicate the pathological status of the liver (Ghadir et al., 2010). In this study, the normal levels of total cholesterol, HDL-cholesterol, triglycerides in the sera of rats following SR (50 and 100 mg/kg) and protocatechuic acid (50 and 100 mg/kg) treatments

indicated that SR (50 and 100 mg/kg) and protocatechuic acid did not produce any sign of hepatotoxicity. The serum levels of urea, uric acid and creatinine indicate renal physiology (Musso et al., 2012; Khanra et al., 2017). The normal levels of urea, uric acid, and creatinine in the sera indicated that SR (50 and 100 mg/kg) and protocatechuic acid (50 and 100 mg/kg) did not produce any sign of nephrotoxicity. Troponins have both diagnostic and predictive importance in the setting of acute coronary syndrome (Daubert and Jeremias, 2010). Additionally, increase in the levels of troponin I and troponin II in the absence of acute coronary syndrome is indicative of myocardial infarction and cardiac damage (Daubert and Jeremias, 2010; Bhattacharjee et al., 2017). The normal levels of troponin I and troponin II in the sera indicated that SR (50 and 100 mg/kg) and protocatechuic acid (50 and 100 mg/kg) did not produce any sign of cardiotoxicity. Finally, the histological observations were also in the agreement to the above findings.

In conclusion, SR (50 and 100 mg/kg) and protocatechuic acid (50 and 100 mg/kg) treated rats did not influence either of haematological, serum biochemical and histological parameter in the rats as compared to normal control. Therefore, SR (50 and 100 mg/kg) and protocatechuic acid (50 and 100 mg/kg) are safe for executing further studies with these doses of SR and protocatechuic acid, which are detailed in the subsequent chapters of this thesis.

References

Agrawal SS, Paridhavi M. Herbal drug technology. Universities press, India. 2007.

Arome D, Chinedu E. The importance of toxicity testing. J Pharm Biosci. 2013;4:146-148.

Bello I, Bakkouri AS, Tabana YM, Al-Hindi B, Al-Mansoub MA, Mahmud R, Asmawi MZ. Acute and sub-acute toxicity evaluation of the methanolic extract of *Alstonia scholaris* stem bark. Med Sci. 2016;4:4.

Bhattacharjee N, Dua TK, Khanra R, Joardar S, Nandy A, Saha A, De Feo V, Dewanjee S. protocatechuic acid, a phenolic from *Sansevieria roxburghiana* leaves, suppresses diabetic cardiomyopathy via stimulating glucose metabolism, ameliorating oxidative stress, and inhibiting inflammation. Front Pharmacol. 2017;8:251.

Bluemel J. Toxicity testing in the 21st century: challenges and perspectives. J Drug Metab Toxicol. 2012;3:e112.

Boukandou Mounanga M, Mewono L, Aboughe Angone S. Toxicity studies of medicinal plants used in sub-Saharan Africa. J Ethnopharmacol. 2015;174:618-627.

Daubert MA, Jeremias A. The utility of troponin measurement to detect myocardial infarction: review of the current findings. Vasc Health Risk Manag. 2010;6:691-699.

Dewanjee S, Das AK, Sahu R, Gangopadhyay M. Antidiabetic activity of *Diospyros peregrina fruit*: Effect on hyperglycemia, hyperlipidemia and augmented oxidative stress in experimental type 2 diabetes. Food Chem Toxicol. 2009;47:2679-2685.

Dewanjee S, Gangopadhyay M, Sahu R, Karmakar S. Cadmium induced pathophysiology: Prophylactic role of edible jute (*Corchorus olitorius*) leaves with special emphasis on oxidative stress and mitochondrial involvement. Food Chem Toxicol. 2013;60:188-198.

Dua TK, Dewanjee S, Khanra R, Bhattacharya N, Bhaskar B, Zia-Ul-Haq M, De Feo V. The effects of two common edible herbs, Ipomoea aquatica and Enhydra fluctuans, on cadmium-induced pathophysiology: a focus on oxidative defence and anti-apoptotic mechanism. J Transl Med. 2015;13:245.

Ellinger JJ, Lewis IA, Markley JL. Role of aminotransferases in glutamate metabolism of human erythrocytes. J Biomol NMR. 2011;49:221-229.

Ghadir MR, Riahin AA, Havaspour A, Nooranipour M, Habibinejad AA. The relationship between lipid profile and severity of liver damage in cirrhotic patients. Hepat Mon. 2010;10:285-288.

Han C-T, Kim M-J, Moon S-H, Jeon Y-R, Hwang J-S, Nam C, Park C-W, Lee S-H, Na J-B, Park C-S, Park H-W, Lee J-M, Jang H-S, Park S-H, Han K-G, Choi YW, Lee H-Y. Acute and

28-day subacute toxicity studies of hexane extracts of the roots of *Lithospermum erythrorhizon* in Sprague-Dawley Rats. Toxicol Res. 2015;31:403-414.

Ishii R, Yoshikawa H, Minakata NT, Komura K, Kada T. Specificity of bioantimutagens in the plant kingdom. Agric Biol Chem. 1984;48:2587-2591.

Jothy SL, Zakaria Z, Chen Y, Lau YL, Latha LY, Sasidharan S. Acute oral toxicity of methanolic seed extract of *Cassia fistula* in mice. Molecules. 2011;16:5268-5282.

Kanu KC, Ijioma SN, Atiata O. Haematological, biochemical and antioxidant changes in Wistar rats exposed to dichlorvos based insecticide formulation used in Southeast Nigeria. Toxics 2016;4:28.

Kemp M, Donovan J, Higham H, Hooper J. Biochemical markers of myocardial injury. Br J Anaesth. 2004;93:63-73.

Khanra R, Bhattacharjee N, Dua TK, Nandy A, Saha A, Kalita J, Manna P, Dewanjee S. Taraxerol, a pentacyclic triterpenoid, from *Abroma augusta* leaf attenuates diabetic nephropathy in type 2 diabetic rats. Biomed Pharmacother. 2017;94:726-741.

Kifayatullah M, Mustafa MS, Sengupta P, Sarker MMR, Das A, Das SK. Evaluation of the acute and sub-acute toxicity of the ethanolic extract of *Pericampylus glaucus* (Lam.) Merr. in BALB/c mice. J Acute Dis. 2015;4:309-315.

Kim WR, Flamm SL, Di Bisceglie AM, Bodenheimer Jr. HC. Serum activity of alanine aminotransferase (ALT) as an indicator of health and disease. Hepatol. 2008;47:1363-1370.

Kimm-Brinson KL, Ramsdell JS. The red tide toxin, brevetoxin, induces embryo toxicity and developmental abnormalities. Environ Health Perspect. 2001;109:377-381.

Lorke D. A new approach to practical acute toxicity testing. Arch Toxicol. 1983;54:275-284.

Musso CG, Gregori JA, Jauregui JR, Núñez JFM. Creatinine, urea, uric acid, water and electrolytes renal handling in the healthy oldest old. World J Nephrol. 2012;1:123-126.

Okoye TC, Akah PA, Ezike AC, Okoye MO, Onyeto CA, Ndukwu F, Ohaegbulam E, Ikele L. Evaluation of the acute and sub-acute toxicity of *Annona senegalensis* root bark extracts. Asian Pac J Trop Med. 2012;5:277-282.

Olaniyan JM, Muhammad HL, Makun HA, Busari MB, Abdullah AS. Acute and sub-acute toxicity studies of aqueous and methanol extracts of *Nelsonia campestris* in rats. J Acute Dis. 2016;5:62-70.

Oliveira CD, Moreira CQ, de Sá LR, Spinosa Hde S, Yonamine M. Maternal and developmental toxicity of ayahuasca in Wistar rats. Birth Defects Res B Dev Reprod Toxicol. 2010;89:207-212.

Parasuraman S. Toxicological screening. J Pharmacol Pharmacother. 2011;2:74-79.

Public Health Service (PHS). Public Health Service Policy on Human Care and Use of Laboratory Animals. Washington, DC: US Department of Health and Human Services, National Institute of Health, Office of Laboratory Animal welfare, 2015.

Raddam QN, Zeidan MM, Abdulrahman MA, Asaad NK. Smoking effects on blood antioxidants level: lactate dehydrogenase, catalase, superoxide dismutase and glutathione peroxidase in university students. J Clin Exp Pathol. 2017;7:6.

Subramanian K, Sankaramourthy D, Gunasekaran M. Toxicity studies related to medicinal plants. In: Natural Products and Drug Discovery. 2018;Chapter-18:491-505.

Yuet Ping K, Darah I, Chen Y, Sreeramanan S, Sasidharan S. Acute and subchronic toxicity study of *Euphorbia hirta* L. methanol extract in rats. Biomed Res Int. 2013;2013:Article ID 182064.

Zepnik H, Völkel W, Dekant W. Toxicokinetics of the mycotoxin ochratoxin A in F 344 rats after oral administration. Toxicol Appl Pharmacol. 2003;192:36-44.

Web references

http://alttox.org/(non-animalmethodsoftoxicitytesting)

http://ecb.jrc.ec.europa.eu/documents/Testing-Methods/ANNEXV/B32web1988

http://www.eoearth.org/view/article/1566.73/

http://www.ich.org/

http://www.oecd.org/dataoecd/20/52/37622194

https://www.fda.gov/

5.1. Introduction

Diabetes mellitus (DM), a chronic metabolic syndrome, contributes considerably in the global health crisis (Kalofoutis et al., 2007). Amongst various types, type 2 diabetes mellitus (T2DM) constitutes > 90 % of total diagnosed DM (Olokoba et al., 2012; https://www.diabetes.co.uk/). DM is characterized by persistent hyperglycemia which damages many organs and tissues via different mechanisms (Khanra et al., 2015). Amongst various anticipated mechanisms, hyperglycemia mediated oxidative stress and inductions of vascular inflammation have been found to play the key roles in diabetic pathophysiology (Manna and Sil, 2012; Khanra et al., 2015). Persistent hyperglycemia causes glucose auto-oxidation leading to the over-production of intercellular reactive oxidative species (ROS) viz. superoxide radical, hydrogen peroxide and hydroxide radical. The excess of ROS provides oxidative stress to the cardiomyocytes and induces cellular damage. Increased amount of ROS activates protein kinase C (PKC) and nuclear factor-κB (NF-κB). The activation of aforementioned signal molecules play key role in hyperglycemia mediated myocardial injury (Khanra et al., 2015; Bhattacharjee et al., 2016). Activation of Poly ADP ribose polymerase (PARP) during diabetic state induces a down regulation of cellular NAD and ATP, leading to energy failure and cell necrosis (Bhattacharjee et al., 2016). Besides, NF-κB activation stimulates inflammatory mediators viz. interleukins (ILs), tumor necrosis factor α (TNF α), monocyte chemo-attractant protein 1 (MCP 1), intercellular adhesion molecule 1 (ICAM 1), vascular endothelial growth factor (VEGF) and thereby induces myocardial inflammation (Szabo 2002; Wolf et al., 2005). In spite of modern therapeutic strategies and educational programs, the incidence of T2DM is still unabated (Cheng, 2005). Commercially available oral hypoglycemic agents also exhibit plenty of adverse effects including congestive heart failure with glitazones (https://www.fda.gov.), gastrointestinal disturbances with glucosidase inhibitors, sulfonylureas and meglitinides (Van de Laar et al., 2005; Bennett et al., 2011). Cardiac problems and weight gain are common adverse effects of sulfonyl ureas (Bastaki, 2005). Therefore, it is a vital need to develop a unique therapeutic agent for T2DM with less toxic/adverse effects. Considering several mechanisms of diabetic pathophysiology, it has been predicted that a multi-target therapeutic agent would be advantageous in the management of T2DM and its associated pathogenesis. Multi-component plant extract would offer the multimodal therapeutic values. Therefore, current study has been designed to explore the antidiabetic potential of a chemically standardize plant extract considering ethnomedicinal knowledge as reference.

S. roxburghiana, commonly known as Indian bowstring heamp, is a perennial herb with short fleshy stem and plump rootstock. This plant is distributed throughout the coastal India and other

tropical and subtropical countries (Eggli, 2002). The roots and rhizomes of *S. roxburghiana* are used in the traditional medicine as the remedies for diabetes, inflammation, pains, fever, asthma, wound, hypertension, oxidative stress and rheumatism (Kirtikar and Basu, 1935; Mortan, 1981; Dhiman, 2006; Pulliah; 2006; Haldar et al., 2010; Philip et al., 2011). Since *S. roxburghiana* is believed to exhibit anti-inflammatory as well as antidiabetic potential, the present study has been undertaken to establish the curative efficacy of *S. roxburghiana* rhizome against T2DM and its related pathogenesis in the cardiac tissues of experimental Wistar rats.

5.2. Material and Methods

5.2.1. Chemicals

Streptozotocin was procured from Hi-media (Mumbai, India). Ammonium sulphate, 1-chloro-2,4-dinitrobenzene, ethylenediaminetetraacetic acid, 2,4-dinitro-phenyl-hydrazine, 5,5-di-thio-bi(2-nitrobenzoic acid), potassium dihydrogen phosphate, N-ethylmaleimide, reduced nicotinamide adenine dinucleotide, nitro blue tetrazolium, sodium pyrophosphate, phenazinemethosulphate, thiobarbituric acid, reduced glutathione, sodium azide, trichloro acetic acid and 5-thio-2-nitrobenzoic acid were obtained from Sisco Research Laboratory (India). Bradford reagent, antibodies and bovine serum albumin were procured from Sigma-Aldrich (St. Louis, USA). The kits for different assays for different biochemical parameters were purchased from Span diagnostic Ltd., India. All other reagents and chemicals used were of analytical grade.

5.2.2. Animals

Wistar rats (♂, 150 ± 25 g) were used in this experiment. Rats were housed in standard polypropylene cages under standard laboratory conditions of light:dark cycle (12 h:12 h), relative humidity (55 ± 5%), temperature (25 ± 2 °C), standard diet and water ad libitum. The animal experiments were performed at the Department of Pharmaceutical Technology, Jadavpur University, India (Committee for the Purpose of Control and Supervision on Experiments on Animals Reg. No. 0367/01/C/CPCSEA, University Grants Commission, Government of India, New Delhi). The animal experiment has been approved by the Jadavpur University animal ethical committee (Ref no. AEC/PHARM/1502/05/2015 dated 30.07.2015) and the principles of laboratory animals care were observed during experiment (Public Health Service, 2015).

5.2.3. Extraction

The powdered rhizomes were extracted with double distilled water containing 1 % of chloroform for 48 h at 30 ± 5 ºC with constant stirring. Particulate matters were removed by filtration and resulting extract was freeze-dried to obtain the powdered crude extract of *S. roxburghiana* rhizomes (SR, ~10.5 % w/w). Lyophilized powder was dissolved in distilled water containing tween 80 (1 %) before in vivo experiment.

5.2.4. Oral Glucose Tolerance Test (OGTT)

Pre-acclimatized Wistar rats (overnight fasted) were divided into 3 groups (n = 6). The animals were given glucose (1.5 g/kg body weight, orally by oral gavage) (Khanra et al., 2015). Immediately after the feeding of glucose solution, 2 groups of rats were treated with SR (50 & 100 mg/kg body weight, orally by oral gavage) and 1 group of animals (normal control) were treated with 1% tween 80 (2 ml/kg, orally by oral gavage). Blood glucose levels were measured @ 0, 30, 60, and 120 min with single touch glucometer (Ascensia Entrust, Bayer Health Care, USA). Total glycemic responses have been calculated from respective areas under the curve (AUC) throughout the observation period of 120 min.

5.2.5. Induction of T2DM and Experimental design

T2DM was induced by high fat diets (25% protein, 17% carbohydrate and 58% fat, as %-age of total kcal) ad libitum and low-dose of streptozotocin as described by Reed et al. (2009). Briefly, the rats were fed high fat diets ad libitum for 2 weeks and then treated with single dose of streptozotocin (35 mg/kg body weight, intraperitonially) (Reed et al., 2009). The composition (Table 5.1) of high fat diet has been described by Srinivasan et al. (2005). One week after streptozotocin injection, the fasting blood glucose levels were appraised and the animals exhibiting fasting blood glucose levels of 170 ± 30 mg/dl were considered to be type 2 diabetic (T2D) rats and included for the further experiments. The rats were continued with high fat diets throughout the course of the study.

Table 5.1. The composition of high fat diet (Reed et al., 2009; Srinivasan et al., 2004).

Ingredients	Diets (g/kg body weight)
Powdered NPD	365
Lard	310
Casein	250
Cholesterol	10
Vitamin and mineral mix	60
Yeast powder	01
Sodium chloride	01

The Wister rats were divided into following groups (n = 6) and received the treatment as follows for 28 days:

Group I: Normal control rats were administered 1% tween 80 (2 ml/kg body weight, orally by oral gavage) in distilled water daily;

Group II: T2DM control rats were administered high fat diets + 1% Tween 80 (2 ml/kg body weight, orally by oral gavage) in distilled water daily;

Group III: T2D rats were administered high fat diets + SR (50 mg/kg body weight, orally by oral gavage) daily;

Group IV: T2D rats were administered high fat diets + SR (100 mg/kg body weight, orally by oral gavage) daily;

Group V: T2D rats were administered high fat diets + glibenclamide (1 mg/kg body weight, orally by oral gavage) daily (Dewanjee et al., 2009).

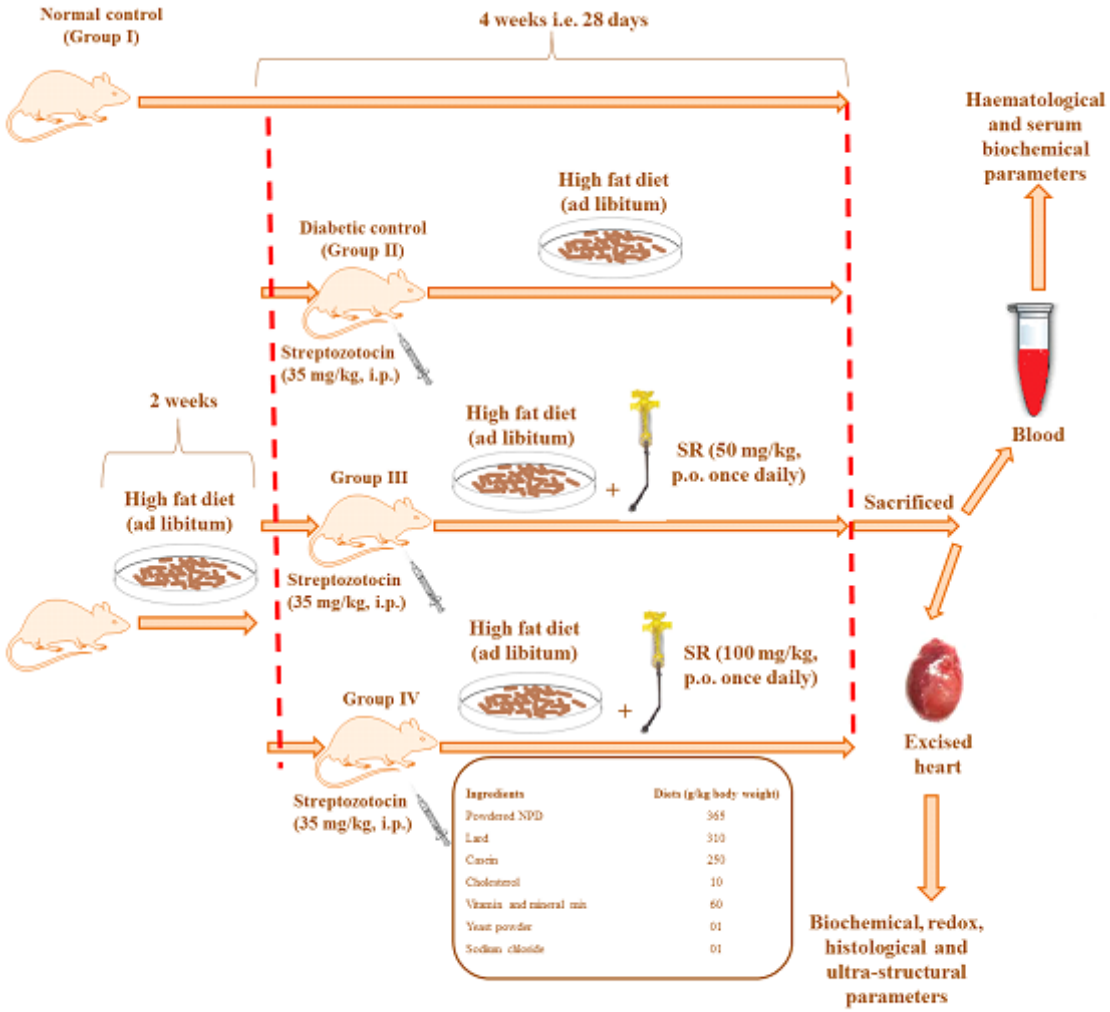

Figure 5.1. A schematic impression of in vivo experiment.

A group (Group VI) has been included, in which rats were administered high fat diets throughout the course of study. This group of animals served as obese control. The selection of doses was entirely based on the OGTT observation. The grouping of animals was done as per the instruction was given by the institutional animal ethical committee and on the basis of statistical analysis. The overall experimental design has been depicted in Figure 5.1. The animals were monitored at 8-hours interval for checking any sign of distress and abnormality.

5.2.6. Determination of fasting blood glucose level and other serum biochemical parameters

Fasting blood glucose levels of overnight fasted rats were estimated on day 0, 1, 3, 7, 14, 21, 28 with single touch glucometer (Ascensia Entrust, Bayer Health Care, USA). After 28 days of the treatment, animals were exposed to CO_2 euthanasia and sacrificed by cervical dislocation (Dewanjee et al., 2015). Before sacrifice, the blood samples were obtained from retro-orbital venous plexus for serum biochemical assays. Retro-orbital bleeding was carried out without general anesthesia, however, tetracaine (0.5 %) ophthalmic anesthetic drop was applied prior to the blood collection. The lactate dehydrogenase (LDH), creatine kinase (CK), HDL cholesterol, triglycerides and total cholesterol contents were measured by commercial kits (Span Diagnostic Limited, India) following the protocol mentioned by the manufacturer. LDL cholesterol was estimated by using Friedewald's equation (LDL cholesterol = Total cholesterol – Triglycerides/5 – HDL cholesterol) (Friedewald et al., 1972). Triglyceride/5 is considered to be the equivalent to VLDL cholesterol level (Mohammed et al., 2016). Troponin I and T contents were determined by ELISA kits (Kamiya Biomedical Company, USA). IL 1β, IL 6 and TNF α contents were analyzed by ELISA kits (Fisher Thermo Scientific Co., USA). Nayak and Pattabiraman's (1981) method was followed to assess the glycosylated hemoglobin concentration. Insulin concentration was measured by ELISA kits (Sigma-Aldrich, USA). Homeostatic model assessments viz. HOMA-IR and HOMA-β scores were calculated employing the following formulae (Mohammed et al., 2016).

HOMA-IR = [(Fasting serum insulin in U/l x Fasting blood glucose in mmol/l)/22.5]

HOMA-β = (Fasting serum insulin in U/l x 20/Fasting blood glucose in mmol/l – 3.5)

MCP 1, ICAM 1 and VEGF levels were estimated by the ELISA using commercially available kits (R&D Systems, Inc. USA) and following manufacture's protocol.

5.2.7. Biochemical parameters of myocardial tissue

The hearts were excised, cleaned immediately with phosphate buffer saline (ice cold; pH 7.4). Cardiomyocytes were isolated from the immediately decapitated hearts of the experimental rats following the method described by Nair and Nair (1997) with little modification (Raghu and Cherian, 2009). Intracellular ROS production was performed in accordance to the method of

LeBel and Bondy (1990) employing 2,7-dichlorofluorescein diacetate (DCF) as a probe. The method has been slightly modified as mentioned by Kim et al. (1996). The DCF development was evaluated at the excitation and the emission wavelengths of 488 and 510 nm, respectively in a fluorescence spectrometer (HITACHI, Model No. F4500, Japan). The hearts were homogenized in 0.1 M Tris-HCl-0.001 M EDTA buffer (pH 7.4) and centrifuged (@ 12,000 g; 30 min; 4 ºC). The supernatants were collected for the biochemical assays. The extent of lipid peroxidation (TBARS level) was estimated following the method of Ohkawa and co-workers (1979). The carbonylation of proteins was measured as per the method described by Uchida and Stadtman (1993). Co-enzymes Q9 and Q10 were appraised employing HPLC as per standard protocol (Zhang et al., 1995). The level of reduced glutathione (GSH) was assayed by the method described by Hissin and Hilf (1973). The levels of endogenous redox enzymes viz. catalase (CAT), superoxide dismutase (SOD), glutathione peroxidase (GPx), glutathione-S-transferase (GST) and glutathione-6-phosphate dehydrogenase (G6PD) were assessed as the per standard methods (Ghosh et al., 2010). The degree of DNA fragmentation in the selected tissues was measured by the diphenylamine reaction as described by Lin et al. (1997). DNA oxidation was assessed by HPLC and was denoted as the ratio of 8-OHdG to 2-dG (Bolner et al., 2011). NAD content was assayed as described by Matsumura and Miyachi (1980). Intracellular ATP concentration was estimated using the commercially available assay kit (Abcam, MA, USA).

5.2.8. Immunoblotting

The protein samples for specific cellular components (whole cell, cytosolic and nuclear fractions) were separated following standard sequential fractionation process as described by Baghirova et al. (2015). Sample proteins (20 µg) isolated from the cardiac tissues of the experimental animals of different groups were subjected to SDS-PAGE (12%) for the separation of proteins and transferred into nitrocellulose membrane following standard transfer protocol (Dua et al., 2015a). These membranes were blocked by blocking buffer (containing 5% non-fat dry milk; 1 h; room temperature) and subsequently incubated with primary antibodies anti-PKC β (1:500), anti-PKC ε (1:500), anti-PKC δ (1:500), anti-NF-κB (1:2000), anti-PARP (1:2000) and anti-IκBα (1:2000) at 4°C overnight followed by washing with tris-buffered saline (TBST; containing 0.1% tween 20). The membranes were then subjected to suitable HRP-conjugated secondary antibody (1: 3000) at room temperature (1 h). The blots were finally recognized by 3,3′-diaminobenzidine tetrahydrochloride (Banglore Genei, India). The membranes were then exposed to mild stripping in stripping buffer containing 1% SDS (pH 2.0) and glycine (25 mM) followed by application of anti-β actin (1:6000) primary antibody (@ 4°C) overnight (Dua et al., 2016). The membranes were then rinsed with TBST followed by secondary antibody treatment as mentioned before.

5.2.9. Histological assessment

Hearts from the animals (normal and experimental) were immediately fixed in formalin (10% buffered) after sacrifice and were processed for paraffin sectioning. Sections (thickness ~ 5 µm) were stained (eosin & hematoxylin) to assess under light microscope (Dewanjee et al., 2017). For scanning electron microscopy (SEM), isolated animal tissues were processed for the complete removal of blood. Then, the tissues were subjected to stepwise dehydration process following tissue perfusion and fixation (Carlson and Hinds, 1981; Liang et al., 2002). Completely dried heart tissues were embedded in araldite. After hardening, resin blocks were subjected to ultra-microtome cutter for ultra-thin sectioning. The sections were observed under analytical SEM (ZEISS EVO 60 scanning electron microscope, Germany) machine with Oxford EDS detector, Germany.

5.2.10. Statistical analysis

One-way ANOVA was utilized for statistical analysis of data and expressed as mean ± SD followed by Dunnett's *t*-test using computerized GraphPad InStat (version 3.05), GraphPad software, USA. The values were considered significant when $p < 0.05$.

5.3. Results

5.3.1. Effect on OGTT

In order to find out the effect of SR on systemic glucose homeostasis, OGTT has been executed (Figure 5.2.A). The OGTT revealed that, the administration of SR (50, 100 mg/kg) significantly

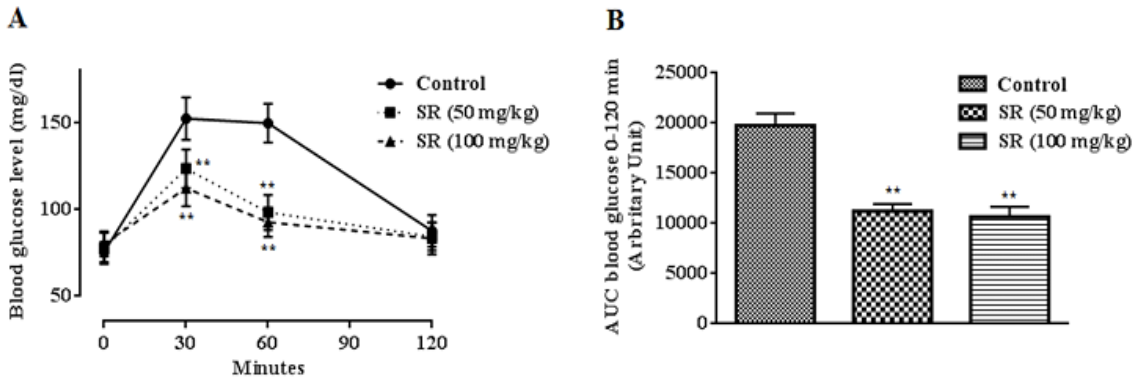

Figure 5.2. Effect of SR on oral glucose tolerance test (A); the areas under the curve (AUC) were calculated using the trapezoid method (B). Data were expressed as mean ± SD (n = 6); *$p < 0.05$ compared with control group; **$p < 0.01$ compared with control group.

reduced ($p < 0.01$) blood glucose concentrations between 30-60 min after glucose (1.5 mg/kg) treatment as compared with normal control group. SR also exhibited a significant persuade on

total hypoglycaemic response revealed by the significant lessening of AUC as compared with the normal control animals (Figure 5.2.B).

5.3.2. Effect on fasting blood glucose level

T2D control rats exhibited a significantly raised ($p < 0.01$) fasting blood glucose level (170 ± 30 mg/dl) before the initiation (Day 0) of the therapeutic regime (Table 5.2.). The principle therapeutic strategy for DM is to maintain the blood glucose level near to normal status. SR (50 and 100 mg/kg) treatment could significantly ($p < 0.05$-0.01) alleviate fasting blood glucose level, which was observed in the fasting blood glucose levels from day 3 onward. Significant reduction of fasting blood glucose levels was observed on day 3 following SR treatment with the values of ~ 16.1 % ($p < 0.05$) and ~ 17.9 % ($p < 0.01$) for the doses of 50 and 100 mg/kg, respectively (compared to that of fasting blood glucose level on day 0). The experimental observation revealed gradual decrease ($p < 0.01$) in fasting blood glucose levels following SR treatment in either of the selected doses. However, maximum therapeutic efficacy was observed on 28th day of the treatment with a decrease of ~ 25.7 % ($p < 0.01$) and ~ 37.4 % ($p < 0.01$) for the doses of 50 and 100 mg/kg body weight, respectively. The standard drug glibenclamide (1 mg/kg) showed maximum decrease of ~ 48.1 % ($p < 0.01$) on day 28 (Table 5.2.).

Table 5.2. Effect of SR on fasting blood glucose level of T2D rats.

Groups	Fasting blood glucose level (mg/dl) in days						
	0	1	3	7	14	21	28
Group I	76.01 ± 5.94	74.28 ± 5.53	77 .04 ± 4.72	76.39 ± 6.11	74.94 ± 3.27	76.50 ± 7.24	75.22 ± 4.56
Group II	171.94 ± 17.71$^{\#}$	173.16 ± 13.58$^{\#}$	176.76± 13.03$^{\#}$	184.31± 19.84$^{\#}$	186.12 ± 18.79$^{\#}$	193.23± 18.62$^{\#}$	191.88 ± 16.67$^{\#}$
Group III	173.15 ± 13.06$^{\#}$	166.27 ± 14.59$^{\#}$	145.22 ± 15.57*	131.04 ± 16.64**	133.04 ± 15.09**	130.15 ± 16.63**	128.67 ± 13.21**
Group IV	173.03 ± 15.90$^{\#}$	159.28 ± 11.95$^{\#}$	142.11 ± 14.88**	125.11± 18.09**	118.07 ± 14.01**	112.69 ± 12.71**	108.39 ± 14.55**
Group V	172.38 ± 13.22$^{\#}$	166.07 ± 16.02$^{\#}$	139.08 ± 17.35**	114.27 ± 14.18**	107.61 ± 8.69**	96.33 ± 11.07**	89.44 ± 10.33**

Data were expressed as mean ± SD (n=6). $^{\#}p< 0.01$ compared with Group I; *p< 0.05 compared with Group II; **p< 0.01 compared with Group II. Group I: Normal control; Group II: T2D control, Group III: T2D rats treated with SR (50 mg/kg, orally); Group IV: T2D rats treated with SR (100 mg/kg, orally); Group V: T2D rats treated with glibenclamide (1 mg/kg, orally).

5.3.3. Effect on serum biochemical parameters

The effects of SR on serum biochemical parameters have been presented in Table 5.3. Significantly increased levels of total cholesterol ($p < 0.01$) and triglycerides ($p < 0.01$) in the T2D rats would corroborate the relationship between hyperlipidemia and hyperglycemia. T2D rats exhibited significantly ($p < 0.01$) low level of serum HDL cholesterol with concomitant increment ($p < 0.01$) of LDL cholesterol level. However, SR (100 mg/kg) treatment could

significantly reinstate the serum lipid ($p < 0.05$-0.01) levels in T2D rats to near normal status. In this study, T2D rats displayed a significantly ($p < 0.01$) high level of glycosylated-haemoglobin. An elevated blood glucose concentration in T2D rats is accountable to the up-regulation of glycosylation of proteins. However, SR (100 mg/kg) treatment significantly ($p < 0.05$) attenuated the glycosylation of haemoglobin to near normal status, which may be due to hypoglycemic effect of SR. The significantly ($p < 0.01$) raised serum levels of membrane bound enzymes, LDH and CK, revealed the cellular injury due to disintegration of sarcoplasmic membrane. SR (50 and 100 mg/kg) could significantly reduce T2D mediated cellular damage resulting significantly ($p < 0.05$) reduced levels of CK and LDH in sera. In this study, C-reactive protein level was significantly ($p < 0.01$) elevated in the sera of T2D animals. An increased level of C-reactive protein stipulated the occurrence of inflammatory disturbances, however, treatment with SR (50 and 100 mg/kg) could significantly ($p < 0.01$) decrease the C-reactive protein levels in T2D rats. Serum levels of troponins I and T are considered to be the specific markers for myocardial cell injury. The significant increases in the levels of serum troponins I ($p < 0.05$) and T ($p < 0.01$) were observed in T2D rats. SR (100 mg/kg) treatment could significantly attenuate the serum troponins I ($p < 0.05$) and T ($p < 0.01$) levels in T2D rats.

Table 5.3. Effect of SR on serum lipid profile, glycosylated haemoglobin, membrane bound enzymes, C-reactive proteins and troponin levels of T2D rats.

Parameters	Group I	Group II	Group III	Group IV	Group V
Total cholesterol (mg/dl)	92.33± 6.54	156.48 ± 13.21$^{\#}$	118.67 ± 9.87*	112.89 ± 6.21**	105.50 ± 8.62**
HDL cholesterol (mg/dl)	31.21 ± 3.12	17.67 ± 2.11$^{\#}$	25.43 ± 2.85	27.86 ± 2.09*	27.98 ± 2.92*
Triglycerides (mg/dl)	116.75 ± 14.56	202.37 ± 19.22$^{\#}$	156.88 ± 17.65	138.76 ± 14.32*	133.56 ± 15.67*
LDL cholesterol (mg/dl)	37.78 ± 3.45	174.22 ± 9.67$^{\#}$	61.47 ± 5.11**	57.28 ± 4.98**	50.81 ± 5.23**
Glycosylated haemoglobin (mg/g haemoglobin)	0.32± 0.11	0.63 ± 0.25$^{\#}$	0.41 ± 0.16	0.38 ± 0.07*	0.34 ± 0.09**
Lactate dehydrogenase (U/l)	187.08± 12.33	285.07 ± 21.15$^{\#}$	218.56 ± 17.92*	215.34 ± 18.50*	202.58 ± 20.80*
Creatine kinase (IU/mg of protein)	9.42 ± 1.45	19.05 ± 2.04$^{\#}$	13.24 ± 1.01*	12.67 ± 1.31*	12.33 ± 1.29**
C-reactive protein (mg/dl)	1.14 ± 0.48	3.01 ± 0.72$^{\#}$	1.67 ± 0.35**	1.41 ± 0.48**	1.32 ± 0.29**
Troponin I (ng/ml)	0.045 ± 0.014	0.087± 0.02$^{\$}$	0.06 ± 0.017	0.048 ± 0.028*	0.048 ± 0.033*
Troponin T (ng/ml)	0.012 ± 0.002	0.027 ± 0.003$^{\#}$	0.02 ± 0.007*	0.017 ± 0.0008**	0.015 ± 0.003**

Data were expressed as mean ± SD (n=6). $^{\$}p< 0.05$ compared with Group I; $^{\#}p< 0.01$ compared with Group I; *$p< 0.05$ compared with Group II; **$p< 0.01$ compared with Group II. Group I: Normal control; Group II: T2D control, Group III: T2D rats treated with SR (50 mg/kg, orally); Group IV: T2D rats treated with SR (100 mg/kg, orally); Group V: T2D rats treated with glibenclamide (1 mg/kg, orally).

In this study, T2D rats exhibited significantly lower ($p < 0.01$) level of serum insulin and HOMA-β score as compared to normal rats (Figure 5.3.). However, a significantly high ($p < 0.01$) HOMA-IR score was observed in T2D rats (Figure 5.3.). 28-day treatment of SR (50 and 100 mg/kg) could significantly reversed serum insulin level ($p < 0.01$), HOMA-IR ($p < 0.05$-0.01) and HOMA-β ($p < 0.01$) scores near to normalcy (Figure 5.3.).

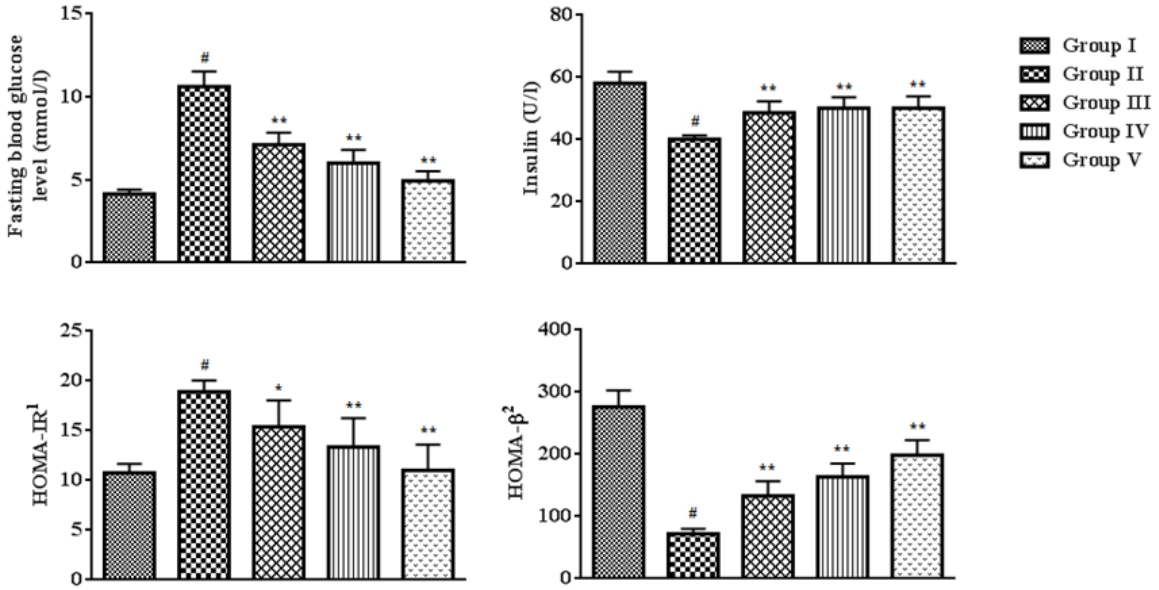

Figure 5.3. Effect of SR on blood glucose, serum insulin, HOMA-IR and HOMA-β. Data were expressed as mean ± SD (n = 6). #$p < 0.01$ compared with Group I; *$p < 0.05$ compared with Group II; **$p < 0.01$ compared with Group II. Group I: Normal control; Group II: T2D control, Group III: T2D rats treated with SR (50 mg/kg, orally); Group IV: T2D rats treated with SR (100 mg/kg, orally); Group V: T2D rats treated with glibenclamide (1 mg/kg, orally).

[1]HOMA-IR = [(Fasting serum insulin in U/l x Fasting blood glucose in mmol/l)/22.5]

[2]HOMA-β = (Fasting serum insulin in U/l x 20/Fasting blood glucose in mmol/l – 3.5)

The blood glucose levels used in these assessments were estimated 24 h before sacrificing the animals. Considering the overall duration of the experiment, it has been postulated that the glucose concentration will not vary significantly within 24 h after 28 days of post-treatment.

5.3.4. Effects on vascular inflammatory markers

The effects of SR on the vascular inflammatory markers have been estimated in this study (Figure 5.4.). VEGF, ICAM 1, MCP 1, IL 1β, IL 6 and TNF α levels in the sera of T2D rats were significantly ($p < 0.01$) up-regulated, which revealed the occurrence of vascular inflammation in T2DM. Treatment with SR (50 and 100 mg/kg) could significantly ($p < 0.05$-0.01) attenuate the

expressions of the ICAM 1, MCP 1, IL 1β and IL 6 in the sera of T2D rats, while, VEGF and TNF α levels were significantly ($p < 0.05$) attenuated at the dose of 100 mg/kg of SR.

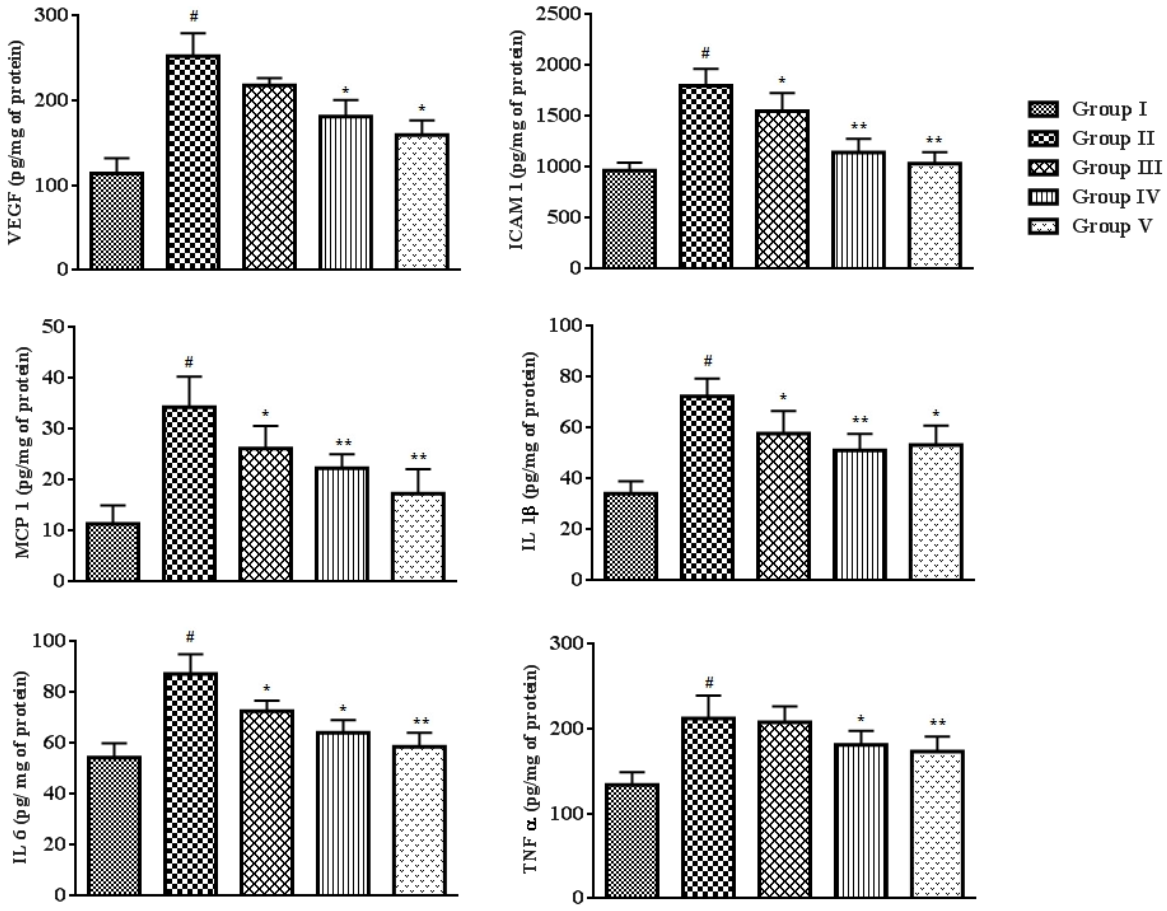

Figure 5.4. Effect of SR on inflammatory markers viz. VEGF, ICAM 1, MCP 1, IL 1β, IL 6 and TNF α in the sera of T2D rats. Data were expressed as mean ± SD (n = 6). $^{\#}p < 0.01$ compared with Group I; $^{*}p < 0.05$ compared with Group II; $^{**}p < 0.01$ compared with Group II. Group I: Normal control; Group II: T2D control, Group III: T2D rats treated with SR (50 mg/kg, orally); Group IV: T2D rats treated with SR (100 mg/kg, orally); Group V: T2D rats treated with glibenclamide (1 mg/kg, orally).

5.3.5. Effects on body weight

In this study, total body weight of experimental rats under different groups was evaluated (Table 4). A significant ($p < 0.01$) increase of total body weight was observed in T2D rats. SR (100 mg/kg) treatment significantly ($p < 0.05$) reduced the weight gain of T2D rats. The effect of SR (100 mg/kg) was comparable to that of glibenclamide (1 mg/kg) treated animals.

Table 5.4. Effect of SR on body weight of T2D rats.

Groups	Body weight (g)
Group I	146.54 ± 12.34
Group II	192.50 ± 17.33$^{\#}$
Group III	178.65 ± 16.43
Group IV	170.33 ± 12.67*
Group V	169.65 ± 11.25*

Data were expressed as mean ± SD (n=6). $^{\#}p< 0.01$ compared with Group I; *p< 0.05 compared with Group II. Group I: Normal control; Group II: T2D control, Group III: T2D rats treated with SR (50 mg/kg, p.o.); Group IV: T2D rats treated with SR (100 mg/kg, p.o.); Group V: T2D rats treated with glibenclamide (1 mg/kg, p.o.).

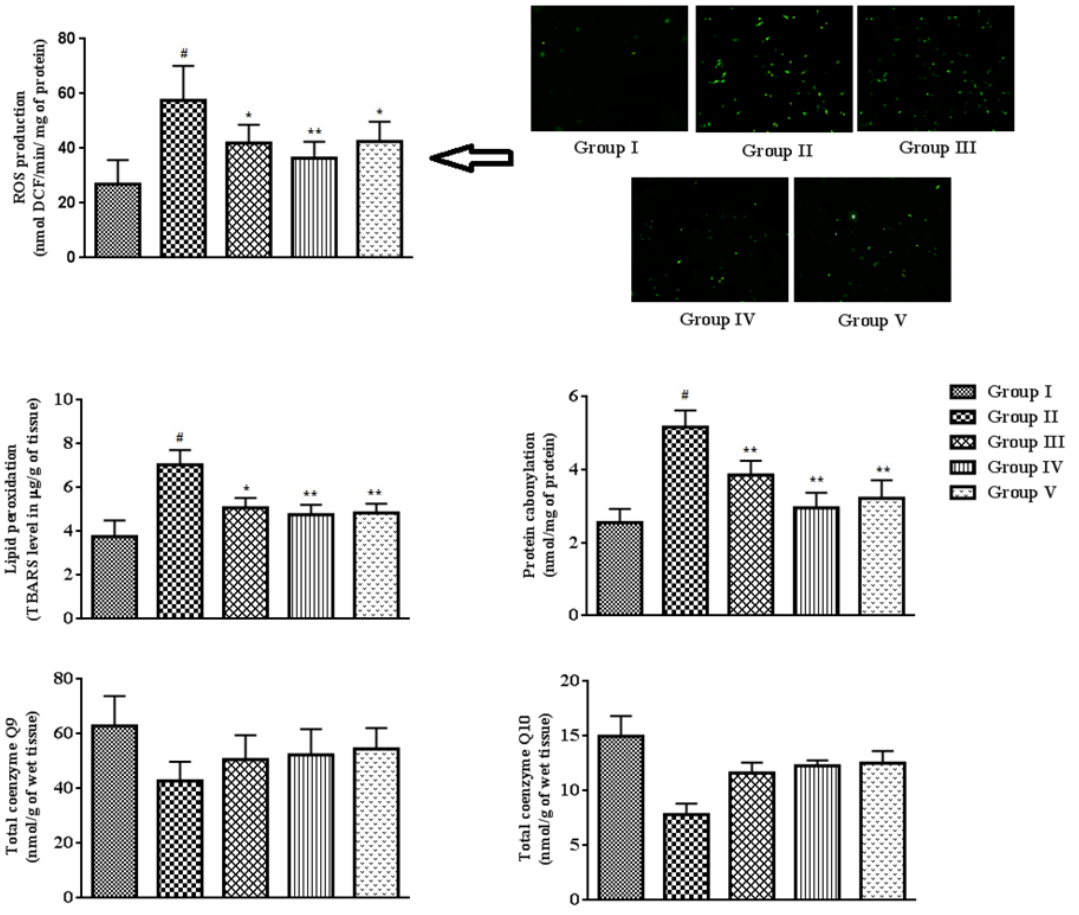

Figure 5.5. Effect of SR on ROS production, lipid peroxidation, protein carbonylation, coenzymes Q levels in the myocardial tissues of T2D rats. Data were expressed as mean ± SD (n

= 6). $^{\$}p < 0.05$ compared with Group I; $^{\#}p < 0.01$ compared with Group I; *p < 0.05 compared with group II; **p < 0.01 compared with Group II. Group I: Normal control; Group II: T2D control, Group III: T2D rats treated with SR (50 mg/kg, orally); Group IV: T2D rats treated with SR (100 mg/kg, orally); Group V: T2D rats treated with glibenclamide (1 mg/kg, orally).

5.3.6. Effects on ROS production, protein carbonylation, lipid peroxidation, co-enzymes Q levels, and endogenous redox markers in the myocardial tissues

In this study, degree of lipid peroxidation, co-enzymes Q levels, ROS production, and protein-carbonylation in the cardiac tissues were estimated (Figure 5.5.). T2D rats revealed significantly high ($p < 0.01$) levels of intercellular ROS in the cardiac tissue. SR (50, 100 mg/kg) treatment

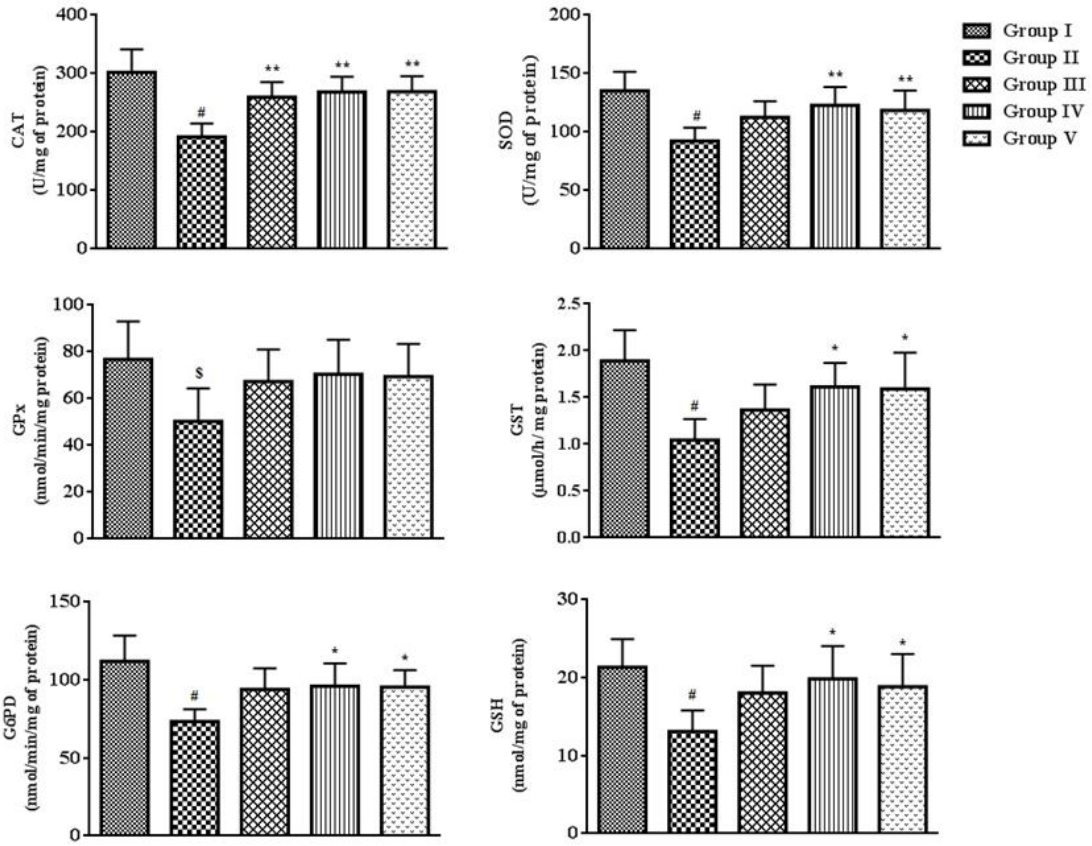

Figure 5.6. Effect of SR on endogenous antioxidant enzymes (SOD, CAT, GPx, GST, G6PD) and GSH levels in the myocardial tissues of T2D rats. Data were expressed as mean ± SD (n = 6). $p < 0.05 compared with Group I; #p < 0.01 compared with Group I; *p < 0.05 compared with Group II; **p < 0.01 compared with Group II. Group I: Normal control; Group II: T2D control, Group III: T2D rats treated with SR (50 mg/kg, orally); Group IV: T2D rats treated with SR (100 mg/kg, orally); Group V: T2D rats treated with glibenclamide (1 mg/kg, orally).

significantly ($p < 0.05$-0.01) arrested hyperglycemia mediated ROS generation in the myocardial tissues. The levels of TBARS (a by-product of lipid peroxidation) and carbonylated proteins were significantly ($p < 0.01$) augmented in the myocardial tissues of T2D rats. SR (50 and 100 mg/kg) treatment, however, could significantly attenuate the extents of protein carbonylation ($p < 0.01$) and lipid peroxidation ($p < 0.05$-0.01). T2D rats displayed significantly ($p < 0.05$-0.01) decreased levels of co-enzyme Q9 and Q10 in the cardiac tissue (Figure 5.5.). Treatment with SR (100 mg/kg) significantly ($p < 0.05$-0.01) restored these alterations of coenzymes Q in the heart of T2D rats. The effects on endogenous antioxidant enzymes and GSH levels measured in homogenates of the cardiac tissues have been depicted in Figure 5.6. The levels of CAT, SOD, GPx, GST, G6PD and GSH were significantly ($p < 0.05$-0.01) decreased in the myocardial tissues of T2D rats as compared with normal animals. Treatment with SR (100 mg/kg) significantly ($p < 0.05$-0.01) improved CAT, SOD, GST, G6PD and GSH levels of T2D rats, while, no substantial improvement was noticed in GPx level.

5.3.7. Effects on ATP level, NAD level, DNA fragmentation and DNA oxidation

The cellular ATP and NAD concentrations give the primary idea about the cellular pathological incidences. In this study, intracellular ATP and NAD levels were significantly ($p < 0.01$) reduced

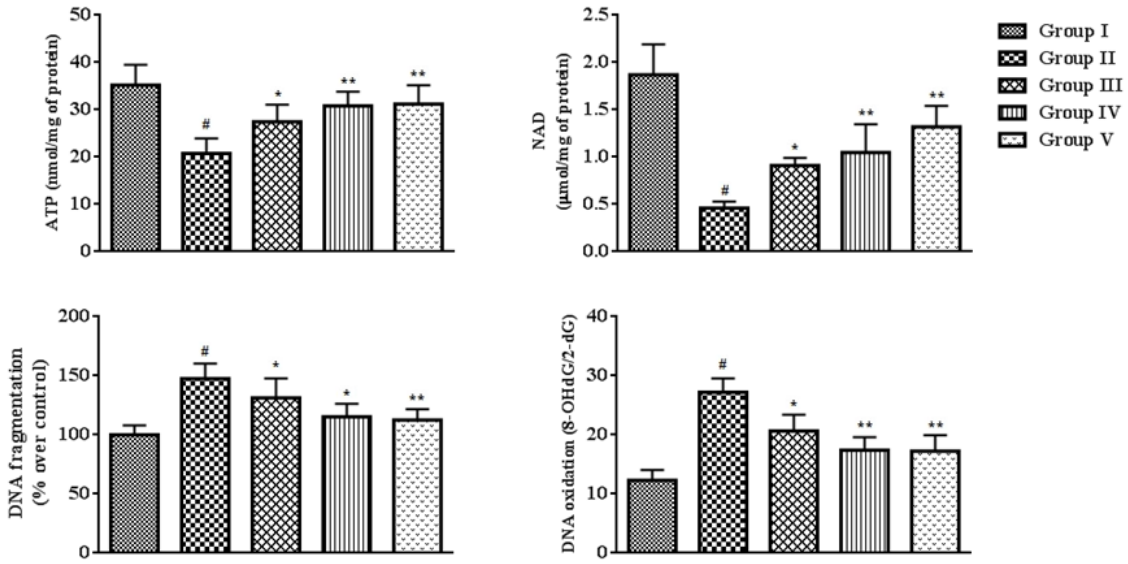

Figure 5.7. Effect of SR on ATP level, NAD level, DNA fragmentation and DNA oxidation in the myocardial tissues of T2D rats. Data were expressed as mean ± SD (n = 6). #$p < 0.01$ compared with Group I; *$p < 0.05$ compared with Group II; **$p < 0.01$ compared with Group II. Group I: Normal control; Group II: T2D control, Group III: T2D rats treated with SR (50 mg/kg, orally); Group IV: T2D rats treated with SR (100 mg/kg, orally); Group V: T2D rats treated with glibenclamide (1 mg/kg, orally).

in the homogenates of the cardiac tissues of T2D rats when compared to that of normal rats (Figure 5.7.). However, treatment with SR (50 and 100 mg/kg) could significantly ($p < 0.05$-0.01) enhance intracellular ATP and NAD contents in the myocardial tissues of T2D rats. The DNA damage and PARP activation play an essential role in diabetic pathophysiology. In current study, the extents of DNA fragmentation and the oxidation of cellular DNA were significantly increased in the myocardial tissues of T2D rats (Fig 5.7.). However, SR (50 and 100 mg/kg) treatment significantly ($p < 0.05$-0.01) attenuated the fragmentation and oxidation of DNA in the cardiac tissues of T2D rats as compared with diabetic control animals. The DNA-protective effect would substantiate the overall cyto-protective potential of SR.

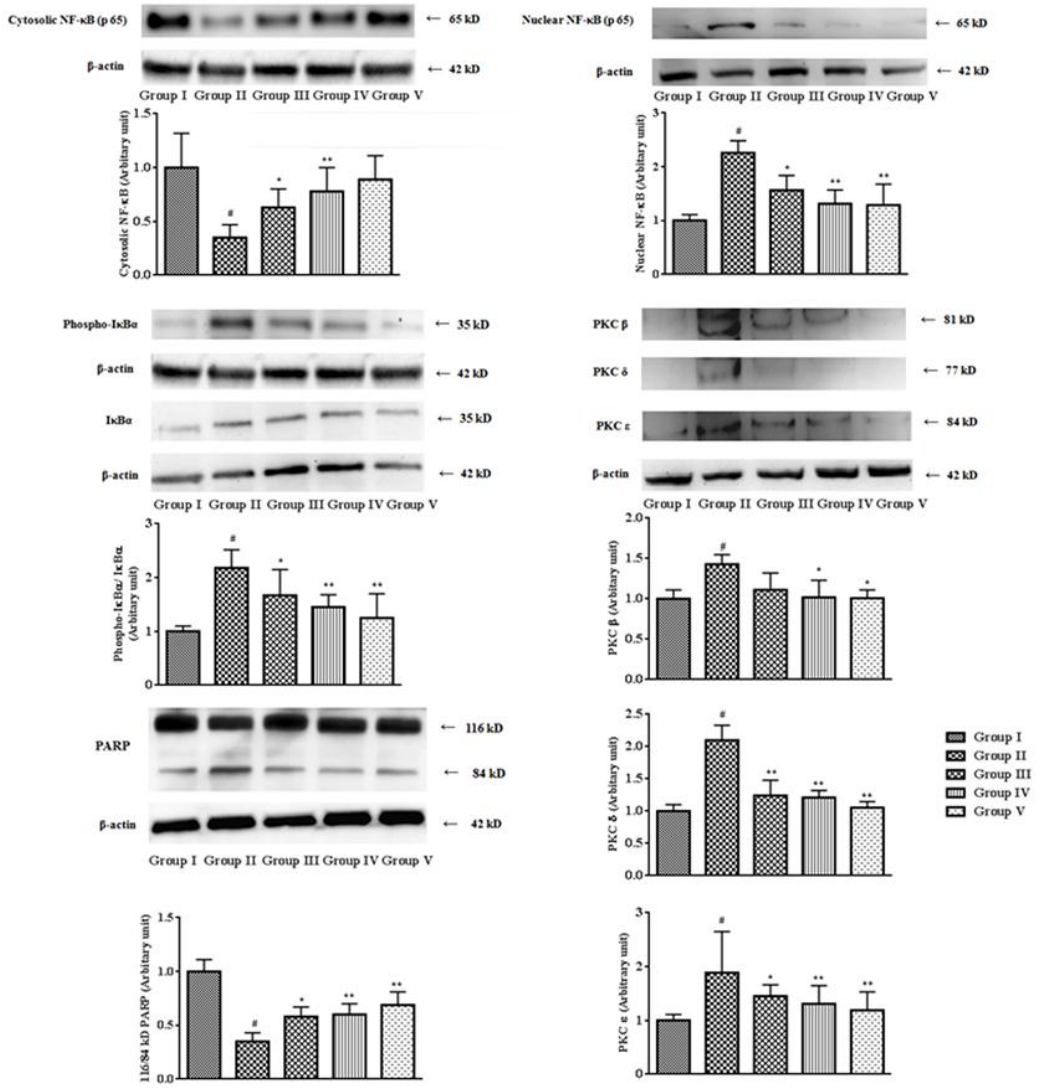

Figure 5.8. Effect of SR on the expressions of NF-κB, IκBα, PKC isoforms, PARP in the myocardial tissues of T2D rats. The relative band strengths were determined and the intensities of normal control (Group I) bands were given the random value of 1. β actin was used as a loading

protein. Data were expressed as mean ± SD (n = 6). $^{\$}p < 0.05$ compared with Group I;$^{\#}p < 0.01$ compared with Group I; *p < 0.05 compared with Group II; **p < 0.01 compared with Group II. Group I: Normal control; Group II: T2D control, Group III: T2D rats treated with SR (50 mg/kg, orally); Group IV: T2D rats treated with SR (100 mg/kg, orally); Group V: T2D rats treated with glibenclamide (1 mg/kg, orally).

5.3.8. Effects on signal proteins

Activations of various PKC isoforms contribute in many vascular and cellular pathophysiologies. PKCs also participate in the activation of NF-κB under redox challenged environment. In this study, significant ($p < 0.01$) up-regulations of PKC-β, PKC-δ and PKC-ε were observed in the myocardial (Figure 5.8.) tissues of T2D rats. However, the treatment with SR (100 mg/kg) could significantly ($p < 0.05$-0.01) attenuate the expression of aforementioned PKC isoforms in T2D rats. Intracellular oxidative challenge activates PARP cleavage which actively participates in the NF-κB activation and DNA damage. In this study, PARP cleavage ($p < 0.01$) from its full length form (116 kDa) to the cleaved form (84 kDa) was observed in the myocardial tissues of T2D rats (Figure 5.8.). However, extract treatment significantly ($p < 0.01$) inhibited PARP cleavage. NF-κB, a redox sensitive protein, participates in the instruction of various inflammatory responses. In this study, immunoblottings revealed significant ($p < 0.01$) up-regulation of nuclear NF-κB (p 65) with concomitant down-regulation ($p < 0.01$) of cytosolic NF-κB (p 65) in the cardiac tissues of T2D rats (Figure 5.8.). The observation suggested that the translocation of the NF-κB (p 65) to the nucleus, which is crucial for the activation of NF-κB to participate in T2D pathogenesis. The western blot analysis of IκBα revealed IκBα phosphorylation was significantly ($p < 0.01$) up-regulated in the cytosol of myocardial tissues of T2D rats, which may be correlated to the activation of NF-κB mediated pathogenesis.

5.3.9. Histological and ultra-structural assessments

The histological heart sections (x 100) of T2D rats revealed the irregular radiating pattern with injured interstitial tissues (Figure 5.9.A). The SEM analyses of hearts of the rats under different groups have been depicted in Figure 5.9.B. Ultrastructural changes of striated muscle of the heart of T2D rats revealed the myofibrillar disorganization. However, treatment with SR could decrease the T2DM mediated histological and ultra-structural aberrations and reinstate the tissue morphology near to normalcy.

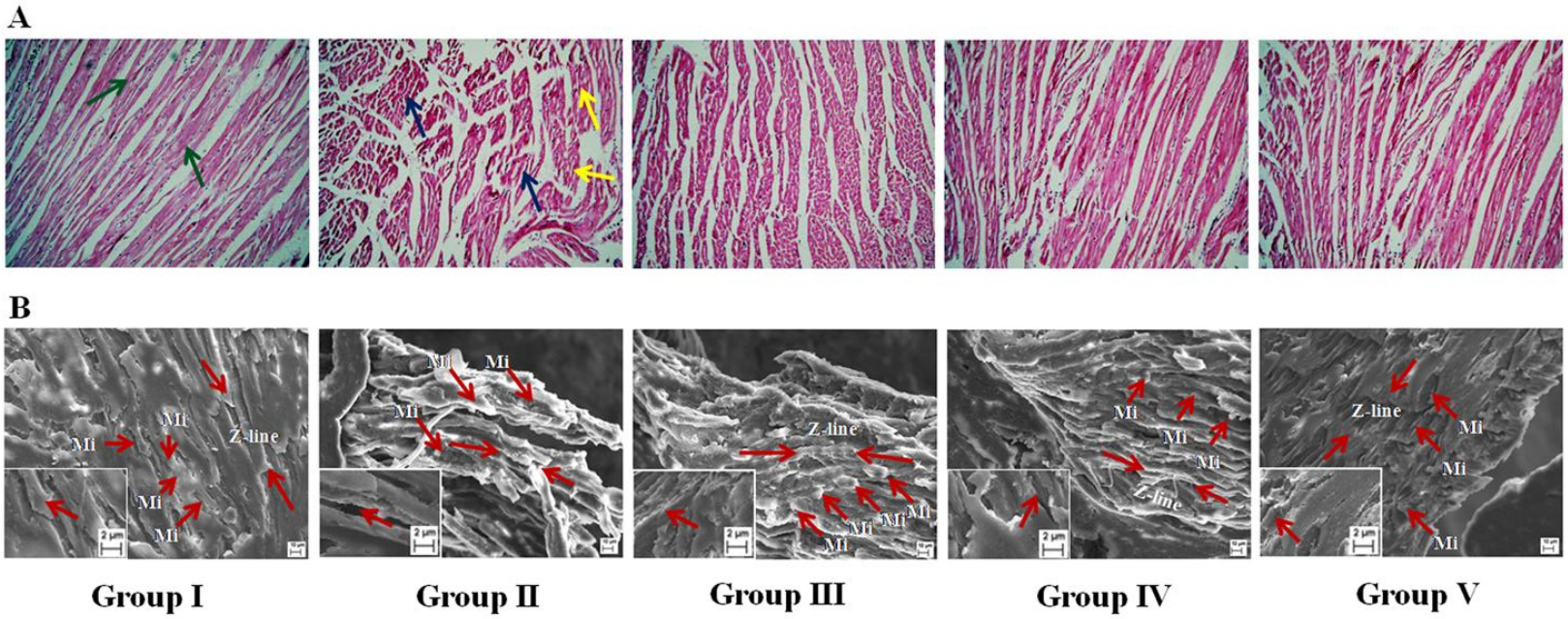

Figure 5.9. Histological (Panel A) and ultrastructural (Panel B) assessments of heart of T2D rats of different groups. Group II exhibited degeneration of interstitial tissues (blue arrows) and change in normal radiating pattern (yellow arrows) in the section of heart, while, Group I exhibited general radiating pattern of heart section. SEM showed ventricular portion of araldite sectioned rat myocardial tissues. Myocardial tissue of normal rats (Group I) exhibited normal myocardial fine structure, with myofibrils comprising regular and continuous sarcomeres which demarcated by Z-lines (Red arrow heads), which were in register with adjacent myofibrils and the rows of moderately electron dense mitochondria (Mi) intervene between myofibrils, while, Group II showed randomly distributed mitochondria (Mi) between poorly organized myofibrils in an electron-lucent sarcoplasm. Group III, IV and V indicated significant improvement in myofibrillar arrangement in heart tissues comparable to that of Group I. Group I: Normal control; Group II: T2D control; Group III: T2D rats treated with SR (50 mg/kg, orally); Group IV: T2D rats treated with SR (100 mg/kg, orally); Group V: T2D rats treated with glibenclamide (1 mg/kg, orally).

The observed effects of SR (50 and 100 mg/kg) were compared with standard drug, glibenclamide (1 mg/kg). The hypoglycemic and hypolipidemic effects of SR (100 mg/kg) were comparable to that of glibenclamide (1 mg/kg). However, SR (100 mg/kg) often exhibited better responses specifically in controlling radox imbalance in T2D rats than the standard drug. Finally, an obese control group was also included in this study to perceive the effect of high fat diets to the experimental rats (Table 5.5., Figure 5.11.). The obese control rats were compared with T2D control and normal control groups. The obese control rats exhibited significantly ($p < 0.01$) high

Table 5.5. Effects on fasting blood glucose and other biochemical parameters in the sera of normal, Type II diabetic and fat fed rats.

Parameters	Group I	Group II	Group VI
Fasting blood glucose (mg/dl)	75.22 ± 4.56	191.88 ± 16.67$^{\#}$	87.75 ± 5.43$^{\$,**}$
Total cholesterol (mg/dl)	92.33± 6.54	156.48 ± 13.21$^{\#}$	136.24 ± 10.89$^{\#,**}$
HDL cholesterol (mg/dl)	31.21 ± 3.12	17.67 ± 2.11$^{\#}$	24.67 ± 2.33$^{\#,**}$
Triglycerides (mg/dl)	116.75 ± 14.56	202.37 ± 19.22$^{\#}$	152.33 ± 14.25$^{\#,**}$
LDL cholesterol (mg/dl)	37.78 ± 3.45	174.22 ± 9.67$^{\#}$	81.10 ± 7.63$^{\#,**}$
Insulin (U/l)	58.16 ± 3.69	40.11 ± 1.24$^{\#}$	65.22 ± 4.54**
Glycosylated haemoglobin (mg/g haemoglobin)	0.32± 0.11	0.63 ± 0.25$^{\#}$	0.36 ± 0.17**
Lactate dehydrogenase (U/l)	187.08± 12.33	285.07 ± 21.15$^{\#}$	199.50 ± 16.28**
Creatine kinase (IU/mg of protein)	9.42 ± 1.45	19.05 ± 2.04$^{\#}$	11.33 ± 1.34**
C-reactive protein (mg/dl)	1.14 ± 0.48	3.01 ± 0.72$^{\#}$	1.21 ± 0.43**

Data were expressed as mean ± SD (n=6). $^{\$}p< 0.05$ compared with Group I; $^{\#}p< 0.01$ compared with Group I; $^{**}p< 0.01$ compared with Group II. Group I: Normal control group; Group II: T2D control group, Group VI: Obese control group.

lipid content in the sera when compared with normal rats. However, the values were also significantly ($p < 0.01$) differing from T2D rats. The serum insulin level was found to slightly higher (statistically insignificant) in obese control rats when compared with normal rats, however, serum insulin level remained significantly ($p < 0.01$) high when compared with T2D rats. Obese control rats also exhibited a significant ($p < 0.05$) increase in fasting blood glucose level when compared with normal control rats, which would have been correlated to the insulin resistance. However, the levels of membrane bound enzymes, glycosylated haemoglobin and C-reactive proteins in the sera remained near normal status. Observing the normalcy in the level of C-reactive proteins in the sera, we did not measure the levels of pro-inflammatory mediators. We also compared the effects of high fat diets in the myocardial tissues (Figure 5.10.). The experimental data revealed that slight (statistically insignificant) disturbances in the intracellular

redox status in the myocardial tissues of obese control rats when compared with normal control rats. However, the tissue parameters were significantly ($p < 0.05$-0.01) varied in obese control rats when compared with T2D rats.

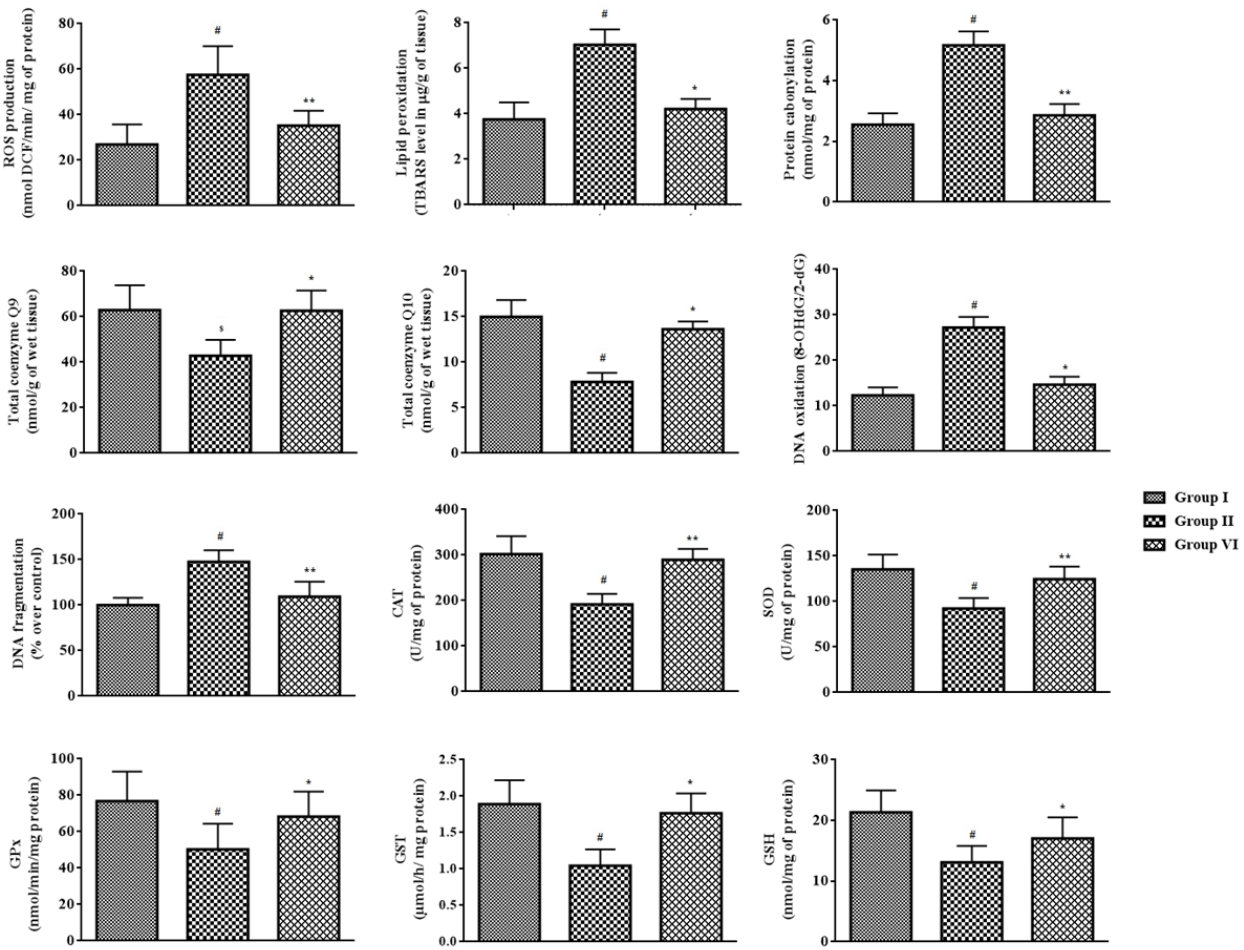

Figure 5.10. Effects on intracellular redox status in the myocardial tissues of normal, Type II diabetic and fat fed rats. Data were expressed as mean ± SD (n=6). $^{\$}p< 0.05$ compared with Group I; $^{\#}p< 0.01$ compared with Group I; **$p< 0.01$ compared with Group II. Group I: Normal control group; Group II: T2D control group, Group VI: Obese control group.

5.4. Discussion

OGTT gives an idea about glucose-insulin homeostasis under different physiological/clinical states. In this study, OGTT was performed prior to the induction of diabetes. OGTT data revealed that the animals developed hyperglycemia to that experimental rats caused by direct glucose feeding, while, SR treatment could reinstate this effect. It would be possible that, SR might cause an improvement of glucose homeostasis through peripheral glucose uptake (Sulyman et al., 2016). Earlier reports revealed that, the phenolic compounds could attenuate intestinal glucose

absorption (Kwon et al., 2007; Schulze et al., 2014). Therefore, presence of phenolic substances within SR might also attribute for the overall OGTT observation. The observed OGTT data could predict the probable hypoglycemic effect of SR. Therefore, SR (50 and 100 mg/kg) was subjected to antidiabetic assay employing established T2D model in experimental rats.

High fat diets are the major cause of obesity with simultaneously insulin resistance in the western countries (Zheng et al., 2012). Streptozotocin has a preferential toxicity toward pancreatic β-cells of islet of Langerhans. Despite the presented literature revealed that β-cells have the ability to regenerate, however, controversies are still existing (Kodama et al., 2003; Dor et al., 2004). The partial destruction of β-cells by the small dose of streptozotocin to high fat fed rats has been claimed to induce T2D by lowering insulin secretion coupled with insulin resistance (Srinivasan et al., 2005; Bhandari et al., 2013). The significantly lower level of serum insulin in T2D control rats indicted the partial destruction of pancreatic β-cells. Besides, significantly low HOMA-β value and significantly high HOMA-IR value in T2D control rats established the induction of insulin resistance (Mohammed et al., 2016). Therefore, high fat diets + low single dose of streptozotocin model has been claimed to be an optimum experimental model for T2D simulating the human T2DM (Srinivasan et al., 2005), which has been employed in this study to evaluate protective effect of SR.

In this study, the animals were divided into five groups. Group I and II represented normal and T2D animals, respectively. The T2D mediated pathological changes were statistically compared with normal animals. Groups III and IV were kept as test groups to observe the protective role of SR. The studied parameters of test groups were statistically compared with respect to T2D control group. Group V represented positive control animals to compare the overall protective effect of SR with respect to commercially available oral hypoglycemic agent, glibenclamide.

Reduction of the blood glucose level is the principle approach of diabetic therapy. Inclusion of low dose of streptozotocin caused incomplete destruction of β-cell population in islet of Langerhans. In this study, significant reduction of serum insulin level was observed. Insulin is known to activate lipoprotein lipase which catalyses the hydrolytic breakdown of lipids during normal physiological status (Khanra et al., 2015). Therefore, lower insulin level coupled with insulin resistance during diabetic condition causes hyperlipidemia. In this study, high concentrations of serum lipids were observed in T2D rats. SR treatment could significantly reverse HOMA-β and HOMA-IR scores with concomitant promotion of insulin secretion. SR treatment could significantly attenuate hyperlipidemia, which would be corroborated with the reversal of insulin resistance coupled with elevation of insulin secretion. Persistent hyperglycemia promotes glycosylation of different functional proteins including haemoglobin (Khanra et al.,

2015). In this study, a significant elevation in the level of glycosylated haemoglobin was observed in the sera of T2D rats. Increased CK and LDH contents in the sera are primary indication of cellular damage (Patel et al., 2014). These membrane bound enzymes come into the blood during cellular injury. In this study, CK and LDH levels in the sera were significantly raised in T2D rats over control, which revealed the occurrence of hyperglycemia mediated cytotoxicity. SR treatment significantly reduced the levels of CK and LDH in the sera of T2D rats, which indicated the cyto-protective role of test extract during DM.

Increased blood glucose level facilitates generation of ROS which directly participate in the pathological incidences in DM. Cardiovascular injury is a critical reason of morbidity and mortality of the DM patients (Manna and Sil, 2012; Khanra et al., 2015). Earlier reports revealed that hyperglycemia mediated excessive ROS generation plays predominant role in diabetic cardiomyopathy (Manna and Sil, 2012; Khanra et al., 2015). In this study, a significantly high ROS production was observed in cardiac tissues of T2D rats. An enhanced generation of ROS would result in the increases in lipid peroxidation, protein carbonylation with concomitant depletion of endogenous antioxidant molecules (Patel et al., 2014; Dua et al., 2015b). Therefore, it would be concluded that myocardial tissues experienced to redox challenge/oxidative stress during DM. SR treatment could significantly attenuate intracellular ROS levels in the myocardial tissues of T2D rats. SR could produce the effect either by direct scavenging ROS and/or indirectly by inhibiting ROS generation through its hypoglycemic effect. A decrease in the levels of ROS in the myocardial tissues in SR treated T2D rats caused the reduction of peroxidative damages of cellular lipids and carbonylation of proteins. SR also ensured better protection against oxidative stress by up-regulating endogenous antioxidant molecules. In a redox challenged cellular environment, an excessive amount of GSH is utilized and subsequently GSH level is decreased (Manna and Sil, 2012). Later encourage generation of many reactive intermediates which cause DNA damage and cell death. The hyperglycemic rats exhibited a significantly increased level of 8-OHdG/2-dG ratio, an index of DNA oxidation and DNA fragmentation. However, SR could significantly prevent DNA oxidation and fragmentation, which would be due to radical scavenging effect synergized with hypoglycemic effect of test material.

Hyperglycemia mediated oxidative stress could simultaneously activate PKCs by the influx of the polyol pathway (Ahmad et al., 2005). Activation of PKC isoforms contributes in the activation of NF-κB in redox challenged cellular environment. PKCs also largely contribute to the accumulation of matrix proteins like collagen and cause fibrosis (Manna and Sil, 2012). In this study, the expressions of PKC β, δ and ε were significantly up-regulated in the myocardial tissues of T2D rats. However, SR treatment significantly reversed the elevated expressions of PKC

isoforms in the myocardial tissues of T2D rats. Intracellular oxidative pressure potentiates PARP cleavage which further promotes the activation of NF-κB (Bhattacharya et al., 2013). NF-κB is one of the redox sensitive proteins, which participates a crucial role in the inflammation process (Khanra et al., 2015). Oxidative stress causes degradation of IκBα via phosphorylation with concomitant translocation of NF-κB to the nucleus from cytosol (Bhattacharya et al., 2013). Translocated NF-κB binds with DNA and regulates the expressions of several molecules like pro-inflammatory cytokines, VEGF, ICAM 1 related to diabetic pathophysiology (Manna and Sil, 2012). In this study, T2D rats exhibited up-regulated expression of NF-κB in nucleus of cardiac tissues following release of inflammatory mediators. However, SR treatment could significantly attenuate the NF-κB mediated inflammatory responses.

GC-MS analysis revealed presence of phenolic compounds, phenolic acids, fatty acids and sterols in SR. The different compounds present within the SR have been reported to display hypoglycemic, anti-inflammatory and antioxidant effects which have been discussed hereunder. Ferulic acid manifests antidiabetic potential by modulating insulin-signaling molecules (Narasimhan et al., 2015). Caffeic acid possesses significant antidiabetic activity (Jung et al., 2006). Besides, caffeic acid and its derivatives exhibited significant anti-inflammatory effect via antioxidant mechanism (da Cunha et al., 2004). Oleic acid has been reported to counteract with the inhibitory effect of inflammatory cytokines in insulin production (Vassiliou et al., 2009). Ergosterol has been reported to possess significant hypoglycemic effect and counteract with diabetic pathophysiology via inhibiting NF-κB mediated inflammatory signals (Ang et al., 2015). Stigmasterol is also known to possess hypoglycemic effect (Nualkaew et al., 2015). Heptadecanoic acid, a saturated fatty acid, has been reported to reverse pre-diabetes condition (Venn-Watson et al., 2015). Sinapyl alcohol has been proposed to inhibit LPS stimulated TNF-α production (Choi et al., 2004). Gallic acid has been reported to exhibit cardioprotective effect via redox balancing in experimentally induced diabetic rats (Patel and Goyal, 2011). 4-hydroxycinnamic acid has been reported to possess hypoglycemic and hypolipidemic effect in diabetic rats (Ambika et al., 2013). Protocatechuic acid exhibited significant antidiabetic, anti-inflammatory and antioxidant effects (Harini and Pugalendi, 2010). 4-hydroxy-3-methoxybenzoic acid has been reported to possess hypoglycemic effect (Gayathri and Kannabiran, 2009). Vanillin has been reported to attenuate the expressions of pro-inflammatory cytokines via anti-oxidant mechanism (Makni et al., 2011). Hydroquinone and 4-hydroxybenzaldehyde have been reported to exhibit anti-inflammatory effect (Lim et al., 2008; Byeon et al., 2013). Besides, a significant number of phenolic acids within SR would attribute significant radical scavenging effect in

diabetic pathophysiology. However, the overall effect would be exerted through the synergy between the aforementioned compounds.

In conclusion, DM is associated with hyperglycemia which largely contributes in generation of excess of ROS. Excess of ROS actively initiates and propagates a number of toxicological incidences including diabetic cardiomyopathy. It has been proposed that, ROS activates the expressions of several redox sensitive proteins which contribute in the toxicological process. ROS mediated activation of PKC isoforms, PARP cleavage and NF-κB translocation to the nucleus constitute integrally in the diabetic cardiomyopathy via activation of inflammatory pathway and leading to necrotic cell death. Besides, excess of ROS attack cellular nucleic acids and participate in cell death process. Considering the multiple mechanisms involved in the diabetic cardiomyopathy (Figure 5.11.), a multi-target therapeutic strategy would be fruitful. The experimental outcome of this study clearly suggested that SR could offer overall protective effect through attenuating hyperglycemia, scavenging ROS and arresting inflammation (Figure 5.11.). The observed effect has been correlated with the existing phytochemicals. Therefore, it could be concluded that SR would have potential to be developed as a novel phytotherapeutic agent for T2DM in future.

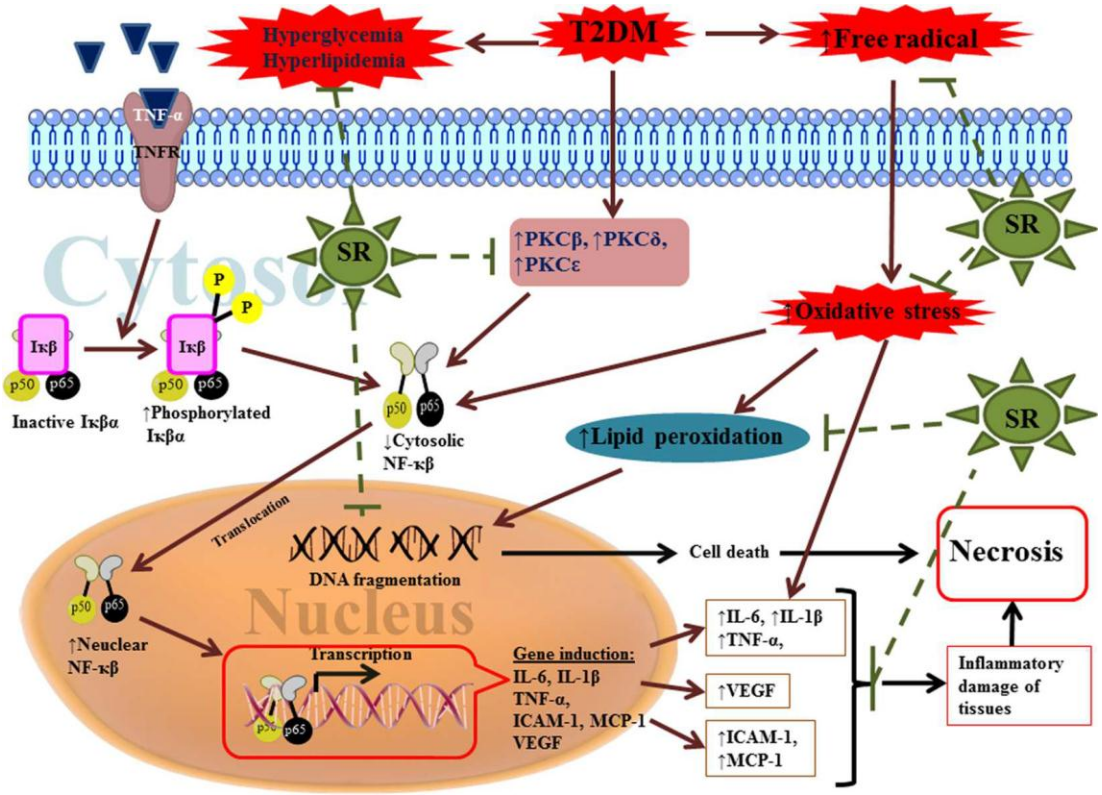

Figure 5.11. A schematic overview of the hypothesis developed in this study regarding probable protective mechanism of SR against diabetic cardiomyopathy. Green dotted lines represented the restricted pathological events by SR.

References

Ahmad FK, Zhiheng H, King GL. Molecular targets of diabetic cardiovascular complications. Curr Drug Targets. 2005;6:487-494.

Ambika S, Saravanan R, Thirumavalavan K. Antidiabetic and antihyperlipidemic effect of p-hydroxycinnamic acid on streptozotocin-induced diabetic rats. Biomed Aging Pathol. 2013;3:253-7.

Ang L, Yuguang L, Liying W, Shuying Z, Liting X, Shumin W. Ergosterol alleviates kidney injury in streptozotocin-induced diabetic mice. Evid Based Complement Alternat Med. 2015;2015:Article ID: 691594.

Baghirova S, Hughes BG, Hendzel MJ, Schulz R. Sequential fractionation and isolation of subcellular proteins from tissue or cultured cells. MethodsX. 2015;2:440-445.

Bastaki S. Diabetes mellitus and its treatment. Int J Diabetes Metab. 2005;13:111-134.

Bennett WL, Wilson LM, Bolen S, Maruthur N, Singh S, Chatterjee R, Marinopoulos SS, Puhan MA, Ranasinghe P, Nicholson WK, Block L, Odelola O, Dalal DS, Ogbeche GE, Chandrasekhar A, Hutfless S, Bass EB, Segal JB. Oral diabetes medications for adults with type 2 diabetes: an update. Effective health care programme. Comparative effectiveness review no. 8, Rockville, USA. 2011.

Bhandari U, Chaudhari HS, Khanna G, Najmi AK. Antidiabetic effects of *Embeli aribes* extract in high fat diet and low dose streptozotocin-induced type 2 diabetic rats. Front Life Sci. 2013;7:186-196.

Bhattacharjee N, Barma S, Konwar N, Dewanjee S, Manna P. Mechanistic insight of diabetic nephropathy and its pharmacotherapeutic targets: An update. Eur J Pharmacol. 2016;791:8-24.

Bhattacharya S, Manna P, Gachhui, R, Sil PC. D-Saccharic acid 1,4-lactone protects diabetic rat kidney by ameliorating hyperglycemia-mediated oxidative stress and renal inflammatory cytokines via NF-κB and PKC signaling. Toxicol Appl Pharmacol. 2013;267:16-29.

Bolner A, Pilleri M, De Riva V, Nordera GP. Plasma and Urinary HPLC-ED Determination of the Ratio of 8-OHdG/2-dG in Parkinson's Disease. Clin Lab. 2011;57:859-866.

Byeon SE, Yu T, Yang Y, Lee YG, Kim JH, Oh J, Jeong HY, Hong S, Yoo BC, Cho WJ, Hong S, Cho JY. Hydroquinone regulates hemeoxygenase-1 expression via modulation of Src

kinase activity through thiolation of cysteine residues. Free Radic Biol Med. 2013;57:105-118.

Carlson EC, Hinds D. Native banded collagen fibrils in the glomerular mesangial matrix of normal human and laboratory animals. J Ultrastruct Res. 1981;77:241-247.

Cheng D. Prevalence, predisposition and prevention of type II diabetes. Nutr Metab (Lond). 2005;2:29.

Choi J, Shin KM, Park HJ, Jung HJ, Kim HJ, Lee YS, Rew JH, Lee KT. Anti-inflammatory and antinociceptive effects of sinapyl alcohol and its glucoside syringin. Planta Med. 2004;70:1027-1032.

da Cunha FM, Duma D, Assreuy J, Buzzi FC, Niero R, Campos MM, Calixto JB. Caffeic acid derivatives: in vitro and in vivo anti-inflammatory properties. Free Radic Res. 2004; 38:1241-1253.

Dewanjee S, Das AK, Sahu R, Gangopadhyay M. Antidiabetic activity of *Diospyros peregrina* fruit: effect on hyperglycemia, hyperlipidemia and augmented oxidative stress in experimental type 2 diabetes. Food Chem Toxicol. 2009;47:2679-2685.

Dewanjee S, Dua TK, Khanra R, Das S, Barma S, Joardar S, Bhattacharjee N, Zia-Ul-Haq M, Jaafar HZ. Water spinach, *Ipomoea aquatica* (Convolvulaceae), ameliorates lead toxicity by inhibiting oxidative stress and apoptosis. Plos One. 2015;10:e0139831.

Dewanjee S, Joardar S, Bhattacharjee N, Dua TK, Das S, Kalita J, Manna P. Edible leaf extract of *Ipomoea aquatica* Forssk. (Convolvulaceae) attenuates doxorubicin-induced liver injury via inhibiting oxidative impairment, MAPK activation and intrinsic pathway of apoptosis. Food Chem Toxicol. 2017;105:322-336.

Dhiman AK. Ayurvedic Drug Plants. Dayal Publishing House. New Delhi, India. 2006.

Dor Y, Brown J, Martinez OI, Melton DA. Adult pancreatic beta-cells are formed by self-duplication rather than stem-cell differentiation. Nature 2004;429:41-46.

Dua TK, Dewanjee S, Gangopadhyay M, Khanra R, Zia-Ul-Haq M, De Feo V. Ameliorative effect of water spinach, *Ipomoea aquatica* (Convolvulaceae), against experimentally induced arsenic toxicity. J Transl Med. 2015a;13:81.

Dua TK, Dewanjee S, Khanra R, Bhattacharya N, Bhaskar B, Zia-Ul-Haq M, De Feo V. The effects of two common edible herbs, *Ipomoea aquatica* and *Enhydra fluctuans*, on cadmium‐induced pathophysiology: a focus on oxidative defence and anti‐apoptotic mechanism. J Transl Med. 2015b;13:245.

Dua TK, Dewanjee S, Khanra R, Barma S, Joardar S, Das S, Zia-Ul-Haq M, De Feo V. Cytoprotective and antioxidant effects of an edible herb, *Enhydra fluctuans* Lour.

(Asteraceae), against experimentally induced lead acetate intoxication. Plos One. 2016;11:e0148757.

Eggli US. Illustrated hand book of succulent plants: monocotyledons. Springer, Berlin, Germany. 2002.

Friedewald WT, Levy RI, Fredrickson DS. Estimation of the concentration of low density lipoprotein in plasma, without use of the preventive ultracentrifuge. Clin Chem. 1972;18:499-502.

Gayathri M, Kannabiran K. Antidiabetic activity of 2-hydroxy 4-methoxy benzoic acid isolated from the roots of *Hemidesmus indicus* on streptozotocin-induced diabetic rats. Int J Diabetes Metab. 2009; 17:53-57.

Ghosh J, Das J, Manna P, Sil PC. Protective effect of the fruits of *Terminalia arjuna* against cadmium induced oxidant stress and hepatic cell injury via MAPK activation and mitochondria dependent pathway. Food Chem. 2010;123:1062-1075.

Haldar PK., Kar B, Bhattacharya S, Bala A, Kumar RBS. Antidiabetic activity and modulation of antioxidant status by *Sansevieria roxburghiana* rhizome in streptozotocin-induced diabetic rats. Diabetologia Croatica.2010;39:115-123.

Harini R, Pugalendi KV. Antihyperglycemic effect of protocatechuic acid on streptozotocin-diabetic rats. J Basic Clin Physiol Pharmacol. 2010; 21:79-91.

Hissin PJ, Hilf R. A fluorometric method for the determination of oxidized and reduced glutathione in tissues. Anal Biochem. 1973;74:214-216.

Jung UJ, Lee MK, Park YB, Jeon S-M, Choi, M-S. Antihyperglycemic and antioxidant properties of caffeic acid in db/db mice. J Pharmacol Exp Ther. 2006; 318:476-483.

Kalofoutis C, Piperi C, Kalofoutis A, Harris F, Phoenix D, Singh J. Type II diabetes mellitus and cardiovascular risk factors: Current therapeutic approaches. Exp Clin Cardiol. 2007;12:17-28.

Khanra R, Dewanjee S, Dua TK, Sahu R, Gangopadhyay M, De Feo V, Zia-Ul-Haq M. *Abroma augusta* L. (Malvaceae) leaf extract attenuates diabetes induced nephropathy and cardiomyopathy via inhibition of oxidative stress and inflammatory response. J Transl Med. 2015;13:6.

Kim J, McCarte RJM, Yu BP. Influence of age, exercise and dietary restriction on oxidative stress in rats. Aging Clin Exp Res. 1996;8:123-129.

Kirtikar KR, Basu BD. Indian Medicinal Plants. Vol. IV. Bishen Singh Mahendra Pal Singh Publisher, New Delhi, India, 1935.

Kodama S, Kuhtreiber W, Fujimura S, Dale EA, Faustman DL. Islet regeneration during the reversal of autoimmune diabetes in NOD mice. Science 2003;302:1223-27.

Kwon O, Eck P, Chen S, Corpe CP, Lee J-H, Kruhlak M, Levine M. Inhibition of the intestinal glucose transporter GLUT2 by flavonoids. FASEB J. 2007;370:366-377.

LeBel CP, Bondy SC. Sensitive and rapid quantitation of oxygen reactive species formation in rat synaptosomes. Neurochem Int. 1990;17:435-440.

Liang Q, Carlson EC, Donthi RV, Kralik PM, Shen X, Epstein PN. Over expression of metallothionein reduces diabetic cardiomyopathy. Diabetes. 2002;51:174-181.

Lim E-J, Kang H-J, Jung H-J, Park E-H, Lim C-J, Park E-H. Anti-inflammatory, anti-angiogenic and anti-nociceptive activities of 4-hydroxybenzaldehyde. Biomol Ther. 2008; 16:231-236.

Lin KT, Xue JY, Sun FF, Wong PYK. Reactive oxygen species participate in peroxinitrile induced apoptosis in HL 60 cells. Biochem Biophys Res Commun. 1997; 230:115-119.

Makni M, Chtourou Y, Fetoui H, Garoui M, Boudawara T, Zeghal N. Evaluation of the antioxidant, anti-inflammatory and hepatoprotective properties of vanillin in carbon tetrachloride-treated rats. Eur J Pharmacol. 2011;668:133-139.

Manna P, Sil PC. Impaired redox signaling and mitochondrial uncoupling contributes vascular inflammation and cardiac dysfunction in type 1 diabetes: Protective role of arjunolic acid. Biochimie. 2012;94:786-797.

Matsumura H, Miyachi S. Cycling assay for nicotinamide adenine dinucleotides. Methods Enzymol. 1980;69:465-470.

Mohammed A, Koorbanally NA, Islam MS. Anti-diabetic effect of *Xylopia aethiopica* (Dunal) A. Rich. (Annonaceae) fruit acetone fraction in a type 2 diabetes model of rats. J. Ethnopharmacol. 2016;180:131-139.

Mortan JF. Atlas of medicinal plants of middle America. Charles C Thomas Publisher, Illinois, US, 1981.

Nair P, Nair RR. Selective use of calcium chelators enhances the yield of calcium tolerant myocytes from heart. Ind J Exp Biol. 1997;35:451-456.

Narasimhan A, Chinnaiyan M, Karundevi B. Ferulic acid exerts its antidiabetic effect by modulating insulin-signalling molecules in the liver of high-fat diet and fructose-induced type-2 diabetic adult male rat. Appl Physiol Nutr Metab. 2015;40:769-781.

Nayak SS, Pattabiraman TN. A new colorimetric method for the estimation of glycosylated haemoglobin. Clin Chim Acta. 1981;109:267-274.

Nualkaew S, Padee P, Talubmook C. Hypoglycemic activity in diabetic rats of stigmasterol-D-glucopyranoside isolated from *Pseuderanthemum palatiferum* (Nees) Radlk. leaf extract. J Med Plants Res. 2015;9:629-635.

Ohkawa H, Ohishi N, Yagi K. Assay for lipid peroxides in animal tissues by thiobarbituric acid reaction. Anal Biochem. 1979;95:351-358.

Olokoba AB, Obateru OA, Olokoba LB. Type 2 Diabetes Mellitus: A Review of Current Trends Oman Med J. 2012;27:269-273.

Patel BM, Raghunathan S, Porwal U. Cardioprotective effects of magnesium valproate in type 2 diabetes mellitus. Eur J Pharmacol. 2014;728:128-134.

Patel SS, Goyal RK. Cardioprotective effects of gallic acid in diabetes-induced myocardial dysfunction in rats. Pharmacognosy Res. 2011; 3:239-245.

Philip D, Kaleena PK, Valivittan K. GC-MS analysis and antibacterial activity of chromatographically separated pure fractions of leaves of *Sansevieria roxburghiana*. Asian J Pharm Clin Res. 2011;4:130-133.

Public Health Service (PHS). Public Health Service Policy on Human Care and Use of Laboratory Animals. Washington, DC: US Department of Health and Human Services, National Institute of Health, Office of Laboratory Animal welfare, 2015.

Pulliah T. Encyclopedia of World Medicinal Plants. Regency Publications. New Delhi, India, 2006.

Raghu KG, Cherian OL. Characterization of cytotoxicity induced by arsenic trioxide (a potent anti-APL drug) in rat cardiac myocytes. J Trace Elem Med Biol.2009;23:61-68.

Reed MJ, Meszaros K, Entes LJ, Claypool MD, Pinkett JG, Gadbois TM, Reaven GM. A new rat model of type 2 diabetes: the fat-fed, streptozotocin-treated rat. Metabolism. 2000;49:1390-1394.

Schulze C, Bangert A, Kottra G, Geillinger KE, Schwanck B, Vollert H, Blaschek W, Daniel H. Inhibition of the intestinal sodium-coupled glucose transporter 1 (SGLT1) by extracts and polyphenols from apple reduces postprandial blood glucose levels in mice and humans. Mol Nutr Food Res. 2014;58:1795-1808.

Srinivasan K, Patole PS, Kaul CL, Ramarao P. Reversal of glucose intolerance by pioglitazone in high-fat diet fed rats. Methods Find Exp Clin Pharmacol. 2004;26:327-333.

Srinivasan K, Viswanad B, Asrat L, Kaul CL, Ramarao P. Combination of high-fat diet-fed and low-dose streptozotocin-treated rat: A model for type 2 diabetes and pharmacological screening. Pharmacol Res. 2005;52:313-320.

Sulyman AO, Akolade JO, Sabiu SA, Aladodo RA, Muritala HF. Antidiabetic potentials of ethanolic extract of *Aristolochia ringens* (Vahl.) roots. J Ethnopharmacol. 2016;182:122-128.

Szabo C. PARP as a drug target for the therapy of diabetic cardiovascular dysfunction. Drug News Perspect. 2002;15:197-205.

Uchida K, Stadtman ER. Covalent attachment of 4-hydroxynonenal to glyceraldehydes-3-phosphate dehydrogenase. A possible involvement of intra- and intermolecular cross-linking reaction. J Biol Chem. 1993;268:6388-6393.

Van de Laar FA, Lucassen PL, Akkermans RP, Van de Lisdonk EH, Rutten GE, Van Weel C. Alpha-glucosidase inhibitors for type 2 diabetes mellitus. Cochrane Database Syst Rev. 2005; 2:CD003639.

Vassiliou EK, Gonzalez A, Garcia C, Tadros JH, Chakraborty G, Toney JH. Oleic acid and peanut oil high in oleic acid reverse the inhibitory effect of insulin production of the inflammatory cytokine TNF-α both in vitro and in vivo systems. Lipids Health Dis. 2009; 8:25.

Venn-Watson SK, Parry C, Baird M, Stevenson S, Carlin K, Daniels R, Smith CR, Jones R, Wells RS, Ridgway S, Jensen ED. Increased dietary intake of saturated fatty acid heptadecanoic acid (C17:0) associated with decreasing ferritin and alleviated metabolic syndrome in dolphins. Plos One. 2015;10:e0132117.

Wolf I, Sadetzki S, Catane R, Karasik A, Kaufman B. Diabetes mellitus and breast cancer. Lancet Oncol. 2005;6:103-111.

Zhang Y, Aberg F, Appelkvist EL, Dallner G, Ernster L. Uptake of dietary coenzyme Q supplement is limited in rats. J Nutr. 1995;125:446-453.

Zheng T, Shu G, Yang Z, Mo S, Zhao Y, Mei Z. Antidiabetic effect of total saponins from *Entada phaseoloides* (L.) Merr. in type 2 diabetic rats. J Ethnopharmacol. 2012;139:814-821.

Web references

https://www.diabetes.co.uk/

https://www.fda.gov.

6.1. Introduction

Diabetes mellitus (DM) is a chronic metabolic syndrome has climbed markedly over past few decades (WHO, 2016). The global prevalence of DM has risen to 8.5% amounting ~422 million in 2014 (WHO, 2016). It has been predicted that, the incidence of this syndrome would be more than double by the year of 2030 (Fernández-Millán et al., 2014). Amongst all diagnosed cases, type 2 diabetes mellitus (T2DM) is more rampant and comprising ~90-95 % of total diabetic cases (Khanra et al., 2015). Hyperglycemia arbitrated glucose toxicity resulted a number of homeostatic disturbances within the organs, which results a number of complications in the critical organs. Diabetic cardiomyopathy (DC) is one of the major complications in T2DM. It has been reported that, adults with T2DM historically have 2-3 times higher risk of cardiovascular problems than the adults without T2DM (WHO, 2016). Persistent hyperglycemia introduces toxic effects through a sequence of secondary transducers. The excess generation of reactive oxygen species (ROS) in the myocardial tissue via activation of polyol pathway is considered to be one of the principle mechanisms in the development of DC. Glucose oxidation resulted production of excess of advanced glycation end-products (AGEs) which leads to myocardial inflammation, collagen deposition and fibrosis (Riaz et al., 2016). AGEs and oxidative stress have been reported to activate nuclear fraction kappa-beta (NF-κB) and protein kinase C (PKC) signaling and thereby induce inflammation (Tsai and Yin, 2012; Bhattacharjee et al., 2016a). Considering the involvements of multiple toxicological events in DC, the attenuation of these events in diabetic population is the looming issue in the field of clinical diabetology. Increased glucose metabolism i.e. glycemic control is one of the principle means to control DC. Reduction of inflammation, oxidative stress and polyol enzymes would further contribute in attenuation of DC. Induction of a sequence of secondary transducers due to persistent hyperglycemia is principally responsible for the development and progression of DC. Therefore, glycemic control would be the principle intention to control DC. Besides hypoglycemic effect, anti-oxidant and anti-inflammatory effects would potentiate the therapeutic efficacy of a therapeutic agent in DC.

S. roxburghiana is a perennial herb with fleshy stem and enviable rootstock. The crude extract of the rhizomes of this plant has been reported to possess prophylactic effect against DC by our group (Bhattacharjee et al., 2016b). Protocatechuic acid has been isolated from the rhizomes of S. roxburghiana. Protocatechuic acid has been reported to possess antioxidant and anti-inflammatory effect (Erukainure et al., 2017; Tsai and Yin, 2012; Adefegha et al., 2016). Protocatechuic acid has also been reported to possess hypoglycemic activity against experimentally induced type I

diabetic rats without effecting the glycemic status of normal rats (Harini and Pugalendi, 2010). However, mechanism of hypoglycemic effect is yet to be explored. Considering the ethnomedicinal evidences of S. roxburghiana rhizomes coupled with reported pharmacological effects of protocatechuic acid, present study was undertaken to evaluate the therapeutic benefit of protocatechuic acid against DC in T2D rats. It has been aimed to explore the mechanism of action. Finally, in silico molecular docking and ADME studies were performed to demonstrate the probable interactions between protocatechuic acid with signal proteins and the possible safety profile of the same compound.

6.2. Material and methods

6.2.1. Chemicals

Streptozotocin was procured from Hi-media (Mumbai, India). Protocatechuic acid (≥ 97 %), Bradford reagent and bovine serum albumin were procured from Sigma-Aldrich (St. Louis, USA). The antibodies were purchased from Santa Cruz Biotechnology (Santa Cruz, USA) and Sigma-Aldrich (St. Louis, USA). The kits/reagents for biochemical assays for estimating different biochemical parameters were bought from Span diagnostic Ltd., India and Sigma-Aldrich, USA. All other reagents, solvents and chemicals used were of analytical grade.

6.2.2. Extraction of protocatechuic acid

The detailed extraction procedure of protocatechuic acid has been discussed in Chapter 3. Briefly, the powdered rhizomes of *S. roxburghiana* were macerated with methanol with constant stirring. The crude extract was fractioned with n-hexane using separating funnel. The residue was chromatographed in a normal phase silica gel column and eluted with n-hexane-ethyl acetate and ethyl acetate-methanol with increasing polarity, to yield 8 major fractions (A-H). Fraction E was further chromatographed with n-hexane-CH_2Cl_2 and CH_2Cl_2-CH_3OH with increasing polarity to yield 4 sub-fractions (E1-4). The sub-fraction E3 was further column chromatographed using same solvent system and finally purified by preparative TLC using solvent system CH_2Cl_2: CH_3COCH_3: CH_3COOH (10: 1.5: 0.5, v/v/v) to yield protocatechuic acid. The structure has been elucidated employing ^{1}H and ^{13}C NMR interpretation and mass spectroscopic data (Gutzeit et al., 2007; Martin et al., 2000).

6.2.3. Animals

Wistar rats (♂, 150 ± 20 g) were housed in separate polypropylene cages under standard laboratory conditions of temperature (24 ± 2 °C), relative humidity (55 ± 5%), light:dark schedule (12 h:12 h), standard rat diet (Agro Corporation Private Ltd., Bangalore, India) and water ad

libitum (Dewanjee et al., 2009). The experiment was performed at the animal house (Registration No. 0367/01/C/CPCSEA, UGC, India) of the Department of Pharmaceutical Technology, Jadavpur University, India. The animal experiment has been permitted by the Jadavpur University animal ethical committee (Ref no. AEC/PHARM/1501/01/2015 dated 18.03.2015) and the principles of laboratory animals care were followed during experiment (PHS, 1986). The animals were acclimatized for 2 weeks before the execution of the in vivo experiment.

6.2.4. Induction of T2DM and Experimental design

High fat fed-low single dose of streptozotocin model for T2DM was used in this study (Reed et al, 2000; Srinivasan et al. 2005). Briefly, the Wistar rats were fed high fat diet (Bhattacharjee et al., 2016b) ad libitum for 2 weeks. After 2 weeks, the rats were injected a single dose of streptozotocin (35 mg/kg body weight, i.p.). 1 week after streptozotocin treatment, the rats exhibited fasting blood glucose levels 170 ± 30 mg/dl were considered to be type 2 diabetic (T2D) rats and included for the further experiments. This experimental model for T2D was validated by our group (Bhattacharjee et al., 2016b). The rats were continued with high fat diet throughout the course of the study. One group of normal rats receiving normal diet was kept as normal control.

The rats were divided into three groups (n = 6) and received the treatment as follows:

Group I: Normal control rats were administered distilled water (2 ml/kg body weight, orally by oral gavage) daily for 28 days;

Group II: T2DM control rats were administered high fat diet + distilled water (2 ml/kg body weight, orally by oral gavage) daily for 28 days;

Group III: T2D rats were administered high fat diet + protocatechuic acid (50 mg/kg body weight, orally by oral gavage) daily for 28 days;

Group IV: T2D rats were administered high fat diet + protocatechuic acid (100 mg/kg body weight, orally by oral gavage) daily for 28 days (Dewanjee et al., 2009).

The animals were monitored at 8-hours interval for checking any sign of distress and abnormality. The body weights, food intake and water intake were monitored in aforementioned timetable. The experimental rats were fasted overnight and the fasting blood glucose levels were measured on day 0, 1, 3, 7, 14, 21 and 28 using single touch glucometer (Ascensia Entrust, Bayer Health Care, USA) (Dewanjee et al., 2009). After the last treatment, animals were fasted overnight and the blood samples were withdrawn from retro-orbital venous plexus after applying tetracaine (0.5 %) ophthalmic drop to the eye of rats (Dua et al., 2016b). The animals were

euthanatized and the hearts were excised, cleaned immediately with cold phosphate buffer saline (pH 7.4) (Dua et al., 2016a). The hearts were immediately subjected to different processing for histological, biochemical and immunoblotting analyses. In search of mechanism of hypoglycemic effect, the soleus muscle (skeletal muscle) were collected from individual rats under different treatments and subjected to lysis. The overall experimental design has been depicted in Figure 6.1.

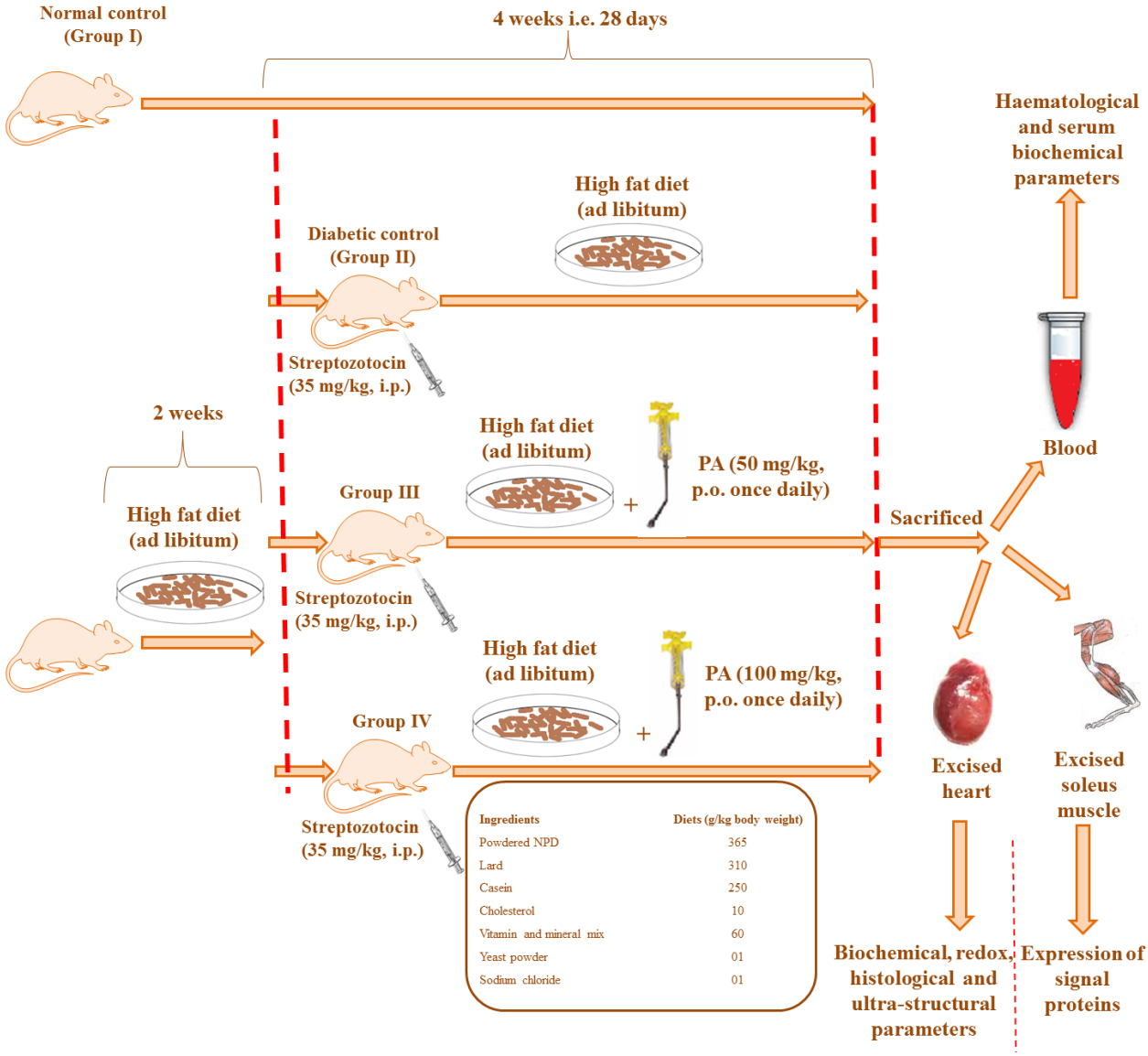

Figure 6.1. A schematic impression of in vivo experiment.

6.2.5. Estimation of serum biochemical parameters

Serum insulin level was measured by ELISA using commercially available kit (Sigma-Aldrich, USA). Homeostatic model assessments were performed by estimating HOMA-IR and HOMA-β using the following equations (Bhattacharjee et al., 2016b):

HOMA-IR = (Fasting serum insulin in U/l x Fasting blood glucose in mmol/l)/22.5

HOMA-β = (Fasting serum insulin in U/l x 20/Fasting blood glucose in mmol/l) – 3.5

The serum lipid profile viz. total cholesterol, HDL cholesterol and triglycerides levels were estimated by commercially available kits (Span Diagnostic Limited, India) following manufacturer's instructions. LDL cholesterol level was estimated following Friedewald's equation, LDL cholesterol = Total cholesterol - Triglycerides/5 – HDL cholesterol (Friedewald et al., 1972). Serum lactate dehydrogenase (LDH) and creatinin kinase (CK) levels were estimated by the commercially available kits (Span Diagnostic Limited, India) following manufacturer's instructions. Glycosylated hemoglobin concentration was estimated according to the protocol described by Nayak and Pattabiraman (1981). The AGEs in the sera were measured by ELISA (Abcam, Cambridge, UK) as per the manufacturer's instructions. Troponin I and T contents were determined by ELISA kits (Kamiya Biomedical Company, USA). IL 1β, IL 6, IL 12 and TNF α levels in the sera were measured by ELISA kits (Fisher Thermo Scientific Co., USA).

6.2.6. Western blotting of signal proteins in skeletal muscle

The soleus muscles of the rats of different groups were homogenized with ice cold lysis buffer. Proteins in the subcellular fractions were obtained by density gradient centrifugation method (Thurmond et al., 1998). Protein samples were quantified by ELISA (Bio-Rad, USA). The protein samples (20 µg) were subjected to SDS-polyacrylamide gel (12 %) electrophoresis and western blotted as described by Dewanjee et al (2015). Briefly, the separated proteins in gel were transferred into nitrocellulose membrane. The membranes were blocked for 1 h at room temperature by treating with blocking buffer (containing 5% non-fat dry milk). The membranes were then incubated with primary antibodies at 4 °C overnight followed by washing with tris-buffered saline (TBST). The membranes were then subjected to suitable HRP-conjugated secondary antibody at room temperature for 1 h. The blots were finally documented by 3, 3' -diaminobenzidine tetrahydrochloride (Banglore Genei, India). The membranes were then subjected to mild stripping using stripping buffer containing 1% SDS (pH 2.0) and glycine (25 mM) followed by treatments with primary and secondary antibodies for detecting the expressions of other proteins in a single membrane. The expressions of phospho-IRS-1(Tyr 895), PI3K (p85),

phospho-Akt (Ser 473), phospho-AMPK (Thr 172) and phospho-P38 (Tyr 180/ Tyr 182) were studied. Normalization of the expressions of proteins was done by using GAPDH as loading control.

6.2.7. Estimation of biochemical parameters of myocardial tissues

The cardiomyocytes were isolated from the immediately decapitated hearts of the experimental rats following the method described by Nair and Nair (1997) with little modification (Raghu et al., 2009). Briefly, decapitated hearts were rapidly immersed in cold Ca^{2+}-free solution. The ventricular myocardial cells were isolated using Langendorff apparatus employing retrograde perfusion through the aorta with enzyme-containing solutions. Finally, Ca^{2+}-replication was done to obtain Ca^{2+}-tolerant cardiomyocytes. Intracellular ROS production was performed in accordance to the method of LeBel and Bondy (1990) employing 2,7-dichlorofluorescein diacetate (DCF) as a probe. The hearts were homogenized in 0.1 M Tris-HCl-0.001 M EDTA buffer (pH 7.4) and centrifuged (@ 12,000 g; 30 min; 4 ^{o}C). The supernatants were collected for the biochemical assays. The extent of lipid peroxidation (thiobarbituric acid reactive substances, TBARS, by-products of lipid peroxidation) was estimated following the method of Ohkawa and co-workers (1979). The carbonylation of proteins was measured as per the method described by Uchida & Stadtman (1993). Co-enzymes Q9 and Q10 were appraised employing RP-HPLC as per standard protocol (Zhang et al., 1995). The level of reduced glutathione (GSH) was assayed by the method described by Hissin & Hilf (1973). The levels of endogenous redox enzymes viz. catalase (CAT), superoxide dismutase (SOD), glutathione peroxidase (GPx) and glutathione reductase (GR) were assessed as the per standard methods (Ghosh et al., 2010). The degree of DNA fragmentation in the selected tissues was measured by the diphenylamine reaction as described by Lin et al. (1997). DNA oxidation was assessed by RP-HPLC and was denoted as the ratio of 8-OHdG to 2-dG (Bolner et al., 20111). Intracellular ATP concentration was estimated using the commercially available assay kit (Abcam, MA, USA). Aldose reductase activity was measured following the method described by Nishinaka and Yabe-Nishimura (2001). The sorbitol dehydrogenase activity was measured following the protocol of Ulrich (1974). Glyoxalase-I activity was measured in accordance to McLellan and Thornalley (1989). The intracellular ATP concentrations were screened by commercial kits (Abcam, Cambridge, USA). Levels of collagen IV in the tissue homogenates were determined using ELISA kits (R&D Systems, Inc. USA) according to the manufacturer's guidelines.

6.2.8. Western blotting of signal proteins in myocardial tissues

The protein samples of hearts of specific cellular components namely cytosolic and nuclear fractions were separated following standard sequential fractionation process as described by Baghirova et al. (2015) and were quantified by ELISA (Bio-Rad, USA). The protein samples (20 µg) were subjected to 10 % SDS-PAGE gel electrophoresis and western blotted as described by Dua et al (2015a). The expressions of phospho-NF-κB (Ser 536), phospho-IκBα (Ser 32), IκBα, PKC β, PKC ε, PKC δ and PARP were studied. The immunoblots were detected by 3,3′-diaminobenzidine tetrahydrochloride (Banglore Genei, India). Normalization of protein expression was done by using GAPDH as loading control.

6.2.9. Histological assessment

Excised hearts of rats were immediately fixed in formalin and were subjected for paraffin blocking followed by sectioning. Sections of ~ 5 µm thickness were stained with hematoxylin & eosin (H & E) to assess under microscope (Dua et al., 2015b). Masson Trichrome (MT) staining was performed following the protocol of Xiao et al. (2015). Finally, the sections were mounted with resinous mounting medium for microscopic observations.

6.2.10. Statistical analysis

The experimental data were interpreted by one-way ANOVA and expressed as mean ± SD followed by Dunnett's t-test using computerized GraphPad InStat (version 3.05), GraphPad software, USA. The significance was considered when $p < 0.05$.

6.2.11. In silico ADME prediction of protocatechuic acid

In silico ADME properties of the protocatechuic acid have been performed by the QikProp module in the Maestro Schrodinger (MS) software (www.schrodinger.com). Here, ADME properties have been checked through Lipinski's rule of five along with some important properties such as mol_MW, FOSA, FISA, PISA, donarHB, accptHB, percent human oral absorption, rtvFG, CNS, QPlogPo/w, QPlogHERG and QPPCaco (Ray et al., 2015).

6.2.12. Molecular docking

The possible interaction patterns of protocatechuic acid with many receptors were investigated. To perform this work, the target proteins such as PKC-δ (PDB: 1PTR), PKC-β (PDB: 2I0E), IRS (PDB: 2Z8C), PI3K (PDB: 3DBS), Akt (PDB: 3D0E), AMPK (PDB: 4QFR), PARP (PDB: 5DS3) and NF-κB (PDB: 1A3Q) were retrieved from the protein data bank (PDB) accessed on July 2015 (http://www.rcsb.org/). Protocatechuic acid, as ligand, was taken from the pubchem database. The preparation of protein structures to complete fault like missing loops, steric clashes

and missing atom names were performed by Protein Preparation Wizar. The ligand, protocatechuic acid, has been prepared in Ligprep of Schrödinger (www.schrodinger.com). The grid was generated to locate the active sites of the protein on the basis of co-crystal ligand attached with the crystal protein. Finally, the SP docking studies (www.schrodinger.com) were performed in Glide. For getting the amino acids which were mainly responsible for the ligand's activity, the docking interactions were compared with the interactions present in the co-crystal ligand available in the PDB site.

6.3. Results

6.3.1. Effects on fasting blood glucose level, body mass gain, foods and water intake

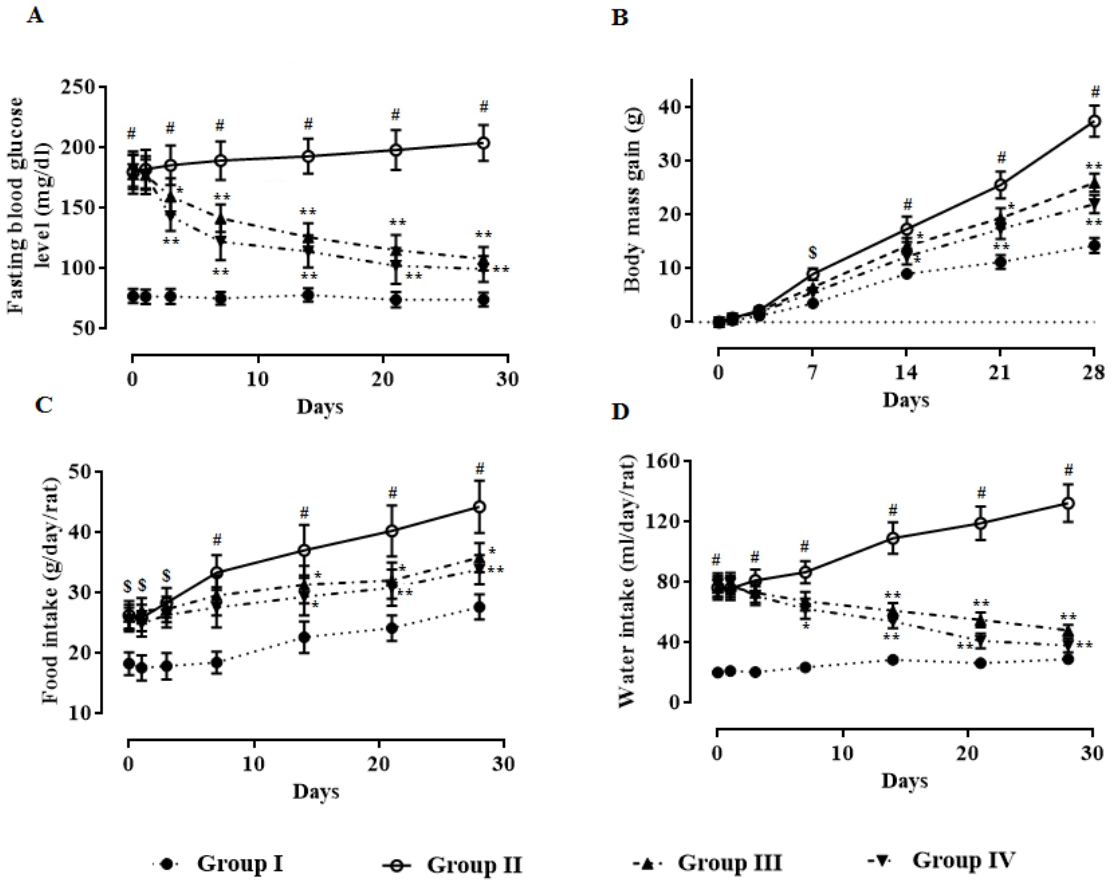

Figure 6.2. Effects of protocatechuic acid on fasting blood glucose level (A), body mass gain (B), foods intake (C), and water intake (D) in T2D rats. Data were expressed as mean ± SD (n = 6). $^{\$}p < 0.01$ compared with Group I; $^{\#}p < 0.01$ compared with Group I; *p < 0.05 compared with Group II; **p < 0.01 compared with Group II. Group I: normal control; Group II: T2D control; Group III: T2D rats treated with protocatechuic acid (50 mg/kg, orally), Group IV: T2D rats treated with protocatechuic acid (100 mg/kg, orally).

High fat fed rats treated with small i.p. dose of streptozotocin exhibited significantly ($p < 0.01$) high fasting blood glucose level (170 ± 30 mg/dl) when compared with normal rats (Figure 6.2.A). Protocatechuic acid (50 and 100 mg/kg) treatment significantly alleviated ($p < 0.05$-0.01) fasting blood glucose level day 3 onward of therapeutic regime. However, maximum therapeutic efficacy was observed on 28th day of treatment with the reduction of ~ 39.32 ($p < 0.01$) and 45.39 % ($p < 0.01$) of fasting blood glucose at the doses of 50 and 100 mg/kg, respectively. The effects of protocatechuic acid on body mass gain, food and water consumption by the experimental rats of different groups were depicted in Figure 6.2. (B-D). In this study, the T2D rats exhibited significant ($p < 0.05$-0.01) increase in body mass gain when compared with normal rats. However, protocatechuic acid (50 and 100 mg/kg) treatment could significantly reduce body mass gain day 14 onward of the therapeutic regime. In this study, the T2D rats exhibited significant raise in food ($p < 0.05$-0.01) and water ($p < 0.01$) consumption when compared with normal rats. However, protocatechuic acid (50 and 100 mg/kg) treatment significantly reversed food ($p < 0.05$-0.01) and water ($p < 0.01$) consumption day 14 onward of therapeutic regime.

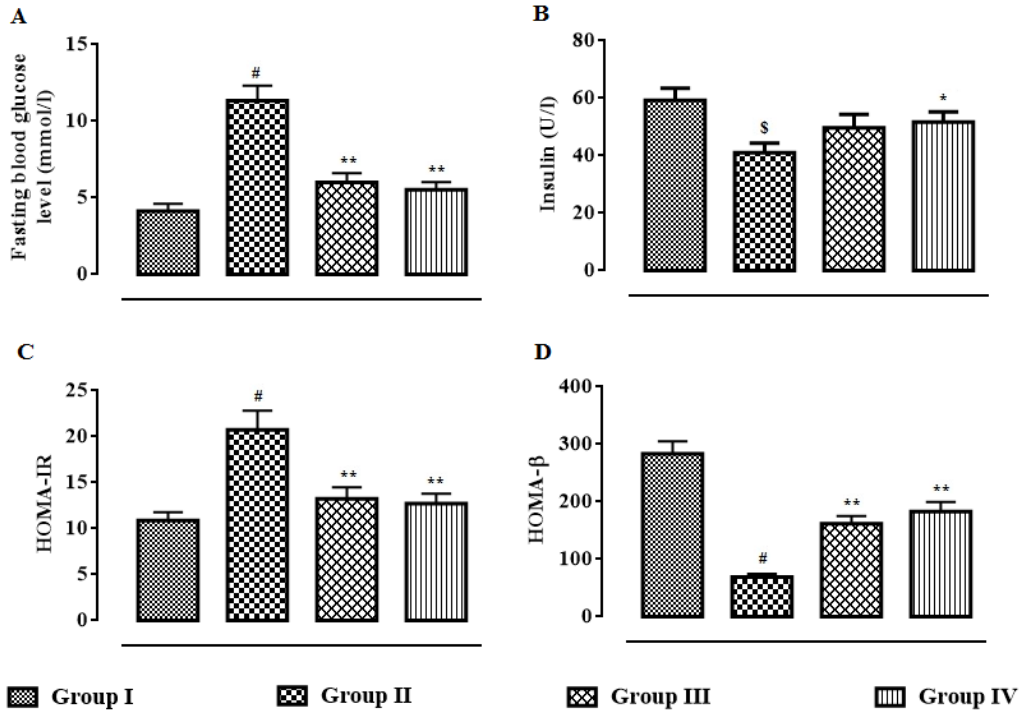

Figure 6.3. Effects of protocatechuic acid on fasting blood glucose level (mmol/l) (A), serum insulin (U/l) (B), HOMA-IR, (C) score and HOMA-β (D) score on day 29 of post treatment in T2D rats. Data were expressed as mean ± SD (n = 6). $^{\$}p < 0.01$ compared with Group I; $^{\#}p < 0.01$ compared with Group I; *$p < 0.05$ compared with Group II; **$p < 0.01$ compared with Group II.

Group I: normal control; Group II: T2D control; Group III: T2D rats treated with protocatechuic acid (50 mg/kg, p.o.), Group IV: T2D rats treated with protocatechuic acid (100 mg/kg, p.o.). HOMA-IR = (Fasting serum insulin in U/l x Fasting blood glucose in mmol/l)/22.5; HOMA-β = (Fasting serum insulin in U/l x 20/Fasting blood glucose in mmol/l) – 3.5.

6.3.2. Effects on serum insulin level, HOMA-IR and HOMA-β

The effects protocatechuic acid (50 and 100 mg/kg) on fasting blood glucose level (mmol/l), serum insulin (U/l), HOMA-IR and HOMA-β have been shown in Figure 6.3. (A-D). T2D rats exhibited significantly ($p < 0.01$) high fasting blood glucose (mmol/l) on day 29 (Figure 6.3.A), while, serum insulin level was significantly ($p < 0.05$) reduced on day 29 when compared with normal rats (Figure 6.3.B). However, protocatechuic acid (50 and 100 mg/kg) treatment could significantly reverse the blood glucose ($p < 0.01$) levels to near normal status. On the other hand, protocatechuic acid (100 mg/kg) could significantly ($p < 0.05$) improve insulin level in the sera of T2D rats. In this study, T2D rats exhibited significantly high ($p < 0.01$) HOMA-IR score (Figure 6.3.C) with concomitant reduction ($p < 0.01$) of HOMA- β score when compared with normal rats (Figure 6.3.D). Aforementioned alteration in fasting blood glucose level, HOMA-IR and HOMA-β scores indicated the establishment of hyperglycemia coupled with insulin resistance. On the other hand, protocatechuic acid (50 and 100 mg/kg) treatment could significantly reverse HOMA-IR ($p < 0.01$) and HOMA-β ($p < 0.01$) scores near to normalcy (Fig 6.3.C and D).

6.3.3. Effects on serum biochemical parameters

In this study, the effects of protocatechuic acid on different biochemical parameters were studied (Table 6.1.). Significant elevation in the levels of total cholesterol ($p < 0.01$), triglycerides ($p < 0.01$) and LDL-cholesterol ($p < 0.01$) was observed in the sera of T2D rats. However, HDL-cholesterol ($p < 0.01$) level was significantly reduced in the sera of T2D rats. On the other hand, protocatechuic acid (50 and 100 mg/kg) treatment could significantly reverse serum lipid profile ($p < 0.01$) of T2D rats near to normalcy. T2D rats exhibited a significantly ($p < 0.01$) high levels of glycosylated-haemoglobin, C-reactive proteins, LDH, CK, AGEs and troponins in the sera. However, protocatechuic acid (50 and 100 mg/kg) treatment could significantly reverse glycosylated-haemoglobin, C-reactive proteins, LDH, CK, AGEs, troponin I and troponin II levels in the sera of T2D rats.

Table 6.1. Effects of protocatechuic acid on serum biochemical parameters of experimental rats.

Parameters	Group I	Group II	Group III	Group IV
Total cholesterol (mg/dl)	87.21± 7.33	164.21 ± 15.08$^{\#}$	136.74 ± 12.89**	132.15 ± 13.54**
HDL cholesterol (mg/dl)	34.50 ± 2.92	15.18 ± 1.67$^{\#}$	26.92 ± 2.11**	27.89 ± 2.37**
LDL cholesterol (mg/dl)	28.13 ± 2.33	108.72 ± 9.42$^{\#}$	76.93 ± 6.81**	73.06 ± 7.18**
Triglycerides (mg/dl)	122.91 ± 10.11	201.55 ± 19.98$^{\#}$	164.43 ± 13.17**	156.02 ± 14.12**
Glyco-haemoglobin (mg/g haemoglobin)	0.32 ± 0.08	0.71 ± 0.08$^{\#}$	0.48 ± 0.03**	0.47 ± 0.08**
LDH (U/l)	156.72± 14.82	272.54 ± 24.50$^{\#}$	197.33 ± 16.48**	182.11 ± 14.75**
CK (IU/mg of protein)	12.07 ± 1.20	18.05 ± 1.62$^{\#}$	15.59 ± 1.37*	13.18 ± 1.02**
C-reactive protein (mg/dl)	1.46 ± 0.15	2.88 ± 0.47$^{\#}$	1.84 ± 0.33**	1.73 ± 0.24**
AGEs (µg/ml)	415.48 ± 32.11	772.23 ± 60.19$^{\#}$	587.01 ± 55.18**	528.44 ± 48.82**
Troponin I (ng/ml)	1.33 ± 0.18	2.78 ± 0.54$^{\#}$	2.12 ± 0.24*	1.97 ± 0.35**
Troponin T (ng/ml)	472.76 ± 45.29	796.01 ± 73.67$^{\#}$	645.00 ± 54.12*	622.71 ± 60.13**

Data were expressed as mean ± SD (n = 6). $^{\#}p< 0.01$ compared with Group I; *p< 0.05 compared with Group II; **p< 0.01 compared with Group II. Group I: normal control; Group II: T2D control; Group III: T2D rats treated with protocatechuic acid (50 mg/kg, orally), Group IV: T2D rats treated with protocatechuic acid (100 mg/kg, orally).

6.3.4. Effects on signal proteins in the skeletal muscle

The western blot analyses of the signal proteins involved in glucose utilization in the skeletal muscle were performed (Figure 6.4). In this study, significant ($p < 0.01$) down-regulation in the expression of PI3K (p 85) was observed in skeletal muscle of T2D rats. On the other hand, protocatechuic acid (50 and 100 mg/kg) treatment could significantly ($p < 0.01$) up-regulate PI3K (p 85) expression in the skeletal muscle of T2D rats. Phosphorylation of IRS 1 protein was significantly down-regulated resulting a significantly ($p < 0.01$) low phospho-IRS 1 rxpression in the skeletal muscle of T2D rats. However, protocatechuic acid (50 and 100 mg/kg) treatment could significantly ($p < 0.01$) reverse phospho-IRS 1 expression to near normal status. A significant reduction ($p < 0.01$) in the expression of phospho-Akt in the skeletal muscle of T2D rats indicated inactivation of Akt signaling. However, protocatechuic acid (50 and 100 mg/kg) treatment could significantly ($p < 0.01$) promote Akt signaling pathway via up-regulation of phosphorylation of Akt protein in the skeletal muscle of T2D rats. In this study, a significant ($p < 0.01$) down regulation in the expression of membrane associated GLUT4 was observed in the skeletal muscle of T2D rats. However, protocatechuic acid (50 and 100 mg/kg) treatment could significantly ($p < 0.01$) up-regulate the expression of membrane associated GLUT4 in the skeletal muscle of T2D rats. In this study, T2D rats exhibited a significant ($p < 0.01$) down-regulation in the expressions of phospho-AMPK and phospho-P38 in the skeletal muscle. However,

protocatechuic acid (50 and 100 mg/kg) treatment could significantly up-regulate ($p < 0.01$) the expressions of phospho-AMPK and phospho-P38 in the skeletal muscle of T2D rats.

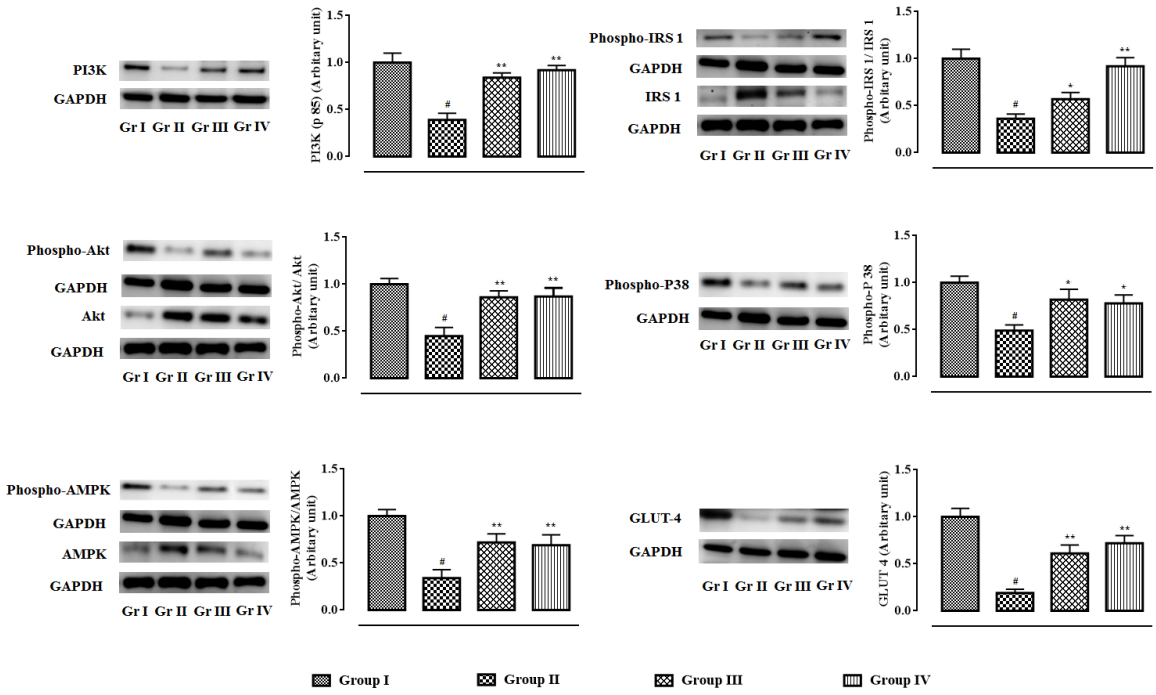

Figure 6.4. Effects of protocatechuic acid in the expressions of signal proteins viz. PI3K, IRS 1, Akt, P38, AMPK in skeletal muscle of T2D rats followed by densitometric analysis of the respective protein levels and the normal control band was given an arbitrary value of 1. GAPDH was used as loading control. Data were expressed as mean ± SD (n = 6). #$p < 0.01$ compared with Group I; *$p < 0.05$ compared with Group II; **$p < 0.01$ compared with Group II. Group I: normal control; Group II: T2D control; Group III: T2D rats treated with protocatechuic acid (50 mg/kg, orally), Group IV: T2D rats treated with protocatechuic acid (100 mg/kg, orally).

6.3.5. Effects on polyol enzymes, ATP and collagenase IV in the myocardial tissue

In this study, significant up-regulation in the levels of aldose reductase ($p < 0.01$) and sorbitol dehydrogenase ($p < 0.01$) with concomitant depletion of glyoxalase-I ($p < 0.01$) were observed in the myocardial tissue homogenate of T2D rats (Figure 6.5.). However, protocatechuic acid (50 and 100 mg/kg) treatment could significantly down-regulate the levels of aldose reductase ($p < 0.01$), sorbitol dehydrogenase ($p < 0.01$) in the heart of T2D rats. However, glyoxalase-I ($p < 0.05$-0.01) level was significantly improved in the myocardial tissue of T2D rats following protocatechuic acid (50 and 100 mg/kg) treatment. In this study, ATP level in the myocardial

tissue homogenate was significantly ($p < 0.01$) reduced in T2D rats when compared to that of normal rats (Figure 6.5.). However, treatment with protocatechuic acid (50 and 100 mg/kg) could significantly ($p < 0.05$-0.01) enhance intracellular ATP content in the myocardial tissues of T2D rats. In this study, T2D rats exhibited a significant ($p < 0.01$) elevation in the levels of collagen IV in the myocardial tissue (Figure 6.5.). However, protocatechuic acid (50 and 100 mg/kg) treatment could significantly reverse collagen IV ($p < 0.01$) levels in hearts of T2D rats.

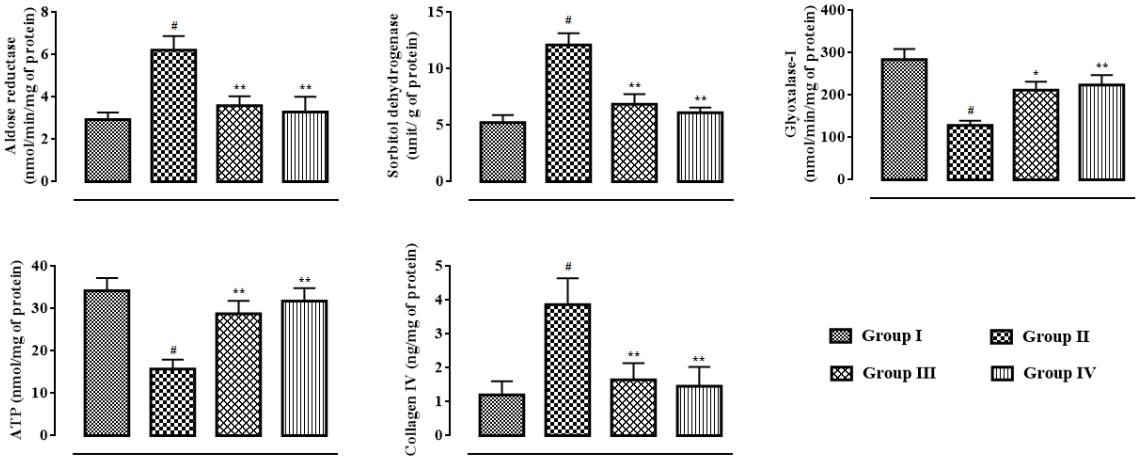

Figure 6.5. Effects of protocatechuic acid on aldose reductase, sorbitol dehydrogenase, glyoxalase-I, ATP and collagen IV levels in myocardial tissues of T2D rats. Data were expressed as mean ± SD (n = 6). #$p < 0.01$ compared with Group I; *$p < 0.05$ compared with Group II; **$p < 0.01$ compared with Group II. Group I: normal control; Group II: T2D control; Group III: T2D rats treated with protocatechuic acid (50 mg/kg, orally), Group IV: T2D rats treated with protocatechuic acid (100 mg/kg, orally).

6.3.6. Effects on redox status within myocardial tissues

In this study, intracellular ROS production, lipid peroxidation, protein carbonylation, endogenous anti-oxidant enzymes, GSH, co-enzymes Q, DNA fragmentation, and DNA oxidation in the cardiac tissues were depicted in Figure 6.6. In this study, T2D rats exhibited significantly high ($p < 0.01$) levels of intercellular ROS in the myocardial tissue. The levels of TBARS and carbonylated proteins were significantly ($p < 0.01$) amplified in the cardiac tissues of T2D rats. However, protocatechuic acid (50 and 100 mg/kg) treatment could significantly alleviate ROS production ($p < 0.01$), lipid peroxidation ($p < 0.05$) and protein carbonylation ($p < 0.05$-0.01) in

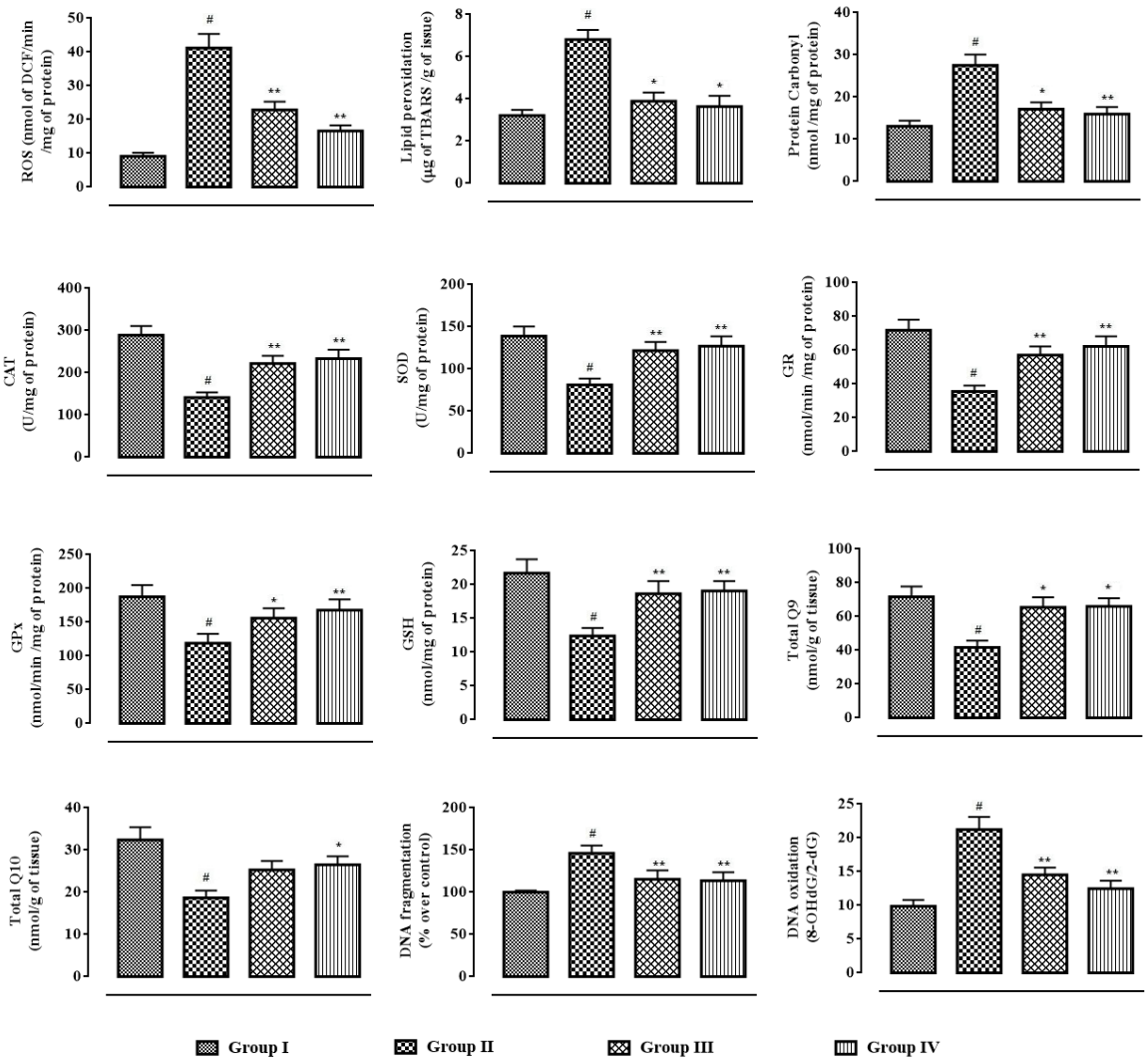

Figure 6.6. Effects of protocatechuic acid on redox status viz. ROS production, lipid peroxidation, protein carbonylation, SOD, CAT, GR, GPx, GSH, co-enzyme Q9, co-enzyme Q10, DNA fragmentation, DNA oxydation in myocardial tissues of T2D rats. Data were expressed as mean ± SD (n = 6). #p < 0.01 compared with Group I; *p < 0.05 compared with Group II; **p < 0.01 compared with Group II. Group I: normal control; Group II: T2D control; Group III: T2D rats treated with protocatechuic acid (50 mg/kg, orally), Group IV: T2D rats treated with protocatechuic acid (100 mg/kg, orally). CAT unit, 'U', is defined as µmoles of H_2O_2 consumed per minute. SOD unit, 'U', is defined as the µmoles inhibition of NBT reduction per minute.

the myocardial tissues of T2D rats. The levels of endogenous antioxidant enzymes, such as CAT, SOD, GPx and GR and antioxidant metabolite, namely GSH were significantly (p < 0.01)decreased in the myocardial tissues of T2D rats when compared with normal rats. However,

treatment with protocatechuic acid (50 and 100 mg/kg) significantly ($p < 0.05$-0.01) improved CAT, SOD, GST, GR and GSH levels in the cardiac tissues of T2D rats. T2D rats exhibited significantly ($p < 0.01$) decreased levels of co-enzyme Q9 and Q10 in the cardiac tissue. However, protocatechuic acid (100 mg/kg) treatment could significantly reiverse co-enzyme Q9 and Q10 in the cardiac tissue of T2D rats. In current investigation, the extents of fragmentation and oxidation of DNA were significantly increased in the cardiac tissue of T2D rats. However, Protocatechuic acid (50 and 100 mg/kg) treatment significantly ($p < 0.01$) reversed the DNA fragmentation and oxidation in the cardiac tissues of T2D rats.

6.3.7. Effects on pro-inflammatory cytokines levels

The effects of protocatechuic acid on the inflammatory bio-markers in the sera were shown in Figure 6.7. In this study, significant ($p < 0.01$) elevation in the levels of IL 1β, IL 6, IL 12 and TNF α in the sera of T2D rats were observed. However, protocatechuic acid (50 and 100 mg/kg) could significantly reversed IL 1β ($p < 0.01$), IL 6 ($p < 0.01$), IL 12 ($p < 0.05$-0.01) and TNF α ($p < 0.01$) levels in the sera of T2D rats to near normal status.

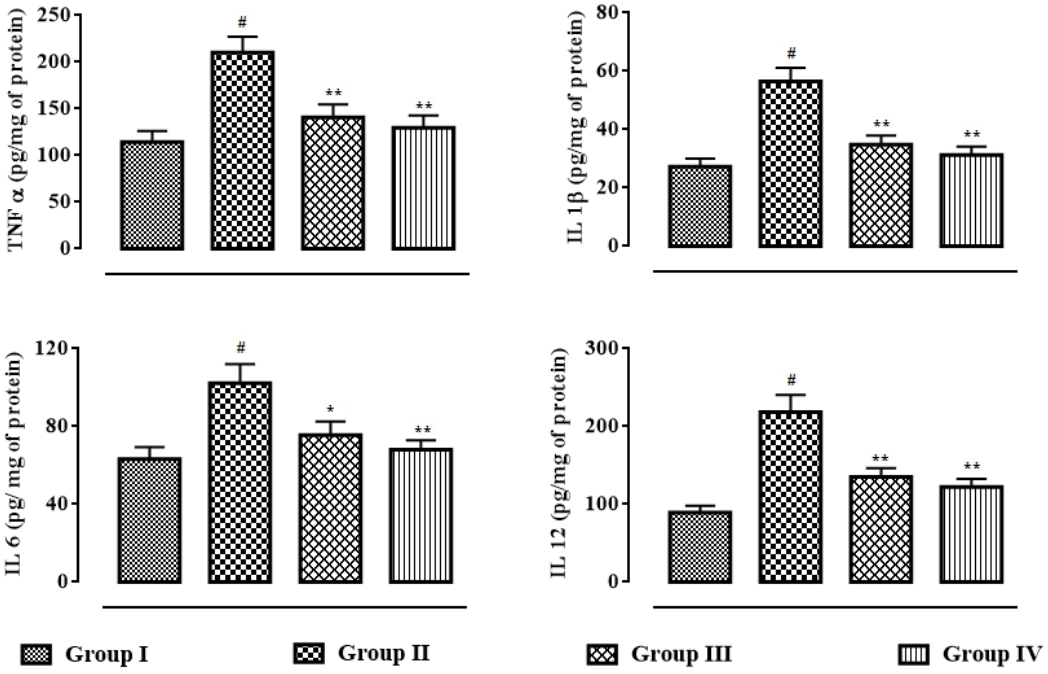

Figure 6.7. Effects of protocatechuic acid on inflammatory biomarkers viz. TNF α, IL 1β, IL 6 and IL 12 in the sera of T2D rats. Data were expressed as mean ± SD (n = 6). Group I: normal control; Group II: T2D control; Group III: T2D rats treated with protocatechuic acid (50 mg/kg, orally), Group IV: T2D rats treated with protocatechuic acid (100 mg/kg, orally).

6.3.8. Effects on signal proteins in hearts

The western blot analyses of the signal proteins involved in inflammatory process in myocardial tissue were performed (Figure 6.8.). In this study, significant ($p < 0.01$) up-regulation in the expressions of PKC isoforms was visible in the cardiac tissue of T2D rats. However, protocatechuic acid (50 and 100 mg/kg) could significantly down-regulate the expressions of PKC β ($p < 0.05$), PKC δ ($p < 0.01$), PKC ε ($p < 0.01$) in the cardiac tissue of T2D rats when compared with T2D control rats. T2D rats exhibited significant ($p < 0.01$) cleavage of PARP into cleaved form (84 kDa) from its full length (116 kDa) in the myocardial tissue. However, protocatechuic acid (100 mg/kg) treatment significantly ($p < 0.05$) attenuated PARP cleavage.

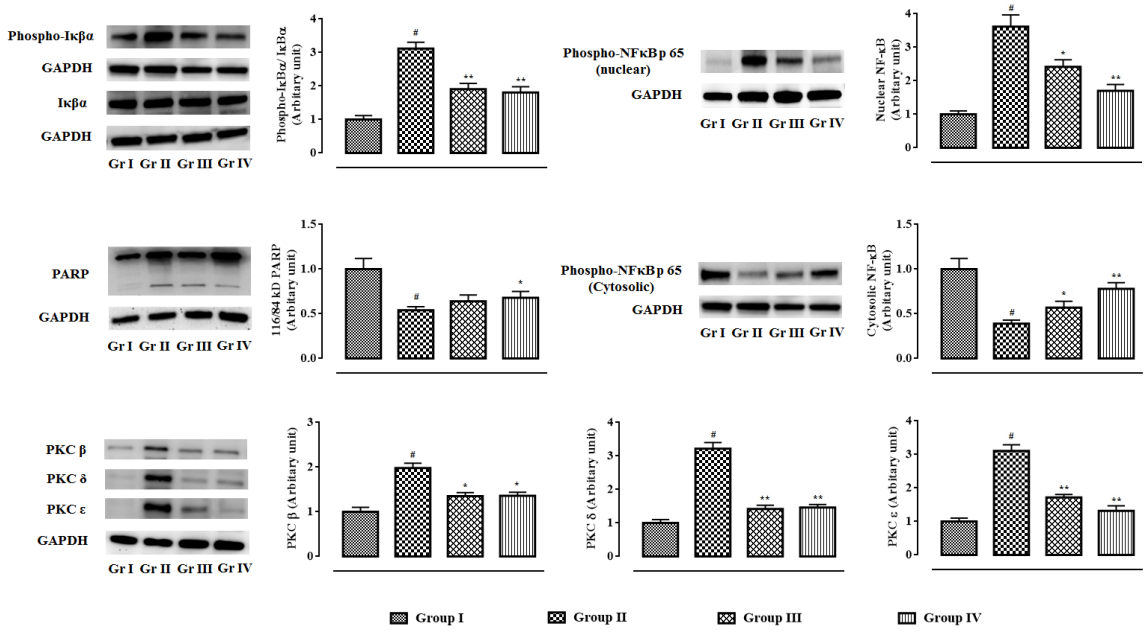

Figure 6.8. Effects of protocatechuic acid on the expressions of signal proteins viz. PARP, PKCs, IκBα, NF-κB involved in the inflammatory patho-physiology in myocardial tissues of T2D rats followed by densitometric analysis of the respective protein levels and the normal control band was given an arbitrary value of 1. GAPDH was used as a loading control. Data were expressed as mean ± SD (n = 6). $^{\$}p < 0.05$ compared with Group I; $^{\#}p < 0.01$ compared with Group I; *$p < 0.05$ compared with Group II; **$p < 0.01$ compared with Group II. Group I: normal control; Group II: T2D control; Group III: T2D rats treated with protocatechuic acid (50 mg/kg, orally), Group IV: T2D rats treated with protocatechuic acid (100 mg/kg, orally).

Immunoblot analysis revealed that significant ($p < 0.01$) degradation of IκBα via its phosphorylation in the myocardial tissue of T2D rats. On other hand, protocatechuic acid (50 and 100 mg/kg) treatment could significantly ($p < 0.01$) reverse IκBα phosphorylation. In this study, significant ($p < 0.01$) up-regulation in the expression of NF-κB (p 65) in the nuclear fraction with concomitant a down-regulation ($p < 0.01$) in the expression of cytosolic NF-κB (p 65) were observed in the myocardial tissues of T2D rats. The aforementioned observations suggested the nuclear translocation of NF-κB protein. However, protocatechuic acid (50 and 100 mg/kg) treatment could significantly reverse the expressions of nuclear and cytosolic NF-κB and thereby prevented the nuclear translocation of NF-κB protein.

6.3.9. Histology of heart sections

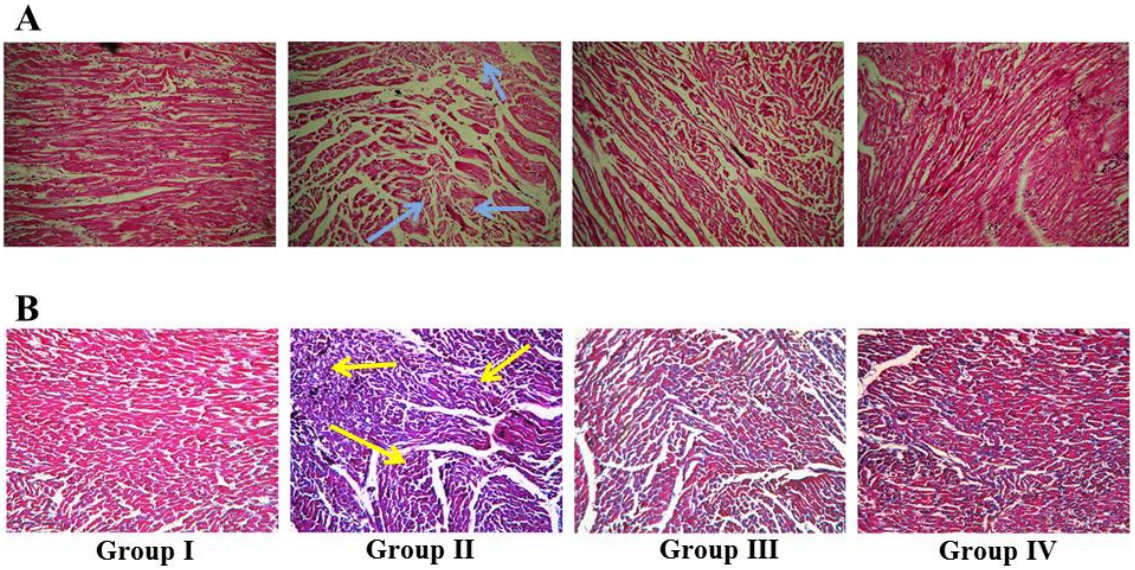

Figure 6.9. Histological assessments of hearts of normal (Group I), T2D rats (Group II), protocatechuic acid (50 mg/kg, orally) treated T2D rats (Group III) and protocatechuic acid (100 mg/kg, orally) treated T2D rats following H & E (A) and MT staining (B).

The histological sections of hearts of rats under different treatments were depicted in Figure 6.9. The H & E stained heart sections (x 100) of T2D rats exhibited the irregular radiating pattern with injured interstitial tissues (blue arrows) (Figure 6.9.A). However, protocatechuic acid (50 and 100 mg/kg) treatment could significantly reduce the T2DM mediated histological abnormality and restored the muscle radiating pattern near to normalcy. MT staining of T2D rats indicated enhanced deposition of collagen (yellow arrows) (Figure 6.9.B). Protocatechuic acid (50 and 100 mg/kg) treatment significantly reduced of blue stained portion, which is an indication of reduction of collagen deposition.

6.3.10. In silico ADME observations

The ADME related descriptors were reported in the Table 6.2. Protocatechuic acid passes all the descriptors related to drug-likeness character of a compound. The QPlogHERG and CNS descriptor suggested that, protocatechuic acid may not produce toxic manifestation to the on heart and central nervous system.

Table 6.2. In silico ADME prediction of protocatechuic acid.

Sl No.	Descriptors	Predicted values for protocatechuic acid
1	rtvFG	0
2	CNS	-1
3	mol_MW	154.122
4	FOSA	0
5	FISA	179.531
6	PISA	84.549
7	Donor HB	3
8	Accpt HB	3.5
9	QPlogPo/w	-0.445
10	QPlogHERG	-0.785
11	QPPCaco	49.774
12	Percent human oral absorption	54.714
13	Rule of five	0

6.3.11. Molecular docking analysis

In the study, it was attempted to explore some possible key residues of the receptors which are especially responsible for the interactions with the protocatechuic acid. Dockings of the signal proteins responsible in glucose transport in the skeletal muscle were shown in Figure 6.10-6.13. In case of PI3K (PDB: 3DBS), three possible H-bond interactions were found with Asp 841 and Tyr 867 along with some hydrophobic interactions with Met 804, Ile 831, Ile 879 etc. (Figure 6.10).

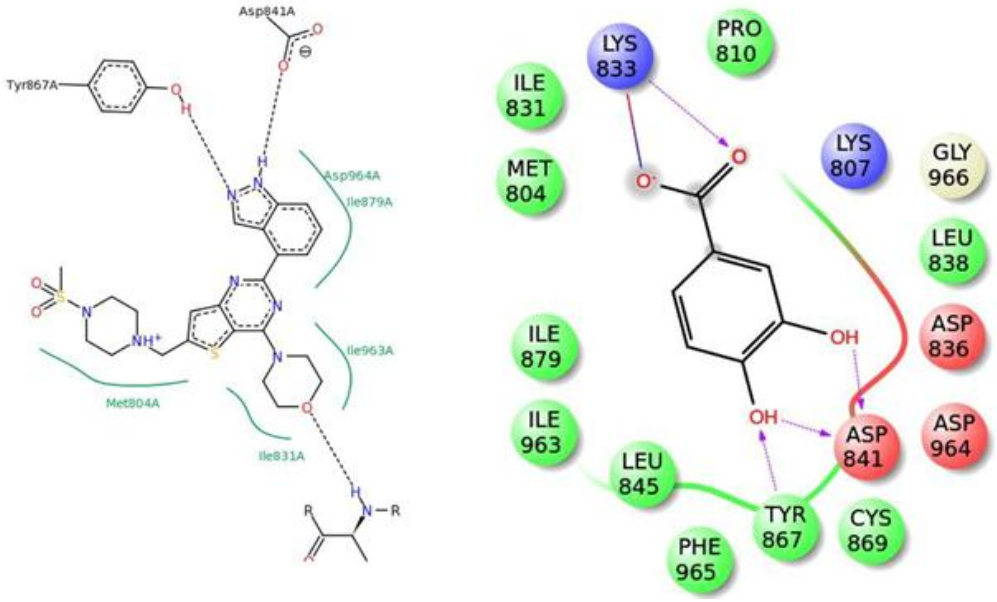

Figure 6.10. Docking interactions of co-crystal ligand with the PI3K protein (PDB: 3DBS) and protocatechuic acid with corresponding amino acid residues of PI3K.

The probable binding interactions of IRS (PDB: 2Z8C) exhibited two H-bonds with Glu 1077 and one important hydrophobic interactions with Leu 1002 (Figure 6.11).

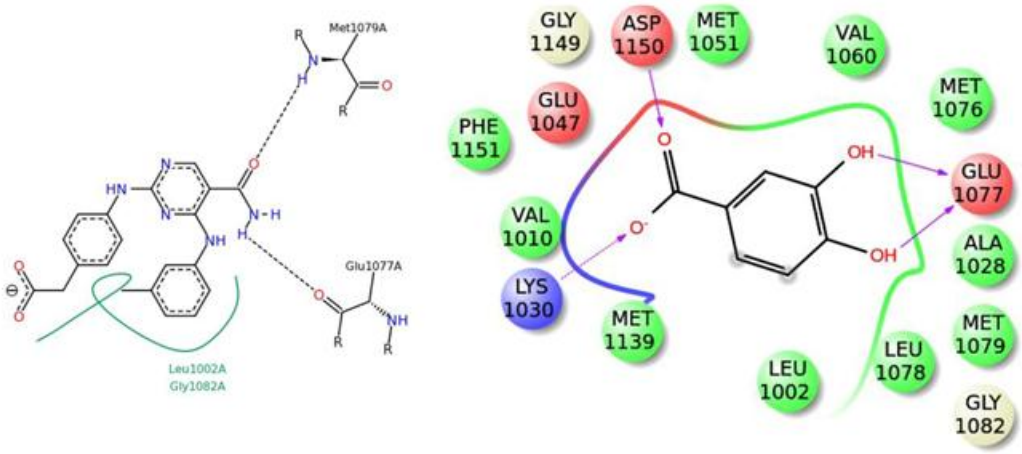

Figure 6.11. Docking interactions of co-crystal ligand with the IRS protein (PDB: 2Z8C) and protocatechuic acid with corresponding amino acid residues of IRS.

Some different interactions were found with the Akt (PDB: 3D0E), such as H-bond interactions with Ala 232 and two co-crystal water molecules, however, the hydrophobic interactions (Met 229 and Val 166 etc) were as similar as mentioned in the PDB file (Figure 6.12).

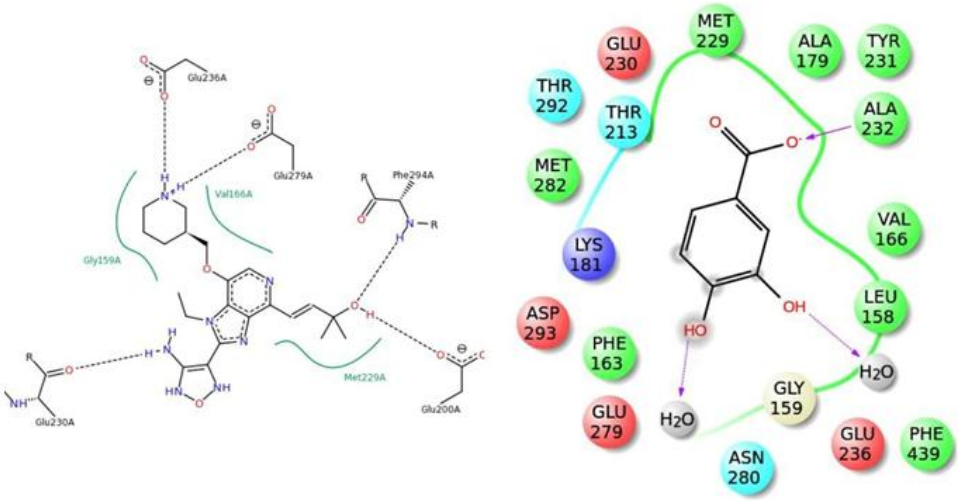

Figure 6.12. Docking interactions of co-crystal ligand with the Akt protein (PDB: 3D0E) and protocatechuic acid with corresponding amino acid residues of Akt.

Another protein AMPK (PDB: 4QFR) produces similar two H-bonds with Val 96 and hydrophobic interactions with Leu 22, Leu 146, Met 93, Ala 156 etc. (Figure 6.13).

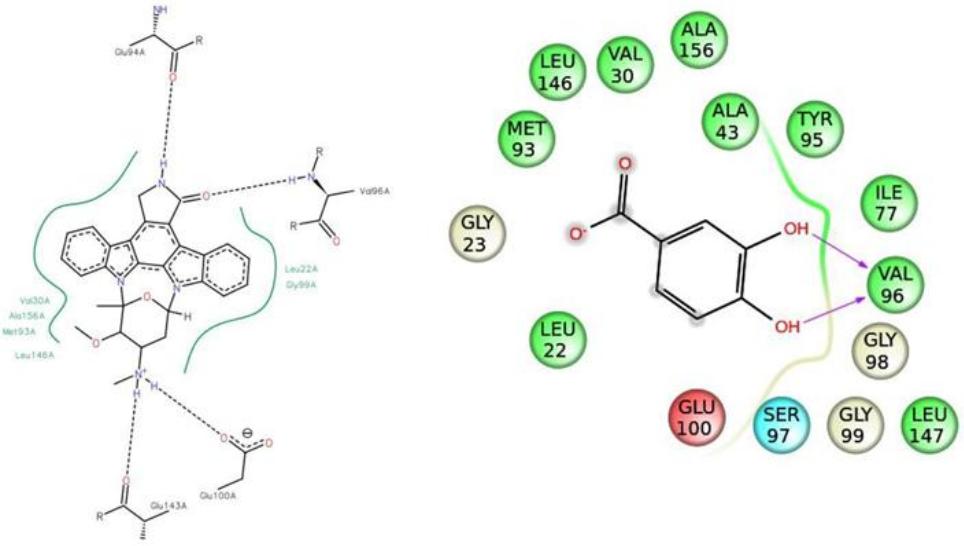

Figure 6.13. Docking interactions of co-crystal ligand with the AMPK protein (PDB: 4QFR) and protocatechuic acid with corresponding amino acid residues of AMPK.

Dockings of the signal proteins responsible in inflammatory pathophysiology in the kidneys were shown in Figure 6.14-6.17. Two H-bond interactions were produced with the catalytic residue (Thr 404 and Val 423) of the protein PKC-β (PDB: 2I0E) and also some hydrophobic interactions were shown with Val 356, Leu 348, Ala 483 etc (Figure 6.14).

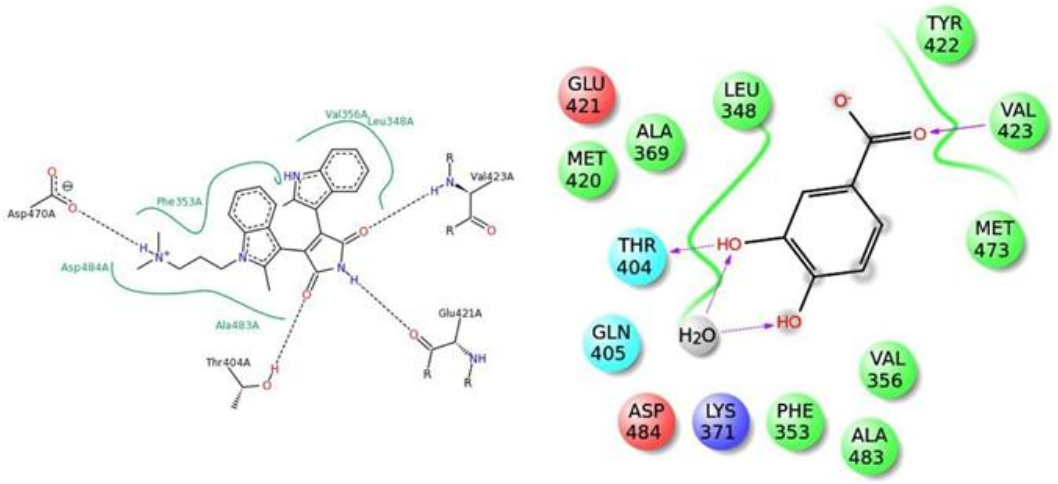

Figure 6.14. Docking interactions of co-crystal ligand with the PKC β protein (PDB: 2I0E) and protocatechuic acid with corresponding amino acid residues of PKC β.

Three H-bond interactions were predicted with most important residues Leu 251 and Thr 242 after binding with PKC-δ (PDB: 1PTR). Other many green ball shaped amino acids were mainly involved for neighbouring hydrophobic interactions of the active cavity site (Figure 6.15).

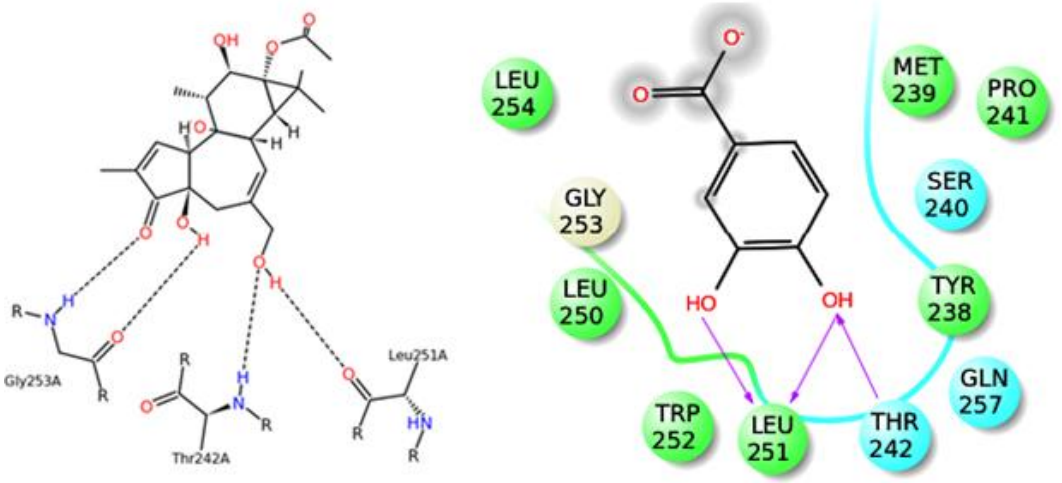

Figure 6.15. Docking interactions of co-crystal ligand with the PKCδ protein (PDB: 1PTR) and protocatechuic acid with corresponding amino acid residues of PKCδ.

The protein, PARP (PDB: 5DS3), exhibited three H-bond interactions with Gly 863 and Ser 904 along with some hydrophobic interactions with Tyr 896, Tyr 907 etc. Also here a similar π- π stacking interaction was prominently seen with Tyr 907 (Figure 6.16).

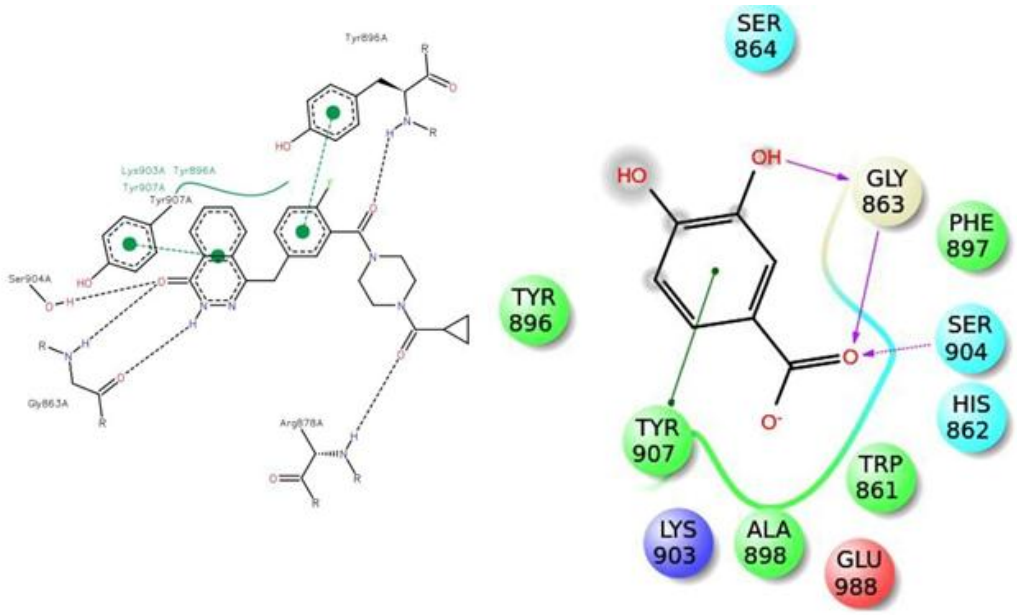

Figure 6.16. Docking interactions of co-crystal ligand with the PARP protein (PDB: 5DS3) and protocatechuic acid with corresponding amino acid residues of PARP.

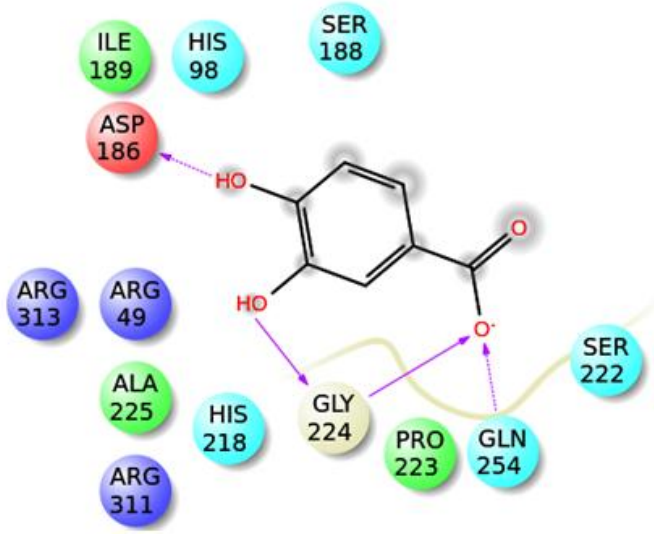

Figure 6.17. Docking interactions of protocatechuic acid with the NF-κB protein (PDB: 1A3Q).

The protein NF-κB (PDB: 1A3Q) prominently showed three H-bond interactions with Gln 254, Gly 224 and Asp 186 along with two hydrophobic interactions with Ala 225 and Pro 223 (Figure 6.17).

6.4. Discussion

T2DM is rapidly becoming a forthcoming epidemic. In spite of several therapeutic strategies were proposed, T2DM and its associated pathogenesis remain increasingly uncontrolled. Persistent hyperglycemia, hyperlipidemia, increased ROS production and myocardial inflammation induce DC via alterations in downstream transcription factors, myocardial substrate utilization, myocyte growth, endothelial function and myocardial compliance (Bhattacharjee et al., 2016b; Riaz et al., 2016). Persistent hyperglycemia exerts its injurious effects through a sequence of secondary transducers. One of the principle abnormalities is the excess generation of AGEs which deactivate NO and thereby, weaken coronary vasodilation (Riaz et al., 2016; Singh et al., 2001). Sustained hyperglycaemia ensures excess generation of ROS which directly activate redox sensitive signaling cascade and participate in DC (Khanra et al., 2015; Singh et al., 2001). An increase in ROS with concomitant decrease in NO levels induces myocardial inflammation and endothelial dysfunction via PARP cleavage (Soriano et al., 2001). ROS also promote NF-κB signaling and thereby induce inflammation (Bhattacharjee et al., 2016a). Persistent hyperglycemia further promotes the activation of PKC signaling cascade in myocardial tissue (Way et al., 2001). The aforementioned toxicological events during T2DM integrally participate in the development and progression of cardiovascular complications to the diabetic patients. Considering the molecular basis of DC, an agent possessing hypoglycemic, anti-oxidant and anti-inflammatory activities would serve as a better therapeutic agent to counteract with DC.

Lowering the blood glucose level is principle approach to control DM and its associated toxic manifestations. In this study, T2DM was experimentally induced to Wister rats by feeding high fat diet following a single small dose of streptozotocin (35 mg/kg, i.p.) (Bhattacharjee et al., 2016b). Low dose of streptozotocin ensured partial damage of pancreatic β cell population while high fat diet resulted insulin resistance to the experimental rats. A significant decrease in serum insulin demonstrated the partial destruction of pancreatic β-cells. Significantly low HOMA-β score with significantly high HOMA-IR ensured the induction of insulin resistance to the rats (Reed et al., 2000). The aforementioned observations ensured the establishment of T2DM to the experimental rats. In this study, protocatechuic acid treatment significantly reduced fasting blood glucose level near to normalcy. The glycemic control ensured the significant drop in the level of glyco-haemoglobin and hyperglycemia mediated augmented ROS generation and thereby lowering the risk of DC (Khanra et al., 2015).

Skeletal muscle participates important role in the regulation of blood glucose level via its utilization/metabolism (Zheng et al., 2015; Li et al., 2015). In search of antihyperglycemic mechanism of protocatechuic acid, the signaling pathways involved in glucose metabolism within the skeletal muscle of T2D rats were investigated. PI3K pathway is an important signaling pathway of glucose utilization systems (Han et al., 2015). Activation of PI3K and Akt are the important steps in insulin action (Li et al., 2015). Akt is an important mediator of the glucose uptake process in the skeletal muscle. Tyrosine phosphorylation of IRS1 (Tyr 895) causes activation of PI3K which further phosphorylation of Akt (Ser 473). Activation of aforementioned signaling cascade further promotes GLUT 4 translocation. In case of T2DM, IRS1/PI3K/Akt/GLUT4 signaling is down-regulated. However, Protocatechuic acid treatment significantly increased the IRS1 phosphorylation, PI3K (p85) expression, Akt phosphorylation, and GLUT4 expression in T2D rats. AMPK regulates cellular energy homeostasis in glucose utilization process (Thakkar et al., 2015). Protocatechuic acid significantly activated AMPK phosphorylation (Thr 172) and thereby regulates cellular energy homeostasis in glucose utilization in the T2D rats. Activation of P 38 via phosphorylation also play important role in glucose transport and utilization (Macko et al., 2008). In this study, protocatechuic acid could significantly up-regulate the phosphorylation of P 38. These results suggest that stimulation of IRS1/PI3K/AKT/AMPK/P 38/GLUT4 signaling pathway by protocatechuic acid in skeletal muscle would have significant role in its antihyperglycemic effect.

T2DM is associated with hyperlipidemia which largely contributes in cell death and thus to cardiac dysfunction (Boudina and Abel, 2010). In this study, significantly elevated levels of membrane bound enzymes, LDH and CK, vindicated the cellular damage in T2D rats. High levels of serum lipids further promote the deposition of cholesterol and triglycerides to the myocardial tissues, which is directly influencing the cardiac toxicological consequences. (Boudina and Abel, 2010). Protocatechuic acid treatment could significantly reverse serum lipid level near to normalcy and thereby attenuate DC.

Oxidative stress plays critical role in the development of DC. The mechanisms of ROS production in diabetic hearts are yet to be clearly understood. However, earlier reports revealed that increased oxidative stress would be correlated with lipid overload, suggesting a role for fatty acid in the generation of ROS (Boudina and Abel, 2010). Hyperglycemia-induced formation of AGEs has also been regarded as the important source of oxidative free radicals (Pal et al., 2014).

In this study, a significantly high ROS level was observed in the myocardial tissues of T2D rats. The excess of ROS further promotes upsurges in lipid peroxidation, protein carbonylation with concomitant diminution of antioxidant enzymes in the myocardial tissues of T2D rats. However, protocatechuic acid treatment could significantly scavenge ROS level in the myocardial tissues resulting offered protection against oxidative damage of lipids and proteins. Protocatechuic acid also could up-regulate endogenous antioxidant molecules and thereby attenuate oxidative stress. T2D rats exhibited significant low level of GSH in the myocardial tissue, which indicated the over-utilization of GSH in a redox challenged cyto-environment. The redox challenge cellular environment further promotes oxidative damage and fragmentation of DNA and causes cell death. In this study, cardiac tissue of T2D rats exhibited significant DNA fragmentation and oxidation. However, protocatechuic acid treatment could significantly attenuate DNA fragmentation and oxidation. The aforementioned prophylactic effect of protocatechuic acid may be due to its radical scavenging and antioxidant effect.

Persistent hyperglycemia leads to activation of polyol pathway which results excess production of AGEs in T2DM (Singh et al., 2014). The interactions between receptors for advanced glycation end products and AGEs result a series of cellular events viz. oxidative stress, inflammation, extracellular matrix accumulation etc., which further led to myocardial dysfunction (Bodiga et al., 2014). In this study, protocatechuic acid significantly inhibited AGEs level in sera of T2D rats. Protocatechuic acid treatment inhibited the activation of polyol pathway by reducing the activities of aldose reductase and sorbitol dehydrogenase and increasing the activity of glyoxalase I. The reduction of AGEs production in protocatechuic acid treated T2D rats would be correlated with its effect on polyol enzymes.

Hyperglycemia-induced low grade myocardial inflammation has significant role in the development of DC. The increased level of C-reactive protein in the sera of T2D rats indicated the establishment of inflammation (Khanra et al., 2015). Besides, T2D rats exhibited significantly higher levels of TNF α, IL 1β, IL 6 and IL 12 in the sera of T2D rats. However, treatment with protocatechuic acid significantly reduced the levels of aforementioned inflammatory markers in the sera. In search of molecular mechanism, the immunoblot was performed with the myocardial proteins. Activation of NF-κB signaling pathways plays an important role in the inflammatory pathophysiology (Khanra et al., 2017). Intracellular oxidative stress promotes PARP cleavage, which further activates NF-κB signaling (Bhattacharya et al., 2013). On the other hand, hyperglycemic redox stress also activates PKC through polyol

activation (Ahmad et al., 2005). PKC activation also contributes in NF-κB activation in redox challenged cyto-environment. PKCs contribute in the accumulation of collagen and cause fibrosis (Bhattacharjee at al., 2016b). NF-κB is activated during inflammation via phosphorylation and degradation of its inhibitor-κB (IκBα) via phosphorylation (Bhattacharjee et al., 2016a). Then phosphor- NF-κB translocates to nucleus and activates the genes encoding inflammatory markers (Khanra et al., 2017). In this study, significant translocation phospho-NF-κB (p 65) to nucleus from cytosol was observed in the myocardial tissue of T2D rats. However, protocatechuic acid could significantly attenuate inflammation in the myocardial tissue via inhibition of PKC/PARP/NF-κB signaling.

The histological assessment revealed that, irregular radiating pattern of cardiac muscle with injured interstitial tissues and collagen deposition in the heart of T2D rats. However, protocatechuic acid treatment could significantly attenuate DC visualized in the heart sections of protocatechuic acid treated T2D rats.

In ADME studies, Lipinski Rule of Five justified the drug-likeness character of protocatechuic acid (Veber et al., 2002). The rule suggested that the drug-like molecule must comply with the following five conditions: (i) log P value must be between 0.4 and +5.6; (ii) molar refractivity must be between 40 and 130; (iii) molecular weight should be between 180 and 500; (iv) The number of atoms must be between 20 and 70 including H-bond donors and acceptors; and (v) The polar surface area must not be greater than 140 Å2 and/or fewer than 10 rotatable bonds. In this earlier study, we have taken different classes of three standard marketed drugs, like aspirin, paracetamol, and rosiglitazone, checked their Rule of Five value in Maestro, and they all produce the acceptable value of 0 (maximum value is 4) (Ray et al., 2015). In this study, protocatechuic acid satisfied aforementioned Lipinski Rule of Five values reflecting the good in silico pharmacokinetic profile and thereby reflected the drug-likeness nature of protocatechuic acid. Finally, in silico molecular docking revealed the probable interactions of protocatechuic acid with PKC β, PKC-δ, NF-κB, PARP, PI3K, IRS, Akt and AMPK. Protocatechuic acid had been predicted to offer H bonding and hydrophobic interactions within the active sites of these proteins and thereby regulate their role to control hyperglycemia and DN.

Protocatechuic acid exhibited protective effect against DC via hypoglycemic, insulin-sensitizing, anti-oxidant and anti-inflammatory effects in T2D rats. The hypoglycemic and insulin-sensitizing effects would be mediated by stimulation of IRS1/PI3K/AKT/AMPK/GLUT4/P 38 signaling pathway in the skeletal muscle, while, anti-inflammatory effects would be documented with the

inhabitation of PARP/PKC/NF-κB signaling cascades in the myocardial tissue. Protocatechuic acid also exerted significant antioxidant and radical scavenging effect in the myocardial tissue of T2D rats, which would be due to its multiple phenolic -OH group within the molecule. The probable protective mechanism of protocatechuic acid has been depicted in Figure 6.18. Molecular docking analysis predicted the probable interactions within the active sites of signal proteins. ADME prediction revealed that, protocatechuic acid supports the drug-likeness character apparent from Lipinski's rule of five. Therefore, protocatechuic acid would have a good possibility to be a new therapeutic agent for DC in future.

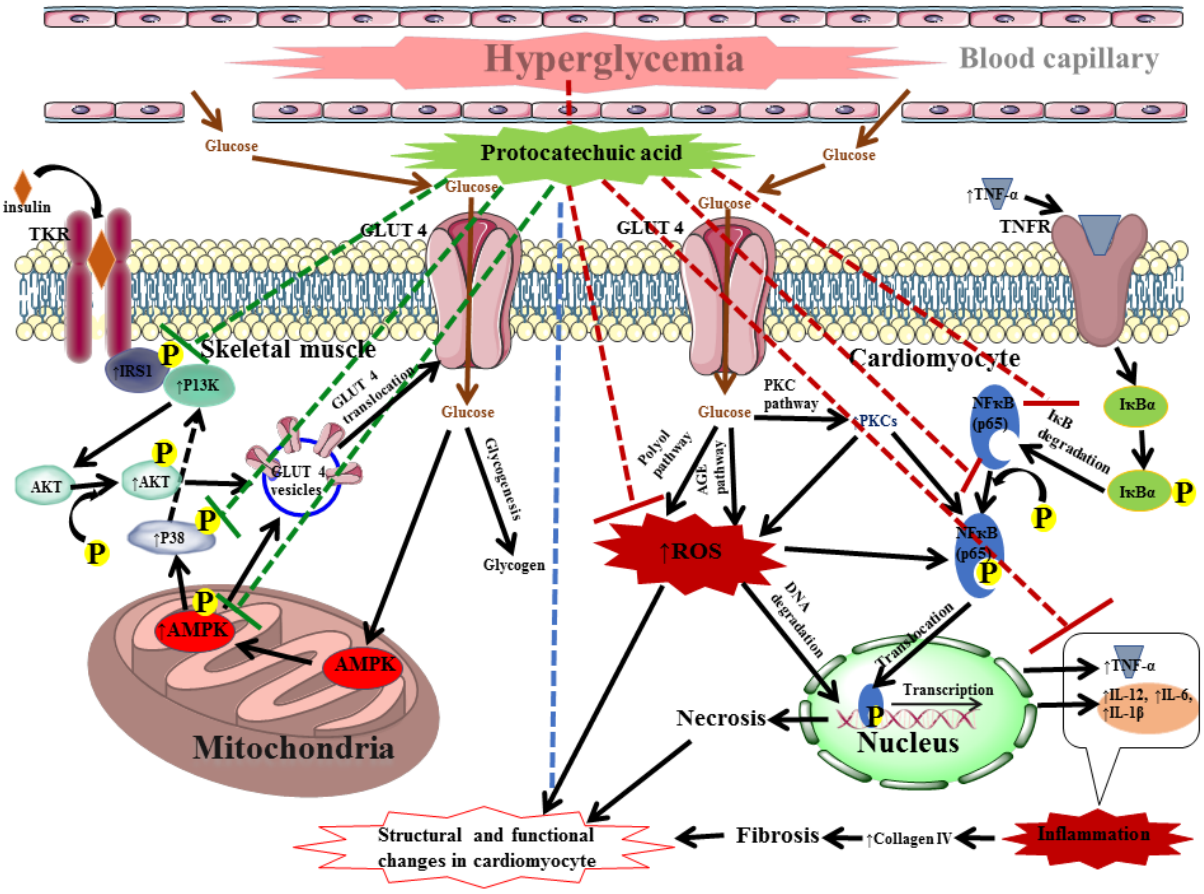

Figure 6.18. The hypothesis developed regarding possible mechanism of protocatechuic acid in the management of DC. Red dotted lines represent inhibition and green lines indicate activation.

References

Adefegha SA, Oboh G, Omojokun OS, Adefegha OM. Alterations of Na^+/K^+-ATPase, cholinergic and antioxidant enzymes activity by protocatechuic acid in cadmium-induced neurotoxicity and oxidative stress in Wistar rats. Biomed Pharmacother. 2016;83:559-568.

Baghirova S, Hughes BG, Hendzel MJ, Schulz R. Sequential fractionation and isolation of subcellular proteins from tissue or cultured cells. MethodsX. 2015;2:440-445.

Bhattacharjee N, Barma S, Konwar N, Dewanjee S, Manna P. Mechanistic insight of diabetic nephropathy and its pharmacotherapeutic targets: An update. Eur J Pharmacol. 2016;791:8-24.

Bhattacharjee N, Khanra R, Dua TK, Das S, De B, Zia-Ul-Haq M, De Feo V, Dewanjee S. *Sansevieria roxburghiana* Schult. & Schult. F. (Family: Asparagaceae) attenuates type 2 diabetes and its associated cardiomyopathy. Plos One. 2016;11:e0167131.

Bodiga VL, Eda SR, Bodiga S. Advanced glycation end products: role in pathology of diabetic cardiomyopathy. Heart Fail Rev. 2014;19:49-63.

Bolner A, Pilleri M, De Riva V, Nordera GP. Plasma and Urinary HPLC-ED Determination of the Ratio of 8-OHdG/2-dG in Parkinson's Disease. Clin Lab. 2011;57:859-866.

Boudina S, Abel ED. Diabetic cardiomyopathy, causes and effects. Rev Endocr Metab Disord 2010;11:31-39.

Dewanjee S, Das AK, Sahu R, Gangopadhyay M. Antidiabetic activity of *Diospyros peregrina* fruit: effect on hyperglycemia, hyperlipidemia and augmented oxidative stress in experimental type 2 diabetes. Food Chem Toxicol. 2009;47:2679-2685.

Dewanjee S, Dua TK, Khanra R, Das S, Barma S, Joardar S, Bhattacharjee N, Zia-Ul-Haq M, Jaafar HZ. Water spinach, Ipomoea aquatica (Convolvulaceae), ameliorates lead toxicity by inhibiting oxidative stress and apoptosis. Plos One. 2015;10:e0139831.

Dua TK, Dewanjee S, Gangopadhyay M, Khanra R, Zia-Ul-Haq M, De Feo V. Ameliorative effect of water spinach, *Ipomoea aquatica* (Convolvulaceae), against experimentally induced arsenic toxicity. J Transl Med. 2015a;13:81.

Dua TK, Dewanjee S, Khanra R, Bhattacharya N, Bhaskar B, Zia-Ul-Haq M, De Feo V. The effects of two common edible herbs, *Ipomoea aquatica* and *Enhydra fluctuans*, on cadmium‐induced pathophysiology: a focus on oxidative defence and anti‐apoptotic mechanism. J Transl Med. 2015b;13:245.

Dua, T. K., Dewanjee, S., Khanra, R. Prophylactic role of *Enhydra fluctuans* against arsenic-induced hepatotoxicity via antiapoptotic and antioxidant mechanisms. Redox Rep. 2016a;21:147-154.

Dua TK, Dewanjee S, Khanra R, Barma S, Joardar S, Das S, Zia-Ul-Haq M, De Feo V. Cytoprotective and antioxidant effects of an edible herb, *Enhydra fluctuans* Lour. (Asteraceae), against experimentally induced lead acetate intoxication. Plos One. 2016b;11:e0148757.

Erukainure OL, Hafizur RM, Choudhary MI, Adhikari A, Mesaik AM, Atolani Q, Banerjee P, Preissner R, Muhammad A, Islam MS. Anti-diabetic effect of the ethyl acetate fraction of *Clerodendrum volubile*: protocatechuic acid suppresses phagocytic oxidative burst and modulates inflammatory cytokines. Biomed Pharmacother. 2017;86:307-315.

Fernández-Millán E, Ramos S, Alvarez C, Bravo L, Goya L. Microbial phenolic metabolites improve glucose-stimulated insulin secretion and protect pancreatic beta cells against tert-butyl hydroperoxide-induced toxicity via ERKs and PKC pathways. Food Chem. Toxicol. 2014;66:245-253.

Friedewald WT, Levy RI, Fredrickson DS. Estimation of the concentration of low density lipoprotein in plasma, without use of the preventive ultracentrifuge. Clin Chem. 1972;18:499-502.

Ghosh J, Das J, Manna P, Sil PC. Protective effect of the fruits of *Terminalia arjuna* against cadmium induced oxidant stress and hepatic cell injury via MAPK activation and mitochondria dependent pathway. Food Chem. 2010;123:1062-1075.

Gutzeit D, Wray V, Winterhalter P, Jerz G. Preparative isolation and purification of flavonoids and protocatechuic acid from sea buckthorn juice concentrate (*Hippophaë rhamnoides* L. ssp. rhamnoides) by high-speed counter-current chromatography. Chromatographia. 2007;65:1-7.

Han Y, Jung HW, Park Y-K. Effects of Icariin on insulin resistance via the activation of AMPK pathway in C2C12 mouse muscle cells. Eur J Pharmacol. 2015;758:60-63.

Hissin PJ, Hilf R. A fluorometric method for the determination of oxidized and reduced glutathione in tissues. Anal Biochem. 1973;74:214-216.

Khanra R, Dewanjee S, Dua TK, Bhattacharjee N. Taraxerol, a pentacyclic triterpene from *Abroma augusta* leaf, attenuates acute inflammation via inhibition of NF-κB signaling. Biomed Pharmacother. 2017;88:918-923.

Khanra R, Dewanjee S, Dua TK, Sahu R, Gangopadhyay M, De Feo V, Zia-Ul-Haq M. *Abroma augusta* L. (Malvaceae) leaf extract attenuates diabetes induced nephropathy and cardiomyopathy via inhibition of oxidative stress and inflammatory response. J Transl Med. 2015;13:6.

LeBel CP, Bondy SC. Sensitive and rapid quantitation of oxygen reactive species formation in rat synaptosomes. Neurochem Int. 1990;17:435-440.

Li S, Chen H, Wang J, Wang X, Hu B, Lv F. Involvement of the PI3K/Akt signal pathway in the hypoglycemic effects of tea polysaccharides on diabetic mice. Int J Biol Macromolec. 2015;81:967-974.

Lin KT, Xue JY, Sun FF, Wong PYK. Reactive oxygen species participate in peroxinitrile induced apoptosis in HL 60 cells. Biochem Biophys Res Commun. 1997;230:115-119.

Macko AR, Beneze AN, Teachey MK, Henriksen EJ. Roles of insulin signaling and p38 MAPK in the activation by lithium of glucose transport in insulin-resistant rat skeletal muscle. Arch Physiol Biochem. 2008;114:331-339.

Martin TS, Kikuzaki H, Hisamoto M, Nakatani N. Constituents of *Amomum tsao-ko* and their radical scavenging and antioxidant activities. J Am Oil Chem Soc. 2000;77:667-673.

McLellan AC, Thornalley PJ. Glyoxalase activity in human red blood cells fractioned by age. Mech Ageing Dev. 1989;48:63-71.

Nair P, Nair RR. Selective use of calcium chelators enhances the yield of calcium tolerant myocytes from heart. Ind J Exp Biol. 1997;35:451-456.

Nayak SS, Pattabiraman TN. A new colorimetric method for the estimation of glycosylated haemoglobin. Clin Chim Acta. 1981;109:267-274.

Nishinaka T, Yabe-Nishimura C. EGF receptor-ERK pathway is the major signaling pathway that mediates upregulation of aldose reductase expression under oxidative stress. Free Radic Biol Med. 2001;31:205-216.

Ohkawa H, Ohishi N, Yagi K. Assay for lipid peroxides in animal tissues by thiobarbituric acid reaction. Anal Biochem. 1979;95:351-358.

Pal PB, Sinha K, Sil PC. Mangiferin attenuates diabetic nephropathy by inhibiting oxidative stress mediated signaling cascade, TNF-α related and mitochondrial dependent apoptotic pathways in streptozotocin-induced diabetic rats. Plos One. 2014;9:e107220.

Public Health Service (PHS). Public Health Service Policy on Human Care and Use of Laboratory Animals. Washington, DC: US Department of Health and Human Services, National Institute of Health, Office of Laboratory Animal welfare, 2015.

Raghu KG, Cherian OL. Characterization of cytotoxicity induced by arsenic trioxide (a potent anti-APL drug) in rat cardiac myocytes. J Trace Elem Med Biol.2009;23:61-68.

Ray SD, Ray S, Zia-Ul-Haq M, De Feo V, Dewanjee S. Pharmacological basis of the use of the root bark of *Zizyphus nummularia* Aubrev. (Rhamnaceae) as anti-inflammatory agent. BMC Complement Altern Med. 2015;15:416.

Reed MJ, Meszaros K, Entes LJ, Claypool MD, Pinkett JG, Gadbois TM, Reaven GM. A new rat model of type 2 diabetes: the fat-fed, streptozotocin-treated rat. Metabolism. 2000;49:1390-1394.

Riaz M, Zia-Ul-Haq M, Saad B. Anthocyanins and Human Health: Biomolecular and Therapeutic Aspects. Springer International Publishing. USA, 2016.

Singh R, Barden A, Mori T, Beilin L. Advanced glycation end products: a review. Diabetologia. 2001;44:129-146.

Singh VP, Bali A, Singh N, Jaggi AS. Advanced glycation end products and diabetic complications. Korean J Physiol Pharmacol. 2014;18:1-14.

Soriano FG, Pacher P, Mabley J, Liaudet L, Szabo C. Rapid reversal of the diabetic endothelial dysfunction by pharmacological inhibition of poly(ADP-ribose) polymerase. Circ Res. 2001;89:684-691.

Srinivasan K, Viswanad B, Asrat L, Kaul CL, Ramarao P. Combination of high-fat diet-fed and low-dose streptozotocin-treated rat: A model for type 2 diabetes and pharmacological screening. Pharmacol Res. 2005;52:313-320.

Thakkar CS, Kate AS, Desai DC, Ghosh AR, Kulkarni-Almeida AA. NFAT-133 increases glucose uptake in L6 myotubes by activating AMPK pathway. Eur J Pharmacol. 2015;769: 117-126.

Thurmond D C, Ceresa BP, Okada S, Elemendorf JS, Coker K, Pessin JE. Regulation of insulin stimulated GLUT4 translocation by Munc 18C in 3T3L1 adipocytes. J Biol Chem. 1998;273:33876-33883.

Tsai S-J, Yin M-C. Anti-glycative and anti-inflammatory effects of protocatechuic acid in brain of mice treated by D-galactose. Food Chem Toxicol. 2012;50:L3198-3205.

Uchida K, Stadtman ER. Covalent attachment of 4-hydroxynonenal to glyceraldehydes-3-phosphate dehydrogenase. A possible involvement of intra- and intermolecular cross-linking reaction. J Biol Chem. 1993;268:6388-6393.

Ulrich HB. Methods of enzymatic analysis. Weinheim, Verlag Chemie, 1974.

Veber DF, Johnson SR, Cheng HY, Smith BR, Ward KW, Kopple KD. Molecular properties that influence the oral bioavailability of drug candidates. J Med Chem. 2002;45:2615-2623.

Way KJ, Katai N, King GL. Protein kinase C and the development of diabetic vascular complications. Diabet Med. 2001;18:945-959.

WHO. Global Report on Diabetes. World Health Organization. 2016.

Xiao X, Wang J, Chang X, Zhen J, Zhou G, Hu Z. Mycophenolate mofetil ameliorates diabetic nephropathy through epithelial mesenchymal transition in rats. Mol Med Rep. 2015;12:4043-4050.

Zhang Y, Aberg F, Appelkvist EL, Dallner G, Ernster L. Uptake of dietary coenzyme Q supplement is limited in rats. J Nutr. 1995;125:446-453.

Zheng T, Yang X, Wu D, Xing S, Bian F, Li W, Chi J, Bai X, Wu G, Chen X, Zhang Y, Jin S. Salidroside ameliorates insulin resistance through activation of a mitochondria-associated AMPK/PI3K/Akt/GSK 3 beta pathway. Br J Pharmacol. 2015;172:3284-3301.

Web references

http://www.schrodinger.com

http://www.rcsb.org/